Photophysical Approach to Study the Interaction between Synthetic Amphiphiles and Proteins

A Dissertation Submitted As Partial
Fulfillment for the Degree of
Doctor of Philosophy

by

Bimlesh Ojha
Roll No. 06612219

Department of Chemistry
Indian Institute of Technology Guwahati
February-2011

Dedicated to my Parents....

INDIAN INSTITUTE OF TECHNOLOGY, GUWAHATI

Department of Chemistry

STATEMENT

I do hereby declare that the matter embodied in this thesis is the result of investigations carried out by me in the Department of Chemistry, Indian Institute of Technology Guwahati, India under the guidance of Dr. Gopal Das, Associate Professor, Department of Chemistry, Indian Institute of Technology Guwahati, India.

In keeping with the general practice of reporting scientific observations, due acknowledgements have been made wherever the work described is based on the findings of other investigators.

February, 2011
IIT Guwahati

Bimlesh Ojha

INDIAN INSTITUTE OF TECHNOLOGY, GUWAHATI

Department of Chemistry

CERTIFICATE

This is to certify that Bimlesh Ojha has been working under my supervision since January, 2007 as a regular registered Ph. D. student. I am forwarding his thesis entitled "**Photophysical Approach to Study the Interaction between Synthetic Amphiphiles and Proteins**" being submitted for the Ph. D. (Science) Degree of this Institute. I certify that he has fulfilled all the requirements according to the rules of this Institute regarding the investigations embodied in his thesis and this work has not been submitted elsewhere for a degree.

February, 2011
IIT Guwahati

Dr. Gopal Das
(Supervisor)
Associate Professor
Department of Chemistry
IIT Guwahati

ACKNOWLEDGEMENT

The results of the works reported in the thesis are based on interdependence rather than independence, which reflect where I have been escorted and supported by many people and that gives me a pleasant opportunity to express my gratitude to all of them. First and foremost, with a deepest sense of gratitude, I would like to express my sincere gratitude to my supervisor Dr. Gopal Das for introducing me into this interdisciplinary topic "Biophysical Chemistry" and giving me the freedom to pursue my own interests. I earnestly thank him for his astute guidance, encouragement, inspiration and creative and scientific ideas, which helped me to enhance my knowledge in this field and made my pursuit really exciting.

I would like to acknowledge my sincere gratitude to all my doctoral committee members, Dr. Manabendra Ray, Dr. Biplab Mondal and Dr. Aiyagari Ramesh for their insightful advices and valuable suggestions. I am also grateful to Prof. Arun Chattopadhyay, Head Department of Chemistry, IIT Guwahati, Prof. A. T. Khan Ex-Head, Department of Chemistry, IIT Guwahati for their valuable suggestions and providing good research environment.

I would also like to extend my sincere gratitude to Dr. Aiyagari Ramesh, Department of Biotechnology for giving me the opportunity to work with him in his lab and for his valuable suggestions and motivation.

I am thankful to the Institute, Indian Institute of Technology Guwahati for providing me with the state of the art infrastructure and facilities for advanced research. My sincere thanks are due to all other faculty members in the Department of Chemistry for their help and encouragement and the non-teaching staffs of the Department for their technical support. I would like to take this opportunity to thank Department of Biotechnology, Centre for Nanotechnology and Centre for Environment for proving me the necessary instrumental facilities during the entire duration of my research tenure. My sincere thanks to Chandan Borgohain, K. Senapati, K. K. Singh and Madhurjya Borah of Central Instruments facility, IIT Guwahati for their help in all the characterizations (SEM, TEM, AFM, NMR *etc.*) required during my research work. I would also like to thank Babulal da, Lipika ba, Abhilasha ba, Parikshit da, Aniruddha da, Diganata da, Shyamal da, Nilyotpal da and Santanu da for their constant help and support during my PhD tenure.

I would like to thank my group members Ballav da, Harjyoti da, Avijit da, Bedabrata, Sandeep, Arghya, Jiban, Chirantan, Romen, Najbul, Kaushik, Hridesh, Mouni and all other former group members Mrinmoy, Subhajit, Nikhil, Madhubrata, Soma and Subrata for their timely help, support and for the wonderful time we shared during this period. I

am also thankful to Dr. P. K. Iyer and his former group members for their help and pleasant association with whom we shared the lab in the initial stage of my research.

I extend my sincerest thanks to my seniors and friends Dr. Sahid Hussain, Dr. Rik Rani, Dr. Bolin Chetia, Dr. Biplab Sarkar, Dr. Santanu Sinha, Dr. Biswa Ranjan Panda, Dr. Saitanya Kumar Bharadwaj, Dr. Mohit Lal Deb, Dr. Saikat Das Sharma, Dr. Manas Ranjan Das, Sonit da, Prasanta da, Gunin da, Pranjal da, Krishna da, Jashmini ba, Jayanto, Dhruba, Rupam, Prasenjit, Musawwer and Roji for their constant help, motivation, enthusiastic company and all the wonderful time we spent in various events.

I also take this opportunity to thank my department seniors. I would like to thank Dr. Atul Kumar Singh, Manab and Uma who helped me with the bio related works. I would like to offer my special thanks to my Cotton College M.Sc. batch mates and friends Subhankar, Partha, Dwipen, Arun, Biswa, Uday, Bulon, Lachit, Papori, Praynga, Mitali and Shayanti for their constant unfailing support, their encouragement and all the help they extended from time to time whenever required. I would also like to extend my gratitude to my old friends Salim, Avijit, Anup, Manoj, Rajesh, Debu, Moni, Munni, Pompa, Dipak, Swarna, Pinku, Aatiqur, Debraj, Mritunjoy and Sushanta.

I wish to express my appreciation to my other friends in the campus and my 2006 Ph.D. batch mates for the wonderful time I had with them. The financial support from Indian Institute of Technology Guwahati is also duly acknowledged.

Finally, my Ph. D. endeavor could not be completed without the endless love, unending support, tolerance and blessings from my family. I wish to express my sincere gratitude to my parents, especially to my father. They are the main soul and inspiration for each and every step that I achieved in my life.

Bimlesh Ojha

SYNOPSIS

The contents of the thesis entitled "**Photophysical Approach to Study the Interaction between Synthetic Amphiphiles and Proteins**" have been divided into five chapters based on the results of experimental works carried out during the research period.

Chapter 1 highlights the definition, properties and importance of synthetic amphiphiles along with their literature background. Amphiphilic molecules consist of hydrophobic tail (usually made of long hydrocarbon chains) and hydrophilic head group (either charged or uncharged polar groups). As a result of having both hydrophobic and hydrophilic structural regions, amphiphilic molecules may dissolve in water and to some extent in non-polar organic solvents. This chapter also gives a brief overview of interaction between synthetic amphiphiles and biomolecules especially protein, where nature of head group and hydrophobic tail along with electrostatic and hydrogen bonding interactions play crucial role. Many amphiphilic molecules are known to interact with peptides and proteins, being that these interactions are of great importance not only *in vivo* but also in several technical applications. This forms the basis of a number of research areas in chemistry, biochemistry and materials science as well. Therefore, study of interaction between synthetic amphiphiles and proteins and the structure of the complexes formed as a result of those interactions have been extensively reviewed in this chapter.

Chapter 2 deals with the common methodology used to synthesize and characterize the compounds along with a brief description of equipments and the different experimental setup to study the interactions between amphiphiles and proteins.

Chapter 3 describes the interaction between 5-(alkoxy)naphthalen-1-amine (**1**-**3**) amphiphile and bovine serum albumin (BSA). The content of this chapter is divided into two sections. The first section reports the selective sensing of BSA by these novel protein binding amphiphilic fluorophores (**1**-**3**) *via.* non-covalent interactions. The weak fluorescent of these probes in an aqueous solution showed a dramatic increase in their fluorescence intensity, quantum yield and lifetime after binding with BSA (Fig. 1). The exclusivity of the system is that it interacts with BSA selectively and signals the event by 'turn on" fluorescence while the responses to various other proteins/enzymes used are negligible under similar set of experimental conditions. The photophysical behaviour of compounds are affected by the interplay with BSA but not with free tryptophan amino acid suggesting the microenvironment created by macromolecule induces some change in

the excited-state of compound. The spectral changes were caused by complex formation, in which the compound is strongly bound at hydrophobic pockets of the BSA supported by hydrophobic interactions. The selective sensing ability of these probes towards BSA can be explained on the basis of proteins hydrophobicity "a suitable cleft" required to bind a host.

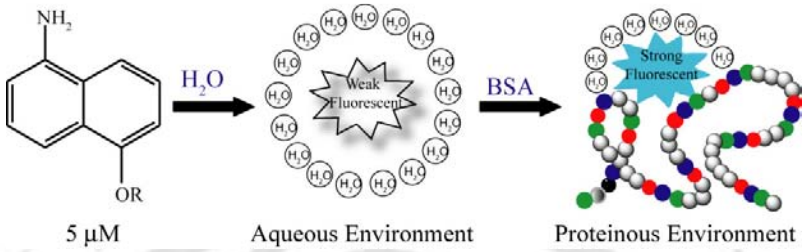

Figure 1. Schematic illustration showing the effect of protein microenvironment on the photophysical response of compounds, where R = C_8H_{17} (**1**), $C_{12}H_{25}$ (**2**), $C_{16}H_{33}$ (**3**).

The second section of chapter 3 describes the effect of these amphiphilic compounds (**1-3**) on the conformation of BSA. The BSA fluorescence exhibits appreciable bathochromic shift along with a reduction in fluorescence intensity and fluorescence lifetime with increasing concentration of compound from 0 to 40 µM. The shifts in emission maxima wavelength along with a reduction in fluorescence intensity of tryptophan residues in protein are generally observed upon unfolding. Compounds quenched the fluorescence of BSA in a concentration dependent manner and deviates positively from linear Stern-Volmer equation indicating the presence of both static and dynamic quenching mechanisms. The calculated quenching rate constants and binding constants were found to depend inversely on compounds alkyl chain length. Compounds bind near Trp-134 in the sub-domain IA of the native BSA and become accessible to Trp-212 when BSA gets unfolded (Fig. 2). The data well supports the idea that BSA loses its structure incrementally during its interaction with compounds.

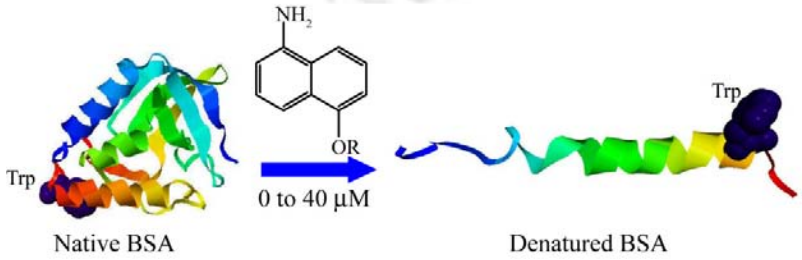

Figure 2. Schematic presentation showing the effect of compounds on the conformation of BSA, where R = C_8H_{17} (**1**), $C_{12}H_{25}$ (**2**), $C_{16}H_{33}$ (**3**).

Chapter 4 discusses the inhibitory effect of cationic amphiphile *viz.* N-methyl-8-(alkoxy)quinolinium iodide (**4-6**) on the aggregation behaviour of hen egg white lysozyme (HEWL) at alkaline pH. Compounds did not protect native HEWL from conformational changes; however they were effective in diminishing HEWL amyloid formation by delaying both nucleation and elongation phases. It is likely that strong binding of these amphiphilic compounds, raise the activation energy barrier for protein misfolding and subsequent aggregation, thereby retarding the aggregation kinetics substantially. In order to understand the inhibitory effect of amphiphilic compounds on HEWL aggregation was either due to cationic head group or as a consequence of hydrophobic tail group, we pursued some additional control experiments with the neutral counterpart of the amphiphilic compound (8-alkoxyquinoline) and the parent non-amphiphilic compound (8-hydroxyquinoline) independently. The control samples were unable to arrest the growth of HEWL aggregation under identical experimental conditions, depicting the fact that cationic head as well as hydrophobic tail group of the compound is indispensable for inhibition of aggregation process. Removal of either head group or hydrocarbon chain from the compound obliterates its ability to do the same. It could be presumed from our results that compounds could directly bind to the partially unfolded protein as the functional groups of protein are more exposed in this form. This relatively stronger binding can assist in stabilizing the protein in this partially unfolded form and subsequently inhibit fibril formation by interfering with the intermediate oligomers (Fig. 3).

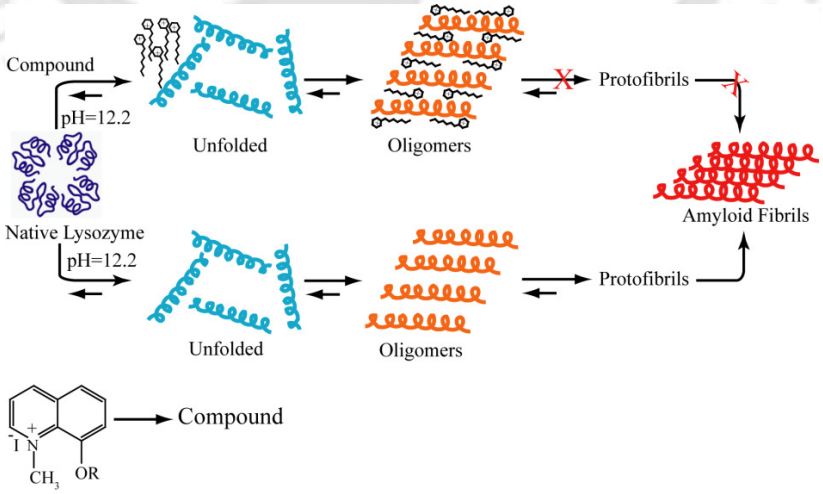

Figure 3. Schematic illustration showing the role of cationic compounds in arresting the growth of HEWL aggregates, where R = C_4H_9 (**4**), C_8H_{17} (**5**) and $C_{12}H_{25}$ (**6**).

Chapter 5 demonstrates the potential of 2-(alkyl)malonic acid amphiphiles (**7-9**) as an inhibitor of metalloenzymes like *Taq* DNA polymerase and α-amylase. A dose-dependent inhibition of *Taq* DNA polymerase was observed when a polymerase chain reaction (PCR) was performed in presence of compounds while in case of α-amylase the enzymatic assay of starch-iodine complex shows the inhibition was independent of inhibitor concentration. Control experiments revealed that both chelating as well as amphiphilic nature of the compound was essential for inhibition of enzymatic activity. Further, addition of Ca^{2+} to the enzyme solution incubated with compound was also unable to recover the enzymatic activity, supporting the fact that the inhibition was irreversible in nature. Steady-state fluorescence quenching studies suggest that the removal of metal ion from the active sites of enzyme leads to a decrease in the solvent accessibility of tryptophan, indicating changes in the tertiary structure of protein. It is proposed that removal of metal ion from the active sites of the enzyme by the amphiphilic compound possibly leads to the disruption of native conformation of enzyme which is responsible for the subsequent loss of its activity (Fig. 4).

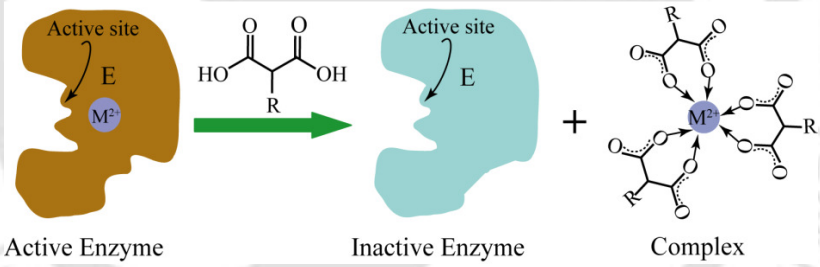

Figure 4. Schematic model showing the extraction of metal from the active sites of enzyme by the compounds, where R = C_8H_{17} (**7**), $C_{12}H_{25}$ (**8**), $C_{16}H_{33}$ (**9**) and M = Calcium or Magnesium.

At the end of the thesis an overall conclusion of the research carried out during the research period along with the future scopes for further research in the area of synthetic amphiphiles and their interaction with biomolecules have been provided.

TABLE OF CONTENTS

Chapter 1

Introduction

1.1 Introduction

Amphiphile (from the Greek amphis: both and philia: love, friendship) is a term describing a chemical compound possessing both hydrophilic (water-loving) and lipophilic (fat-loving) properties (Fig. 1.1). The lipophilic group is usually a hydrocarbon moiety (also called the tail group), such as a long chain of the form $CH_3(CH_2)_n$, with n>4, while the hydrophilic group (also called the head group), falls into the categories like charged or polar uncharged groups. The polar charged region may be anionic or cationic. Molecules possessing such properties are called amphiphilic or amphipathic.[1.1] As a result of having both lipophilic and hydrophilic regions, amphiphilic compounds may dissolve in water and to some extent in non-polar organic solvents. Based on the occurrence amphiphilic molecules may be natural or synthetic. Phospholipids, glycolipids fatty acids, bile acids and cholesterols etc. are the common examples of natural amphiphiles found in biological systems, while sodium dodecyl sulfate (SDS), cetyl trimethylammonium bromide (CTAB), didecyldimethylammonium bromide (DDAB) and triton X etc. are the common examples of some synthetic amphiphiles. Amphiphilic molecules have a surface activity and are controlling features in many important systems, including emulsification, detergency, foaming, wetting, lubrication, water repellence, waterproofing, spreading and dispersion, and colloid stability.

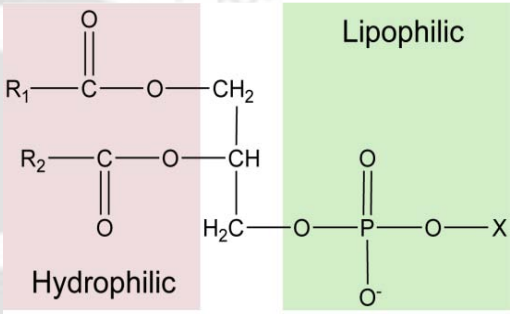

Figure 1.1. General structure of an amphiphilic molecule showing the hydrophilic head (polar) and lipophilic tail (apolar) group.

Often, amphiphilic species have several lipophilic parts, several hydrophilic parts, or several of both (Fig. 1.2). Proteins and some block copolymers are examples of such kind. Amphiphiles having two hydrophilic head group at the two ends of the long hydrocarbon chain are called bolaamphiphiles, while molecule having a head groups with two oppositely charged is called zwitterionic amphiphiles. There is another kind of amphiphilic molecules called gemini surfactants made up of two long hydrocarbon chains and two ionic groups linked by a spacer. The spacer can be attached directly to the (identical) ionic groups, each of which is in turn bonded to an identical hydrocarbon chain. The spacer can vary in length, hydrophobicity and flexibility. This thesis mainly deals with synthetic amphiphilic molecules having single-headed and single-tailed.

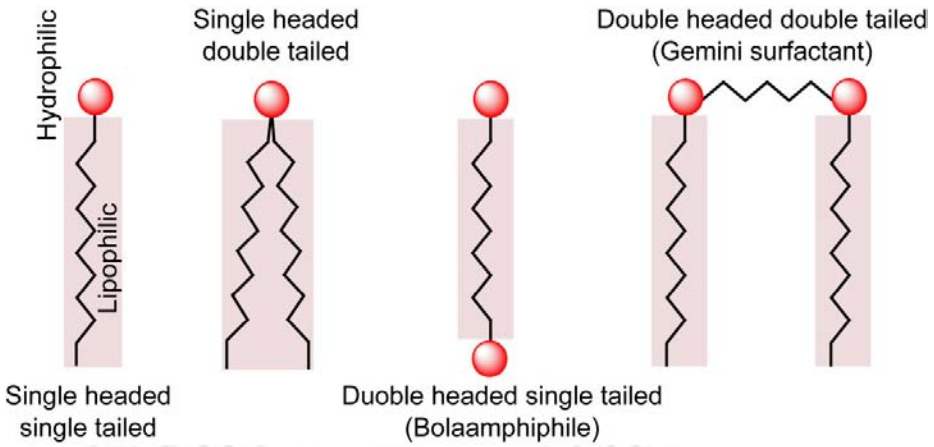

Figure 1.2. Amphiphilic molecules having different number of hydrophilic and lipophilic regions.

Amphiphilic molecules are also referred as surfactants (surface active agents) as they have the tendency to reduce the surface tension of water by adsorbing at the liquid gas interfaces. In this report, the term amphiphiles has been used rather than surfactants. Depending on the environmental conditions like temperature, concentration and structure of the amphiphiles they can also assemble in the bulk solution to give different types of aggregates having different morphology (Fig. 1.3). Some of these aggregates are known as micelles, vesicles bilayers etc.[1.2] The morphology of the aggregates can be controlled through variations in the amphiphiles composition, the concentration in the solution, the nature of the common solvent, the amount of water present in the medium, the temperature, the presence of additives such as ions and other surfactants etc.[1.2] The driving force for the aggregation of amphiphiles in water is considered to be the hydrophobic effect[1.3] above a certain critical concentration. The concentration at which amphiphiles begin to aggregate is known as the critical micelle concentration or CMC. When micelles form in water, their tails form a core that can encapsulate an oil droplet, and their (ionic/polar) heads form an outer shell that maintains favorable contact with water. When amphiphiles assemble in oil, the aggregate is referred to as a reverse

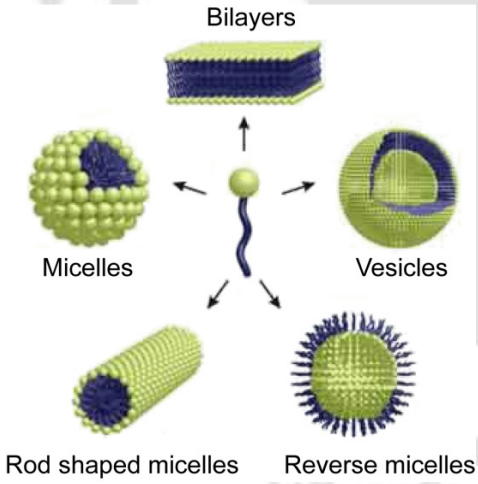

Figure 1.3. Amphiphilic molecules showing the morphology of different types of organized structure in solution (Adopted from reference 1.3d).

micelle. In a reverse micelle, the heads are in the core and the tails maintain favorable contact with oil. The aggregated amphiphiles, in a solution remain in equilibrium with free, unaggregated or monomeric amphiphiles.

1.2. Advantages of Photophysical Approach

During the last two decades, there has been an enormous increase in the use of photophysical methods in different field of chemistry, biochemistry and material science as well. Photophysical methods generally offer numerous advantages of crucial importance for biophysicists, particularly high sensitivity, *i.e.*, reliable output at low concentration along with the possibility of selectively probing individual chromophoric parts of molecules and supramolecules.[1.4] The accessibility of the information from dilute samples (typically 10^{-5} to10^{-7} M) is important, as the typical features studied in biophysical chemistry, such as protein-ligand association and formation and dissociation of supramolecular associates and complexes, typically suffer from side effects such as self-association of components at higher concentrations (>10^{-4} M). Additional advantages of photophysical methods are the usually nondestructive nature of the measurements and the small sample volume required for the experiments. Most importantly, however, photoexcitation methods allow the detection of transient species. While an entity with a lifetime of 50 ns or less can be comfortably analyzed by transient absorption or fluorescence spectrometry, other physical methods of steady-state character are likely to fail.[1.4]

For example, the timescale of most NMR experiments is longer than *ca*. 100 ms, which renders this method unsuitable for studies of short-lived species. Moreover, the typical tools of supramolecular chemistry, such as NMR spectrometry, require concentrations usually in excess of 10^{-4} M, and other favorite methods such as mass spectroscopy [fast-atom bombardment (FAB), electrospray ionization (ESI), matrix-assisted laser desorption ionization (MALDI)], and vapor-pressure osmometry do not directly provide information about supramolecular behavior in solution. The most favorite method, x-ray analysis, suffers from the limitation posed by the ultimate requirement of being able to grow single crystals. While this is, in numerous instances, possible in the case of pure molecular entities, supramolecules, being mixed molecular objects by nature, are usually difficult to grow in the form of a single crystal. Thus the photo-techniques offer researchers another

level of information in the field of biophysical chemistry, where these techniques may be particularly useful.[1.4]

1.3 Interaction of Synthetic Amphiphiles with Biomolecules

Thermodynamics of the amphiphilic systems are of great importance, theoretically and practically. This is because the amphiphilic systems represent a system between ordered and disordered states of matter. Amphiphilic solutions may contain an ordered phase (aggregates) and a disordered phase (free amphiphilic molecules and/or ions in the solution). This forms the basis for a number of research areas in chemistry and biochemistry. In this context the interaction of amphiphiles with biomolecules specially protein have been a subject of extensive studies because of their relevance to the field of pharmaceutics, paints and coatings, adhesives, oil recovery, and so forth.[1.5] Moreover, such investigations can provide insight relevant to the field of biochemistry like

- Denaturing or renaturing action of amphiphiles on protein
- Solubilizing or precipitating action of amphiphiles on protein
- Sensing of biomolecules
- Suppression of protein-protein interactions etc.

1.3.1. Denaturing or Renaturing Action of Amphiphiles on Protein

Interactions of protein with amphiphiles generally depend on the features of amphiphiles. Compared to the anionic, cationic and neutral amphiphiles weakly interact with the proteins as a consequence of smaller relevance of electrostatic interactions at the pH of interest.[1.6] However, the binding isotherms of both types of amphiphiles have been found to be similar.[1.6,1.7] Establishing a protein's structure in its native state is a complex proposition. Many physical methods are cumulatively necessary for its elucidation. Moreover, the structure of proteins varies significantly in solution and solid phases. Although many native protein structures are presently known at the level of atomic resolution, a clear understanding of the physical principles of their organization and stabilization in space is still lacking. A useful approach to this problem is studying the denaturation of the native structure by external probes. The commonly used denaturants are urea, guanidine hydrochloride, and ionic amphiphiles or surfactants. Urea and guanidine hydrochloride affect the denaturing process in several ways,[1.7] one of which is affecting the water structure[1.8] The process is therefore passive, and consequently, the

required denaturant concentration is relatively large. While the ionic amphiphiles bound to the oppositely charged amino acid residues of protein leading to unfolding of the biopolymers (denaturate native protein structure) at low denaturant concentrations. There is evidence that, at the initial stage, the interaction is of electrostatic nature, which causes the protein to unfold, resulting in the exposure of more binding sites. For general aspects of interactions between ionic amphiphiles and water soluble proteins, sodium dodecyl sulfate (SDS) and bovine serum albumin (BSA) have been often used as a representative system.[1.9] The interaction of proteins with the amphiphilic molecules can change the conformation of proteins in the bulk (Fig. 1.4) and at the interfaces.[1.10] In electrophoresis, proteins are classically treated with SDS to denature the native tertiary and quaternary structures, allowing the separation of proteins according to their molecular weight. Therefore, understanding of interaction between the amphiphiles and proteins in the bulk and at the interfaces, formation of protein-amphiphile complexes and displacement of protein molecules from the interfaces by amphiphilic molecules is important from scientific as well as practical viewpoints. A number of papers deal with the theoretical and experimental studies on the adsorption behavior of protein amphiphile mixtures and different mechanisms for the displacement of protein molecules from the interfaces by the amphiphiles have been suggested such as orogenic displacement[1.11] or competitive adsorption.[1.12]

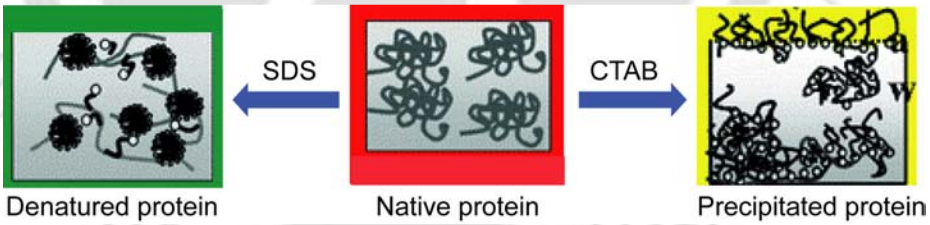

Figure 1.4. Schematic illustration showing the effect of amphiphiles on the physicochemical and conformational properties of protein (Adopted from reference 1.10b).

Klein-Seetharaman *et al.*[1.13] have identified that sodium dodecyl sulfate (SDS), alone or incombination with other chemicals, for the formation of a compact unfolding intermediate state with flexible surface elements in a membrane protein. In agreement with the pattern of secondary structure changes detected by circular dichroism described by them and also the distinct tertiary structural changes over four SDS concentration ranges based on the expected predominant micellar structures. Dodecyl maltoside

(DM)/SDS mixed micelle spheres (0.05-0.3% SDS) turn into SDS spheres (0.3-3% SDS) that gradually (3-15% SDS) become cylindrical (above 15% SDS). Denatured states in SDS spheres and cylinders show a relatively greater burial of cysteine and tryptophan residues and are more compact as compared to the states observed in mixed micellar structures. Protein structural changes at the membrane/water interfaces region are most prominent at very low SDS concentrations but reach transient stability in the compact conformations in SDS spheres (Fig. 1.5).[1.13]

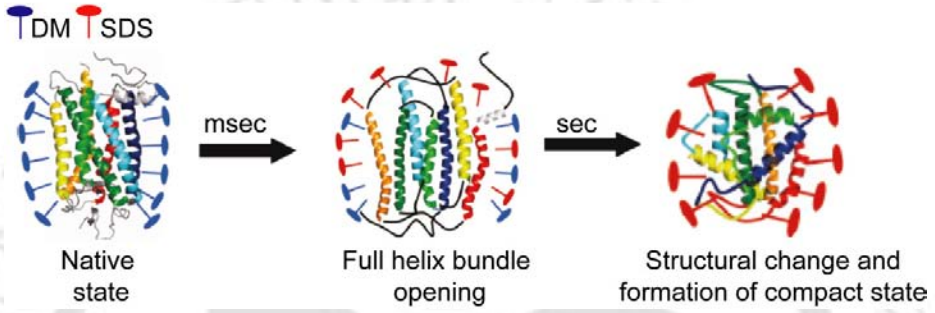

Figure 1.5. Schematic model depicting structural changes in rhodopsin due to the addition of SDS. Where DM and SDS stands for dodecyl maltoside and sodium dodecyl sulfate (Adopted from reference 1.13a).

1.3.2. Sensing of Biomolecules

Molecules based on amphiphilic building blocks are capable of providing diverse self-assembled structures, because of their differential interaction energy with the solvent surface.[1.14] Such amphiphilic assemblies could find use in a variety of applications ranging from biology to materials.[1.15] There is significant interest in amphiphile-based supramolecular assemblies, because of their container properties in aqueous solutions (*e.g.*, micelles and vesicles)[1.16] that these macromolecules are capable of providing in which both the hydrophilic and the hydrophobic moieties are incorporated within the monomer unit.[1.17] Polymeric versions of these assemblies have been extensively explored due to their greater stability, and the lower critical aggregation concentrations. Sensing through "pattern generation" is promising due to the simpler molecular design principles, compared to the typical lock and key sensor.[1.18] This approach will be even more attractive if the components of the sensor are assembled noncovalently[1.19] in such a fashion that the differential response could be achieved from a single receptor for multiple analytes. However, pattern generation does require numerous synthetic receptors. Hence, it is interesting to develop strategies that either simplify the assembly of the receptors or reduce the need for multiple receptors. In this direction, Thayumanavan

et al. have recently introduced an approach that uses a single receptor scaffold, but with multiple fluorescent transducers for pattern recognition of metalloproteins.[1.20] The basis of their hypothesis is when polyelectrolytes complex to complementary small molecule ionic amphiphiles, the combination should provide supramolecular assemblies with apolar interiors that can sequester hydrophobic guest molecules in water. Since polymeric amphiphiles typically exhibit lower critical aggregation constant (CAC), it is reasonable to expect the polymer-amphiphile complex to exhibit lower CACs than the small molecule amphiphile by itself.[1.21] At a concentration between these two CACs, the guest molecules will be released if the interaction between the polymer and the amphiphile is interrupted (Fig. 1.6).

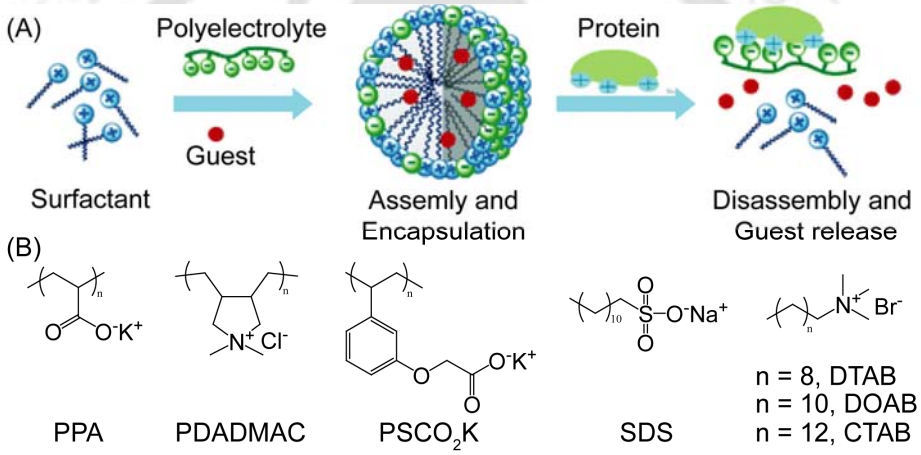

Figure 1.6. (A) Schematic of the assembly and disassembly upon protein binding and (B) Structures of polymers and amphiphiles used (Adopted from reference 1.20b).

This is because the amphiphile by itself is not capable of forming a micelle at this concentration. Since polyelectrolytes are known to effectively bind globular proteins, the protein binding should cause the release of the guest molecules. However, to generate the targeted analyte (protein)-dependent patterns, the binding affinity of the polymer to different proteins has to be necessarily different. It is understandable nonetheless that a negatively charged protein can bind to a similarly charged polymer because proteins are polyampholytes and polymers are polyelectrolytes.[1.22] They have also noted that the sizes of protein also seem to play a crucial role in these polymer binding events along with the charge of the protein and that provides the requisite unpredictability and therefore the opportunity for analyte-dependent fingerprints.

Fluorescent sensors for biological species are receiving considerable attention because of their high selectivity, sensitivity, and simplicity to facilitate both qualitative and quantitative analysis, which may have wide implications in proteomics, medical diagnostics, and pathogen detection.[1.23] Various synthetic receptors have been used for detecting biomedical analytes including adenosine-triphosphate (ATP),[1.24] heparin,[1.25] protein,[1.26] and IP3.[1.27] In particular, fluorescent probes whose emission intensity increases upon association with biomolecules, such as DNA or proteins, are useful markers in genomics and proteomics, because the binding event to the host molecule may be followed by the appearance of an intense fluorescence emission ("light-up probes").[1.28] Their major applications are staining of nucleic acids and proteins in gel electrophoresis and the quantification of these biomacromolecules.[1.29] The fluorescent protein stains include, among others, 1-anilino-8-naphthalenesulfonate (1,8-ANS),[1.30] Nile Red,[1.31] or the SYPRO dye family.[1.32]

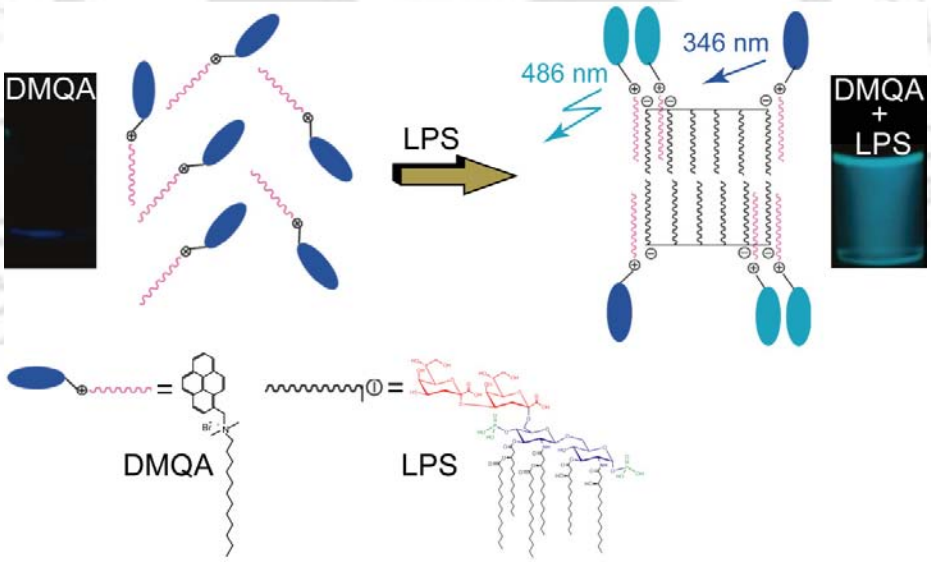

Figure 1.7. Proposed assembly mechanism between DMQA and LPS in aqueous solution (Adopted from reference 1.33).

Nevertheless, studies aimed at a better understanding of the origin of the fluorescence properties of a given fluorophore, in particular the dependence on the environment, are scarcely addressed in the literature. Even less investigated is the mechanism of protein detection by light-up probes. Recently Lee *et al.* have reported a synthetic amphiphilic fluorescent sensor for lipopolysaccharide (LPS) a bacterial endotoxin[1.33] based on pyrenyl

quaternary ammonium (DMQA) as shown in figure 1.7. Such a modified cationic amphiphile DMQA can interact with the highly negatively charged LPS by the electrostatic interaction and hydrophobic interaction in aqueous solution.[1.34] Their prediction is that the negatively charged carboxylate and phosphate groups located nearby in LPS molecule could catch two DMQA molecules *via* electrostatic interaction. Meanwhile, the long alkyl chain (lipophilic group) in DMQA could assemble with lipid A (lipid component the innermost region of LPS) by the hydrophobic interactions. In this process, pyrenyl groups from two DMQA molecules would stack onto each other *via* π-π interaction. Upon photoexcitation, this molecular ensemble should thus give an enhanced pyrene excimer photoluminescence and applied as fluorescent probe for LPS detection (Fig. 1.7). Their work not only provides a simple method to detect LPS but also opens a new perspective to rationally design sensors *via* supramolecular assembly.

1.3.3. Suppression of Protein-Protein Interactions

Self-assembly of proteins into their native conformations has been one of the seminal topics in biochemistry for more than half a century.[1.35] Proper native protein conformations play an essential role in normal cell functioning. If the correct folding of proteins does not occur appropriate cellular repair machinery fail to function, protein aggregation and amyloid formation may occur. The abnormal assembly of proteins is implicated in over 30 human disorders, which include Alzhemers, Parkinsons disease etc. In vitro and vitro studies have suggested that protein aggregation is a multi-step process with several intermediates (Fig. 1.8) and amyloid fibril formation is a nucleation-dependent process that can be accelerated dramatically by fibril seeds in vitro and in vivo.[1.36] In vitro studies revealed that the monomeric Aβ can self-assemble into amyloid fibrils with facile conversion in physiological conditions. Recent studies revealed that these soluble oligomers, including Aβ-derived diffusible ligands (ADDLs)[1.37] and Aβ*56[1.38] have been thought to be the most important features showing higher toxicity to neuronal cells than the monomeric form and mature amyloid fibrils. The structural definition of the soluble oligomers has not been accomplished, because the oligomers are metastable. Circular dichroism (CD) studies indicated that the oligomers are composed of β-sheet structures.[1.39] These ongoing experiments have also demonstrated that the rate of fibrillization and the morphology of the final fibrillar state are strongly influenced by environmental factors (pH, salt, temperature, agitation, etc.); chemicals (proteins, lipids,

cholesterol, metals, etc.); and by the nature of the seeding agent.[1.40] In the case of Aβ, evidence from both in vitro and in vivo studies strongly suggest that soluble oligomeric Aβ forms with β-sheet secondary structure are responsible for neurological toxicity.

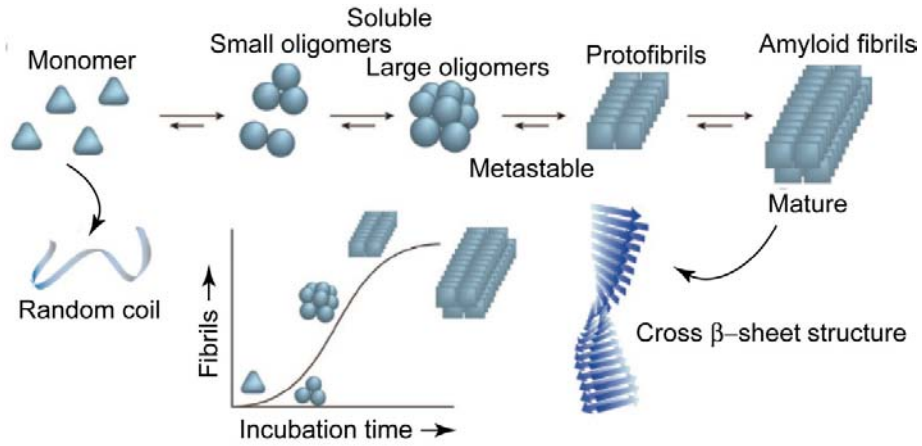

Figure 1.8. Schematic model showing the pathway for fibrillogenesis of Aβ monomer *via* different metastable intermediates (Adopted from reference 1.39).

One of the promising strategies to prevent protein aggregation is to stabilize their native state by small molecules.[1.41] As the native structure of protein undergoes partial unfolding before aggregation, stabilization of the native state may increase the activation energy barrier, thereby slowing the aggregation kinetics and moving away from amyloidgenic state (Fig. 1.9).[1.42] A number of small molecules like ligands, substrates or enzyme inhibitors, can selectively bind to native protein conformer and prevent its structural fluctuation.[1.43] As amphiphilic molecules provide a molecular basis for the role of biological membranes and the effects of the most representative anionic surfactant, namely, sodium dodecyl sulfate (SDS), on fibril formation have been extensively studied and described by many authors.[1.44]

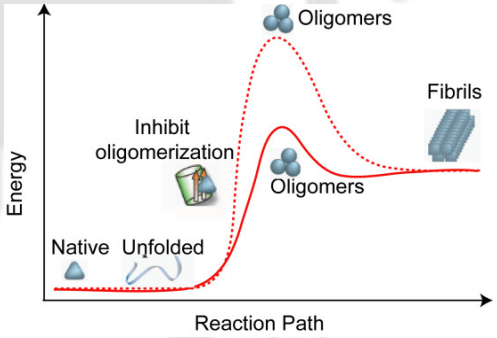

Figure 1.9. Schematic illustration showing reaction energy pathway for fibrillogenesis of native protein in absence (solid line) and presence of inhibitor (dotted line).

Estelrich *et al.* have studied the effect of cationic amphiphiles on the propensity of the peptide to form fibrils. Their findings have demonstrated that the cationic amphiphiles

can have dual effect, depending on the concentration: they both stimulate and inhibit the formation of aggregates and amyloid material.[1.45] Below a determined surfactant concentration (close to the corresponding critical micellar concentration in medium without peptide), surfactants favor aggregation, presumably by means of electrostatic interactions that destabilize the native conformation of a protein (Fig. 1.10).

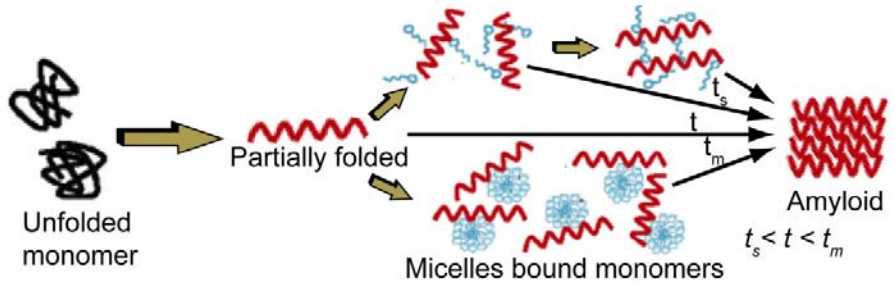

Figure 1.10. Scheme showing the effect of alkyl bromide surfactants on the aggregation process of protein. Where t is the time needed to reach a complete aggregation in absence of surfactant, t_s in the presence of submicellar surfactant concentrations and t_m in the presence of supramicellar surfactant concentrations (Adopted from reference 1.45).

1.4. Scope of the Work

From the above literature review it is evident that the interaction of synthetic amphiphiles with biomolecules is of great importance not only in vivo but also in several technical applications and that forms the basis of a number of research areas in chemistry, biochemistry and materials science as well.

From the foregoing overview it also emerges that there still exists a wide application of synthetic amphiphiles in various fields of biology and chemistry. The objective of the research project was to synthesize different types of amphiphilic molecules having different head group and alkyl chain length and to study their interaction with proteins using photophysical method. Upto now the effect of the amphiphilic molecules on the photophysics of biomolecules especially on proteins have been extensively studied, here in addition to that the photophysics of some fluorophoric amphiphilic molecules in presence of protein have been studied too. The research interests also aimed towards the design and development of inhibitors of protein-protein interactions and biosensors for selective detection of proteins. Therefore, study of interaction between synthetic amphiphiles and proteins and the structure of the complexes formed as a result of those interactions have been extensively reviewed in the thesis.

References

[1.1] Feiters, M. C.; Notle, R. J. M. *Advances in Supramolecular Chemistry*, Vol. 6, Ed.; Gokel, G. W., Jai Press, Inc Stamdfort CT, U.S.A. 2000.

[1.2] (a) Mueller, A.; O'Brien, D. F. *Chem. Rev.* **2002,** *102*, 727; (b) Hartgerink, J. D.; Zubarev, E. R.; Stupp, S. I. *Curr. Opin. Solid St. Mat. Sci.* **2001,** *5*, 355; (c) Lehn, J. M. *Supramolecular Chemistry;* New York: VCH, 1995; (d) Sone, E. D.; Zubarev, E. R.; Stupp, S. I. *Angew. Chem. Int. Ed. Engl*. **2002**, *41*, 1705; (e) Arnt, L.; Tew, G. N. *J. Am. Chem. Soc.* **2002**, *124*, 7664.

[1.3] (a) Tanford, C. *The Hydrophobic Effect, Formation of Micelles and Biological Membranes*, Wiley Interscience, Newyork, U.S.A., 1973; (b) Blockzijl, W.; Engberts, J. B. F. N. *Angew. Chem. Int. Ed. Engl.* **1993**, *32*, 1545; (c) Evans, D. F.; Wennerstrom, H. *The Colloidal Domain, Where Physics, Chemistry, Biology and Technology Meet*, VCH: Newyork/Weinheim Cambridge, 1994.

[1.4] Anzenbacher, P.; Rodgers, M. A. J. *Encyclopedia of Supramolecular Chemistry,* Taylor & Francis, London, 2004.

[1.5] (a) Ananthapadmanabhan, K. P. *Interactions of Surfactants with Polymers and Proteins*, Eds.; Goddard, E. D.; Ananthapadmanabhan, K. P., CRC Press, Inc: London, U.K., 1993; (b) Jones, M. N. *Chem. Soc. Rev*. **1992**, *21*, 127; (c) Jones, M. N. *Food Polymers, Gels and Colloids,* Ed.; Dickenson, E., The Royal Society of Chemistry: Cambridge, U.K., 1991; (d) McClements, D. J. *Food Emulsions: Principles, Practice and Techniques*, 2nd ed.; CRC Press: Boca Raton, FL, 2004.

[1.6] Few, A. V.; Ottewill, R. H.; Parreira, H. C. *Biochim. Biophys. Acta* **1955**, *18*, 136.

[1.7] (a) Nozaki, Y.; Reynolds, J. A.; Tanford, C. *J. Biol. Chem.* **1974**, *249*, 4452; (b) Ramos, C. H. I.; Baldwin, R. L. *Protein Sci.* **2002**, *11*, 1771; (c) Timasheff, S. N. *Annu. Rev. Biophys. Biomol. Struct.* **1993**, *22*, 67; (d) Bostrom, M.; Williams, D. R. M.; Ninham, B. W. *Biophys. J.* **2003**, *85*, 686; (e) Russo, A. T.; Rosgen, J.; Bolen, D. W. *J. Mol. Biol.* **2003**, *330*, 851; (f) Schellman, J. A. *Biophys. J.* **2003**, *85*, 108.

[1.8] Das Gupta, P. K.; Moulik, S. P. *J. Phys. Chem.* **1987**, *91*, 5826.

[1.9] Takeda, K.; Moriyama, Y.; Hachiya, K. *Protein Interactions with Ionic Surfactants Part I: Binding and Induced Conformational Changes, Encyclopedia of Surface and Colloid Science*, 2nd ed.; Eds.; Somasundaran, P.; Hubbard, A., Taylor and Francis: London, U.K., 2006.

[1.10] (a) Gelamo, E. L.; Silva, C. H.; Imasato, H.; Tabak, M. *Biochim. Biophys. Acta* **2002**, *1594*, 84; (b) Chakraborty, T.; Chakraborty, I.; Ghosh, S. *Langmuir* **2006,** *22,* 9905; (c) Kotsmar, Cs.; Pradines, V.; Alahverdjieva, V. S.; Aksenenko, E. V.; Fainerman, V. B.; Kovalchuk, V. I.; Kragel, J.; Leser, M. E.; Noskov, B. A.; Miller, R. *Adv. Colloid Interface Sci.* **2009**, *150*, 41.

[1.11] Mackie, A. R.; Gunning, A. P.; Ridout, M. J.; Wilde, P. J.; Morris, V. J. *Langmuir* **2001**, *17*, 6593.

[1.12] Miller, R.; Fainerman, V. B.; Leser, M. E.; Michel, M. *Colloids Surf. A* **2004**, *233*, 39.

[1.13] (a) Dutta, A.; Kim, T. Y.; Moeller, M.; Wu, J.; Alexiev, U.; Klein-Seetharaman, J. *Biochemistry* **2010**, *49*, 6329. (b) Dutta, A.; Tirupula, K. C.; Alexiev, U.; Klein-Seetharaman, J. *Biochemistry* **2010**, *49*, 6317.

[1.14] (a) Israelachvili, J. N. *Intermolecular and Surface Forces*, 2nd ed.; Academic Press: New York, 1991; (b) Bucknall, D. G.; Anderson, H. L. *Science* **2003**, *302*, 1904; (c) Mckee, M. G.; Layman, J. M.; Cashion, M. P.; Long, T. E. *Science* **2006**, *311*, 353; (d) Chen, W. H.; Shao, X.-B.; Regen, S. L. *J. Am. Chem. Soc.* **2005**, *127*, 12727; (e) Loewik, D. W. P. M.; van Hest, J. C. M. *Chem. Soc. Rev*. **2004**, *33*, 234; (f) Menger,

F. M.; Keiper, J. S. *Angew. Chem., Int. Ed.* **2000**, *39*, 1906; (g) Ryu, E. H.; Zhao, Y. *Org. Lett.* **2004**, *6*, 3187.

[1.15] (a) Hartgerink, J. D.; Beniash, E.; Stupp, S. I. *Science* **2001**, *294*, 1684; (b) Gaucher, G.; Dufresne, M. H.; Sant, V. P.; Kang, N.; Maysinger, D.; Leroux, J. C. *J. Controlled Release* **2005**, *109*, 169; (c) Torchilin, V. P. *J. Controlled Release* **2001**, *73*, 137; (d) Shuai, X.; Ai, H.; Nasongkla, N.; Kim, S.; Gao, J. *J. Controlled Release* **2004**, *98*, 415; (e) Gao, Z.; Lukyanov, A. N.; Singhal, A.; Torchilin, V. P. *Nano Lett.* **2002**, *2*, 979; (f) Wang, Y. L.; Banziger, J.; Dubin, P. L.; Filippelli, G.; Nuraje, N. *Environ. Sci. Technol.* **2001**, *35*, 2608.

[1.16] Evans, D. F.; Wennerstrom, H. *The Colloidal Domain*, 2nd ed.;Wiley-VCH: New York, 1999.

[1.17] Basu, S.; Vutukuri, D. R.; Shyamroy, S.; Sandanaraj, B. S.; Thayumanavan, S. *J. Am. Chem. Soc.* **2004**, *126*, 9890.

[1.18] (a) Wright, A. T.; Anslyn, E. V. *Chem. Soc. Rev.* **2006**, *35*, 14; (b) Zhou, H.; Baldini, L.; Hong, J.; Wilson, A. J.; Hamilton, A. D. *J. Am. Chem. Soc.* **2006**, *128*, 2421; (c) Zadmard, R.; Schrader, T. *J. Am. Chem. Soc.* **2005**, *127*, 904; (d) Kolusheva, S.; Zadmard, R.; Schrader, T.; Jelinek, R. *J. Am. Chem. Soc.* **2006**, *128*, 13592; (e) Zhang, C.; Suslick, K. S. *J. Agric. Food Chem.* **2007**, *55*, 237; (f) You, C. C.; Miranda, O. R.; Gider, B.; Ghosh, P. S.; Kim, I. B.; Erdogan, B.; Krovi, S. A.; Bunz, U. H. F.; Rotello, V. M. *Nat. Nanotechnol.* **2007**, *2*, 318.

[1.19] (a) Grandini, P.; Mancin, F.; Tecilla, P.; Scrimin, P.; Tonellato, U. *Angew. Chem., Int. Ed.* **1999**, *38*, 3061; (b) Berton, M.; Mancin, F.; Stocchero, G.; Tecilla, P.; Tonellato, U. *Langmuir* **2001**, *17*, 7521.

[1.20] (a) Sandanaraj, B. S.; Demont, R.; Thayumanavan, S. *J. Am. Chem. Soc.* **2007**, *129*, 3506; (b) Savariar, E. N.; Ghosh, S.; Daniella Gonzalez, C.; Thayumanavan, S. *J. Am. Chem. Soc.* **2005**, *127*, 13200; (c) Basu, S.; Vutukuri, D. R.; Thayumanavan, S. *J. Am. Chem. Soc.* **2005**, *127*, 16794; (d) Sandanaraj, B. S.; Simard, J.; Vutukuri, D. R.; Hong, R.; Rotello, V. M.; Thayumanavan, S. *J. Am. Chem. Soc.* **2005**, *127*, 10693.

[1.21] Kong, L.; Cao, M.; Hai, M. *J. Chem. Eng. Data* **2007**, *52*, 721.

[1.22] Roy, R.; Sandanaraj, B. S.; Klaikherd, A.; Thayumanavan, S. *Langmuir* **2006**, *22*, 7695.

[1.23] (a) Kodadek, T. *Chem. Biol.* **2001**, *8*, 105; (b) Wang, D.; Gong, X.; Heeger, P. S.; Rininsland, F.; Bazan, G. C.; Heeger, A. J. *Proc. Natl. Acad. Sci. U. S. A.* **2002**, *99*, 49; (c) Pinto, M. R; Schanze, K. S. *Proc. Natl. Acad. Sci. U.S.A.* **2004**, *101*, 7505.

[1.24] (a) Kim, S. K.; Lee, D. H.; Hong, J.-I.; Yoon, J. *Acc. Chem. Res.* **2009**, *42*, 23; (b) Lee, D. H.; Kim, S. Y.; Hong, J. I. *Angew. Chem., Int. Ed.* **2004**, *43*, 4777; (c) Lee, D. H.; Im, J. H.; Son, S. U.; Chung, Y. K.; Hong, J. I. *J. Am. Chem. Soc.* **2003**, *125*, 7752; (d) Ojida, A.; Miyahara, Y.; Wongkongkatep, J.; Tamaru, S.; Sada, K.; Hamachi, I. *Chem. Asian J.* **2006**, *1*, 555.

[1.25] (a) Wright, A. T.; Zhong, Z.; Anslyn, E. V. *Angew. Chem., Int. Ed.* **2005**, *44*, 5679; (b) Wang, S.; Chang, Y. T. *Chem. Comm.* **2008**, 1173.

[1.26] (a) Lavigne, J. J.; Anslyn, E. V. *Angew. Chem., Int. Ed.* **2001**, *40*, 3119 (b) Chen, N.; Huang, Y.; Yang, L.; Liu, R.; Yang, J. J. *Chem. Eur. J.* **2009**, *15*, 9311; (c) Honda, K.; Fujishima, S.; Ojida, A.; Hamachi, I. *ChemBioChem.* **2007**, *8*, 1370; (d) Suzuki, Y.; Yokoyama, K. *Angew. Chem., Int. Ed.* **2007**, *46*, 4097.

[1.27] (a) Aoki, S.; Zulkefeli, M.; Shiro, M.; Kohsako, M.; Takeda, K.; Kimura, E. *J. Am. Chem. Soc.* **2005**, *127*, 9129; (b) Oh, D. J.; Ahn, K. H. *Org. Lett.* **2008**, *10*, 3539; (c) Anslyn, E. V.; Shear, J. B. H. *Chem. Biol.* **2002**, *9*, 779.

[1.28] Prentø, P. *Biotech. Histochem.* **2001**, *76*, 137.

[1.29] (a) Jin, L. T.; Choi, J.-K. *Electrophoresis* **2004**, *25*, 2429; (b) Herr, A. E.; Singh, A. K. *Anal. Chem.* **2004**, *76*, 4727; (c) Giordano, B. C.; Jin, L.; Couch, A. J.; Ferrance, J. P.; Landers, J. P. *Anal. Chem.* **2004**, *76*, 4705.

[1.30] Horowitz, P. M.; Bowman, S. *Anal. Biochem.* **1987***, 165,* 430.

[1.31] Daban, J. R.; Bartolome, S.; Samso, M. *Anal. Biochem.* **1991**, *199*, 169.

[1.32] (a) Berggren, K.; Chernokalskya, E.; Steinberg, T. H.; Kemper, C.; Lopez, M. F.; Diwu, Z.; Haugland, R. P.; Patton, W. F. *Electrophoresis* **2000**, *21*, 2509; (b) Steinberg, T. H.; Jones, L. J.; Haugland, R. P.; Singer, V. L. *Anal. Biochem.* **1996**, *239*, 223.

[1.33] Zeng, L.; Wu, J.; Dai, Q.; Liu, W.; Wang, P.; Lee, C. S. *Org. Lett.* **2010,** *12*, 4014.

[1.34] (a) Peng, L.; Zhang, G.; Zhang, D.; Xiang, J.; Zhao, R.; Wang, Y.; Zhu, D. *Org. Lett.* **2009**, *11*, 4014; (b) Peng, L.; Wang, M.; Zhang, G.; Zhang, D.; Zhu, D. *Org. Lett.* **2009**, *11*, 1973; (c) Zeng, L.; Wang, P.; Zhang, H.; Zhuang, X.; Dai, Q.; Liu, W. *Org. Lett.* **2009**, *11*, 4294.

[1.35] (a) Thornton, J. M.; Orengo, C. A.; Todd, A. E.; Pearl, F. M. *J. Mol. Biol.* **1999**, *2*, 333; (b) Ohnishi, S.; Takano, K. *Cell. Mol. Life. Sci.* **2004**, *61*, 511; (c) Dobson, C. M. *Semin. Cell. Dev. Biol.* **2004**, *1*, 3.

[1.36] (a) Kihara, M.; Chatani, E.; Sakai, M.; Hasegawa, K.; Naiki, H.; Goto, Y. *J. Biol. Chem.* **2005**, *280*, 12012. (b) Bieschke, J.; Zhang, Q.; Bosco, D. A.; Lerner, R. A.; Powers, E. T.; Wentworth, P.; Kelly, J. W. *Acc. Chem. Res.* **2006**, *39*, 611.

[1.37] Klein, K. L. *Neurochem. Int.* **2002**, *41*, 345.

[1.38] Lesne, S.; Koh, M. T.; Kotilinek, L.; Kayed, R.; Glabe, C. G.; Yang, A.; Gallagher, M.; Ashe, K. H. *Nature* **2006**, *440*, 352.

[1.39] Takahashi, T.; Mihara, H. *Acc. Chem. Res.* **2008**, *41*, 1309.

[1.40] Rochet, J. C.; Lansbury, P. T. *Curr. Opin. Struct. Biol.* **2000**, *10*, 60.

[1.41] Johnson, S. M.; Wiseman, R. L.; Sekijima, Y.; Green, N. S.; Adamski-Werner, S. L.; Kelly, J. W. *Acc. Chem. Res.* **2005,** *38,* 911.

[1.42] Hammarstrom, P.; Wiseman, R. L.; Powers, E. T.; Kelly, J. W. *Science* **2003**, *299*, 713.

[1.43] (a) Rochet, J. C. *Exp. Rev. Mol. Med.* **2007**, *9*, 1; (b) May, B. C.; Govaerts, C.; Cohen, F. E. *Neurology* **2006**, *66*, 118; (c) Loo, T. W.; Clarke, D. M. *Exp. Rev. Mol. Med.* **2007** *9*, 1; (d) Papp, E.; Csermely, P. *Handb Exp. Pharmacol.* **2006**, *172,* 405.

[1.44] (a) Marcinowski, K. J.; Shao, H.; Clancy, E. L.; Zagorski, M. G. *J. Am. Chem. Soc*. **1998**, *120*, 11082; (b) Montserret, R.; McLeish, M. J.; Böckmann, A.; Geourjon, C.; Penin, F. *Biochemistry* **2000**, *39*, 8362; (c) Xiong, L. W.; Raymond, L. D.; Hayes, S. F.; Raymond, G. J.; Caughey, B. *J. Neurochem.* **2001**, *79*, 669; (d) Pertinhez, T. A.; Bouchard, M.; Smith, R. A. G.; Dobson, C. M.; Smith, L. J. *FEBS Lett.* **2002**, *529*, 193; (e) Kuroda, Y.; Maeda, Y.; Sawa, S.; Shibata, K.; Miyamoto, K.; Nakagawa, T. *J. Pept. Sci*. **2003**, *9*, 212.

[1.45] Sabate, R.; Estelrich, J. *Langmuir* **2005,** *21,* 6944.

Chapter 2

Experimental Section

2.1. Introduction

A comprehensive account of the materials used in synthesis of compounds and the relevant particulars of instruments/equipments used for their characterization has been provided in this chapter.

2.2. Materials

All the chemicals and solvents used for the present work were for analytical grade quality and were used without purification unless otherwise specified. 5-aminonaphthalen-1-ol, 8-hydroxyquinoline, alkyl halides, congo red (CR) and thioflavin T (ThT) were purchased from Sigma, USA while diethyl malonate, malonic acid, tryptophan were from Merck, India and used as received. Bovine serum albumin (BSA) (Fluka and Sigma), α-amylase (from hog pancreas, Fluka), amiloglucosidase (AMG) (from *Aspergillus niger*, Fluka), Proteinase K, Hen egg white lysozyme (HEWL) (Sigma, USA), DNA isolation kit (Sigma, USA) and *Taq* DNA polymerase (Sibenzyme, Novosibirsk, Russia) were used as received. All the solvents used for spectroscopic studies were of spectroscopy grade and the water used in different experiments is Ultrapure water (Milli-Q system, Millipore, USA).

2.3. Synthetic Procedures

2.3.1. Synthesis of 5-(Alkoxy)naphthalene-1-amine (1-3)

5-(alkoxy)naphthalene-1-amine were prepared following the literature method (Scheme 2.1).[2.1] To a solution of 5-aminonaphthalen-1-ol (1 mol) in dry *n*-propanol crushed sodium hydroxide (5 mol) was added. The reaction mixture was stirred for 1 h at RT followed by the addition of corresponding alkyl halide (1.2 mol). The mixture was refluxed for another 6 h, followed by work up to isolate the product. The products thus obtained were re-crystallized from ethanol and finally characterized by NMR, IR and melting point (Appendix).

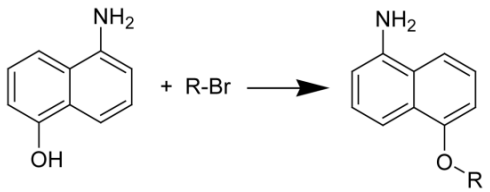

Where, R= C_8H_{17} (**1**), $C_{12}H_{25}$ (**2**) and $C_{16}H_{33}$ (**3**)

Scheme 2.1. Synthesis of compounds (**1**-**3**).

2.3.2. Synthesis of N-methyl-8-(alkoxy)quinolinium iodide (4-6)

At first 8-(alkoxy)quinoline were prepared following the literature method (Scheme 2.2) [2.2] followed by N-alkylation to get the desired product. To a solution of 8-hydroxyquinoline (1 equivalent) in dry *n*-propanol crushed sodium hydroxide (5 equivalents) was added. The reaction mixture was stirred for 1 h at RT followed by the addition of corresponding alkyl halide (1.2 equivalents). In order to complete the reaction, the mixture was refluxed for another 6 h, followed by work up using ethyl acetate and water to obtain 8-(alkoxy)quinoline. To a solution of 8-(alkoxy)quinoline (1 equivalent) in dry acetonitrile methyl iodide (1.2 equivalent) was added and refluxed for 6 h to get N-methyl-8-(alkoxy)quinolinium iodide. The products (Scheme 2.2) thus obtained were re-crystallized from methanol and finally characterized by NMR, IR and melting point (Appendix).

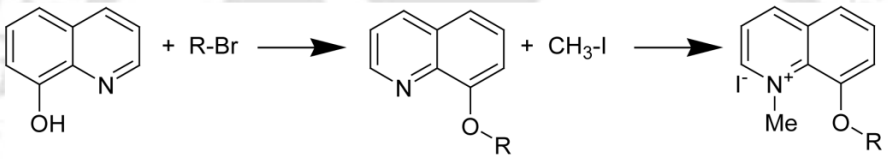

Where, R= C_4H_9 (**4**), C_8H_{17} (**5**) and $C_{12}H_{25}$ (**6**)

Scheme 2.2. Synthesis of compounds (**4-6**).

2.3.3. Synthesis of 2-(alkyl)malonic acid (7-9)

Compounds were prepared following the literature method as shown in scheme 2.3.[2.3,2.4] One equivalent of diethylmalonate was dissolved in dry acetonitrile followed by the addition of ten equivalent of potassium carbonate and refluxed for about 45 minutes at 80 ^{o}C. After that the solution was cooled and corresponding alkyl halide (1.2 equivalents) was added followed by reflux at 80 ^{o}C for about 20 h. The warm solution was filtered and acetonitrile was removed on rotavapour, followed by work up using ethyl acetate and water to get the 2-(alkyl)diethylmalonate. Finally, 2-(alkyl)diethylmalonate was treated with potassium hydroxide solution of water: ethanol mixture to obtain 2-(alkyl)malonic acid in refluxing conditions for around 6 hrs. Ethanol was distilled from the reaction mixture as much as possible and the residue was dissolved in small amount of water. The solution was cooled in a large ice containing beaker and then dilute sulfuric acid was added slowly with vigorous stirring until the solution is acidic to litmus paper. The obtained precipitate was filtered, washed with little amount of water and dried in vacuum

desicator to get the compound. The products obtained were re-crystallized from methanol and characterized by NMR, IR and melting point (Appendix).

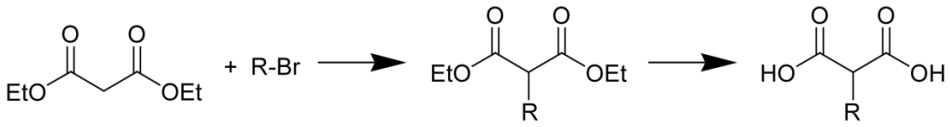

Where, R= C_8H_{17} (**7**), $C_{12}H_{25}$ (**8**) and $C_{16}H_{33}$ (**9**)

Scheme 2.3. Synthesis of compounds (**7-9**).

2.4. Particulars of Instruments/Equipments Used for Different Types of Studies

2.4.1. Melting Point Measurement

Melting points of compounds were recorded using a Type B-540 Buchi melting point apparatus. The heating rate was maintained at either 5 ^oC or 10 ^oC.

2.4.2. Infrared Spectra (IR)

IR spectra of compounds were recorded at 4 cm^{-1} resolution with 5 or 10 scan using a Perkin Elmer-Spectrum One FT-IR spectrometer from 4000 to 450 cm^{-1}. A background spectrum was measured for pure KBr.

2.4.3. ^1H and ^{13}C NMR (Nuclear Magnetic Resonance) Spectra

^1H and ^{13}C NMR spectra were recorded on a Varian 400 MHz spectrometers using tetramethylsilane (TMS) as internal standard.

2.4.4. pH measurement

pH values of different solutions were recorded or adjusted with a Systronics Type 355 and VSI-01 digital pH meter.

2.4.5. Absorption Spectra

UV-visible spectra were recorded, on a Hitachi UV-visible U-2001 spectrophotometer or on a Perkin Elmer Lambda 25 UV-visible spectrophotometer using 10 mm path length quartz cuvettes at room temperature.

2.4.6. Fluorescence Spectra

The steady state fluorescence spectra of different samples were recorded on a Varian Cary-Bio spectrofluorimeter or Jobin-Yvon Fluoromax-4 or FSP-920 spectrofluorimeter (Edinburgh instrument) using 10 mm path length quartz cuvettes.

2.4.7. Time-resolved Fluorescence Spectra

Time-resolved intensity decays of different samples were measured using a Life Spec II spectrofluorimeter (Edinburgh instrument). The decay curves were analyzed by FAST software using discrete exponential method, provided by Edinburgh instrument along with the fluorescence instrument. The generated curves for intensity decay were fitted in the functions of equation 2.1.

$$I(t) = \sum_i \alpha_i \exp(\frac{-t}{\tau_i}) \qquad (2.1)$$

Where, τ_i is the initial intensity of the decay component i, having a lifetime α_i. The mean lifetime (τ_m) of samples under different experimental condition was calculated following the equation 2.2.[2.5]

$$\tau_m = \frac{\sum_i \alpha_i \tau_i}{\sum_i \alpha_i} \qquad (2.2)$$

2.4.8. Steady State Anisotropy Measurement

Steady state fluorescence anisotropy of different samples was recorded on a FSP-920 spectrofluorimeter (Edinburgh instrument). Steady state anisotropy (r) was defined by equation 2.3, where I_{VV} and I_{VH} are the intensities obtained with the excitation polarizer orientated vertically, and the emission polarizer oriented vertically and horizontally, respectively, where, the G factor is defined as sown in equation 2.4,

$$r = \frac{I_{VV} - GI_{VH}}{I_{VV} + 2GI_{VH}} \qquad (2.3)$$

$$G = \frac{I_{HV}}{I_{HH}} \qquad (2.4)$$

2.4.9. Time Resolved Anisotropy Measurement

Time-resolved anisotropy decays of different samples were measured using a Life Spec II spectrofluorimeter (Edinburgh instrument). The decay curves were analyzed by FAST

software using discrete exponential method. The calculated time-resolved anisotropy was represented by the following function of equation[2.6]

$$r(t) = \beta_r \exp\left(\frac{-t}{\tau_r}\right) \qquad (2.5)$$

The fitting parameters β_r and τ_r are the amplitudes and correlation times for the exponential terms involved in the deconvoluted time-resolved anisotropy function.

2.4.10. Scanning Electron Microscope (SEM)

Scanning electron micrograph (SEM) images of samples glued on an aluminum stub and gold sputtered were obtained by means of a LEO-1430 VP electron microscope.

2.4.11. Atomic Force Microscope (AFM)

AFM imaging of different samples were taken on Picoplus microscope (Molecular Imaging, USA) under non contact or MAC MODE.

2.4.12. Calculation of Quantum Yield (Φ)

For quantum yield calculation, 2-aminopyridine (Φ = 0.6) in 0.1 N H_2SO_4 was used as the standard. The quantum yields of fluorescence were calculated using the equation 2.6.[2.7]

$$\Phi_u = \frac{A_s F_u n_u^2}{A_u F_s n_s^2} \Phi_s \qquad (2.6)$$

Where, Φ_s and Φ_u are the fluorescence quantum yields, F_s and F_u are the integrated fluorescence area and A_s and A_u are the absorbance of the standard and unknown compound respectively, while n_s and n_u are the refractive indices of the solvents used for the standard and unknown.

2.4.13. Calculation of Association Constant (K_a)

The intrinsic binding constant (K_a) was determined from the half reciprocal plot of [BSA]/$\Delta\varepsilon_{ap}$ vs. [BSA], where $\Delta\varepsilon_{ap} = [\varepsilon_a - \varepsilon_f]$ and $\Delta\varepsilon = [\varepsilon_b - \varepsilon_f]$. The apparent extinction coefficient, ε_a, is obtained by calculating $A_{[obsd]}$/[compound]. ε_b and ε_f correspond to the extinction coefficient of bound form of compound and free compound respectively. The data were fitted to equation 2.7 with a slope equal to $1/\Delta\varepsilon$ and a y-intercept equal to $1/\Delta\varepsilon K_a$. ε_b was determined from $\Delta\varepsilon$, and K_a was obtained from the ratio of the slope to the y-intercept.[2.8]

$$\frac{[BSA]}{\Delta\varepsilon_{app}} = \frac{[BSA]}{\Delta\varepsilon} + \frac{1}{\Delta\varepsilon K_a} \qquad (2.7)$$

2.4.14. Calculation of Change in Free Energy (ΔG)

Change in free energy (ΔG) associated with the complexation between compound and BSA, was determined using the equation 2.8,[2.9]

$$\Delta G = -2.303RT\log K_a \qquad (2.8)$$

2.4.15. Calculation of Non-radiative Decay Rate Constant (k_{nr})

In order to calculate the non-radiative decay rate constant (k_{nr}), the equation 2.9 was used,[2.10]

$$k_{nr} = k_r\left[\frac{1}{\Phi} - 1\right] \qquad (2.9)$$

Where, k_r is radiative decay rate constant, Φ = fluorescence quantum yield of compound. Radiative decay rate constant k_r can be determined using the equation 2.10,

$$k_r = \frac{\Phi_f}{\tau_f} \qquad (2.10)$$

Where, τ_f is lifetime of compound and Φ_f is fluorescence quantum yield of the compound.

References

[2.1] Ward Jr. K.; *J. Am. Chem. Soc*. **1935**, *57*, 914.

[2.2] Andree, L.; Jean, S.; Farchid, V. Z. *Bull. Soc. Chim. Fr.* **1987**, *6*, 1027

[2.3] Aggett, J.; Timperley, M. H. *Anal. Chim. Acta* **1969**, *47*, 551.

[2.4] Nokami, J.; Yamamoto, T.; Kawada, M.; Izumi, M.; Ochi, N.; Okawara, R. *Tetrahedron Lett.* **1979**, *12*, 1047.

[2.5] Swaminathan, R.; Krishnamoorthy, G.; Periasamy, N. *Biophys. J.* **1994**, *67*, 2013.

[2.6] Chen, J.; Toptygin, D.; Brand L.; King, J. *Biochemistry* **2008**, *47*, 10705.

[2.7] Eaton, D. F. *Pure & Appl. Chem.* **1988**, *60*, 1107.

[2.8] Urien, S.; Nguyen, P.; Berlioz, S.; Bree, F.; Vacherot F.; Tillement, J. *Biochem. J.* **1994**, *302*, 69.

[2.9] Wolfe, A.; Shimer, G. H.; Meehan, T. *Biochemistry* **1987**, *26*, 6392.

[2.10] Kamat, P. V.; Das, S.; Thomas, K. G.; George, M. V. *J. Phys. Chem.* **1992**, *96*, 195.

APPENDIX

A2.1 Characterization Data of Compounds

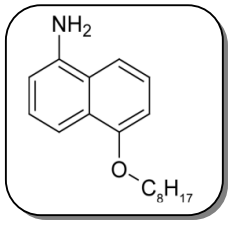

Compound 1 [5-(octyloxy)naphthalene-1-amine]: IR (KBr): 3434-3100, 2919, 1724 cm^{-1}; ^1H NMR (400 MHz, $CDCl_3$): δ 0.89 (t, *J* = 6, 3H), 1.36 (m, 10 H), 1.92 (m, 2H), 4.11 (t, *J* = 6.4, 2H), 6.81 (m, ArH), 7.27 (m, ArH), 7.36 (m, ArH), 7.73 (m, ArH) (Fig. A2.1). ^{13}C NMR (100 MHz, $CDCl_3$): δ 14.3, 22.9, 26.5, 29.5, 68.4, 104.9, 110.6, 113.2, 124.8, 141.9 and 155.5 (Fig. A2.1). Deep brown viscous liquid at RT.

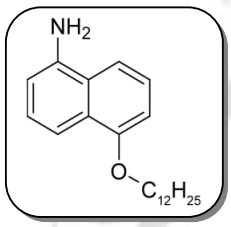

Compound 2 [5-(dodecyloxy)naphthalene-1-amine]: IR (KBr): 3410-3100, 2900, 1720 cm^{-1}; ^1H NMR (400 MHz, $CDCl_3$): δ 0.86 (t, *J* = 6.1, 3H), 1.36 (m, 18H), 1.89 (t, *J* = 6.8, 2H), 4.11 (t, *J* = 6.2 2H), 6.81 (m, ArH), 7.28 (m, ArH), 7.34 (m, ArH), 7.77 (m, ArH) (Fig. A2.2). ^{13}C NMR (100 MHz, $CDCl_3$): δ 14.3, 23.9, 27.0, 30.2, 68.3, 105.2, 112.3, 115.5, 125.3, 142.4 and 156.9 (Fig. A2.2). Deep brown semi solid at RT

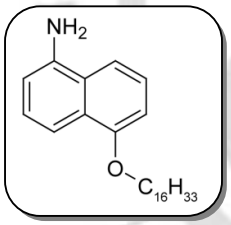

Compound 3 [5-(hexadecyloxy)naphthalene-1-amine]: IR (KBr): 3436-3100, 2922, 1721 cm^{-1}; ^1H NMR (400 MHz, $CDCl_3$): δ 0.81 (t, *J* = 6.4, 3H), 1.19 (m, 30 H), 1.84 (t, *J* = 6.8, 1H), 4.04 (t, *J* = 6.4, 2H), 6.81 (m, ArH), 7.21 (m, ArH), 7.32 (m, ArH), 7.74 (m, ArH) (Fig. A2.3). ^{13}C NMR (100 MHz, $CDCl_3$): δ 14.6, 23.9, 28.6, 30.3, 67.9, 106.3, 113.2, 115.9, 126.5, 143.3 and 155.3 (Fig. A2.3). Light brown solid, Melting point: 58 ^oC.

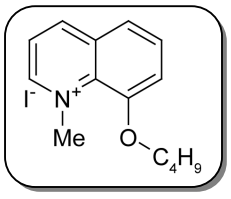

Compound 4 [N-methyl-8-(butoxy)quinolinium iodide]: IR (KBr): 2921, 1597, 1533, 1467 cm^{-1}; ^1H NMR (400 MHz, $CDCl_3$): δ 1.01 (t, *J* = 7.2, 3H), 1.51 (m, 2H), 1.95 (m, 2H), 4.23 (t, 2H), 5.06 (s, 3H), 7.47 (d, ArH), 7.79 (m, ArH), 8.09 (m, ArH), 8.89(m, ArH), 10.15 (d, ArH) (Fig. A2.4). ^{13}C NMR (100 MHz, $CDCl_3$): δ 13.8, 19.6, 30.9, 53.5, 70.9, 109.9, 116.7, 122.4, 122.7, 130.5, 130.9, 130.14, 147.5, 151.0 and 152.1 (Fig. A2.4). Light brown solid, Melting point 163 ^oC.

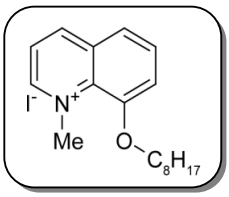

Compound 5 [N-methyl-8-(octyloxy)quinolinium iodide]: IR (KBr): 2925, 1599, 1530, 1465 cm^{-1}; ^1H NMR (400 MHz, $CDCl_3$): δ 0.90 (t, *J* = 6.8, 3H), 1.31 (m, 8H), 1.53 (m, 2H), 1.99 (m, 2H), 4.25 (t, *J* = 6.8, 2H), 5.09 (s, 3H), 7.49 (d, ArH), 7.81 (m, ArH), 8.13 (m, ArH), 8.92 (m, ArH), 10.19 (d, ArH) (Fig. A2.5). ^{13}C NMR (100 MHz, $CDCl_3$): δ 14.2, 22.7, 26.4, 29.0, 29.3, 29.4, 31.9, 53.1, 71.2, 116.5, 122.4, 122.9, 130.9, 132.2, 147.4, 151.2 and 152.4 (Fig. A2.5). Light brown solid, Melting point 117 ^oC.

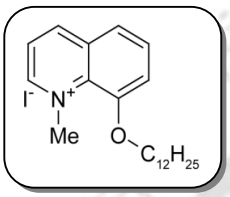

Compound 6 [N-methyl-8-(doecyloxy)quinolinium iodide]: IR (KBr): 2930, 1595, 1535, 1470 cm^{-1}; ^1H NMR (400 MHz, $CDCl_3$): δ 0.88 (t, *J* = 7.2, 3H), 1.27 (m, 16H), 1.53 (m, 2H), 2.00 (m, 2H), 4.25 (t, *J* = 6.4, 2H), 5.09 (s, 3H), 7.50 (d, ArH), 7.82 (m, ArH), 8.13 (m, ArH), 8.96 (m, ArH), 10.19 (d, ArH) (Fig. A2.6). ^{13}C NMR (100 MHz, $CDCl_3$): δ 14.2, 22.8, 26.4, 29.0, 29.4, 29.5, 29.6, 29.7, 31.9, 53.1, 71.2, 116.6, 122.5, 122.9, 123.1, 130.9, 132.2, 147.5, 151.1 and 152.3 (Fig. A2.6). Light brown solid, Melting point 110 ^oC.

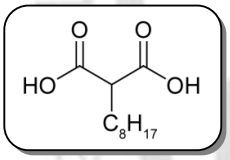

Compound 7 [2-(octyl)malonic acid]: IR (KBr): 3434-3100, 2919, 1724 cm^{-1}; ^1H NMR (400 MHz, CD_3OD): δ 0.926 (t, *J* = 6, 3H), 1.377 (m, 14 H), 1.852 (t, *J* = 6.8, 1H) (Fig. A2.7). ^{13}C NMR (100 MHz, CD_3OD): δ 14.637, 23.901, 27.901, 28.442, 30.233, 30.574, 33.184, 53.235 and 173.465 (Fig. A2.7). Colorless solid, m.p. 113 ^oC.

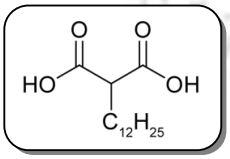

Compound 8 [2-(dodecyl)malonic acid]: IR (KBr): 3410-3100, 2900, 1720 cm^{-1}. ^1H NMR (400 MHz, CD_3OD): δ 0.85 (t, *J* = 6.1, 3H), 1.36 (m, 22 H), 1.83 (t, *J* = 6.8, 1H) (Fig. A2.8); ^{13}C NMR (100 MHz, CD_3OD): δ 14.6, 23.9, 28.7, 30.2, 30.5, 30.6, 33.2, 53.3 and 173.5 (Fig. A2.8). Colorless solid; m.p. 119 ^oC.

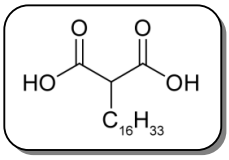

Compound 9 [2-(hexadecyl)malonic acid]: IR (KBr): 3436-3100, 2922, 1721 cm^{-1}; ^1H NMR (400 MHz, CD_3OD): δ 0.89 (t, *J* = 6.4, 3H), 1.32 (m, 30 H), 1.83 (t, *J* = 6.8, 1H) (Fig. A2.9). ^{13}C NMR (100 MHz, CD_3OD): δ 14.6, 23.9, 28.7, 30.3, 30.5, 30.6, 33.2, 53.3 and 173.5 (Fig. A2.9). Colorless solid, m.p. 121 ^oC.

A2.2 NMR Spectra of Compounds

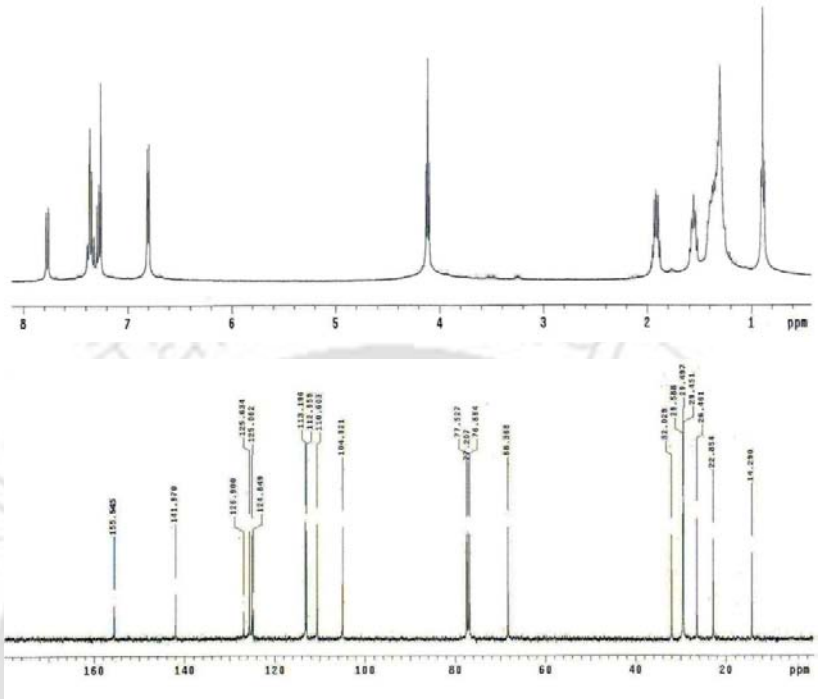

Figure A2.1. ^{1}H (top) and ^{13}C (bottom) NMR spectra of compound **1**.

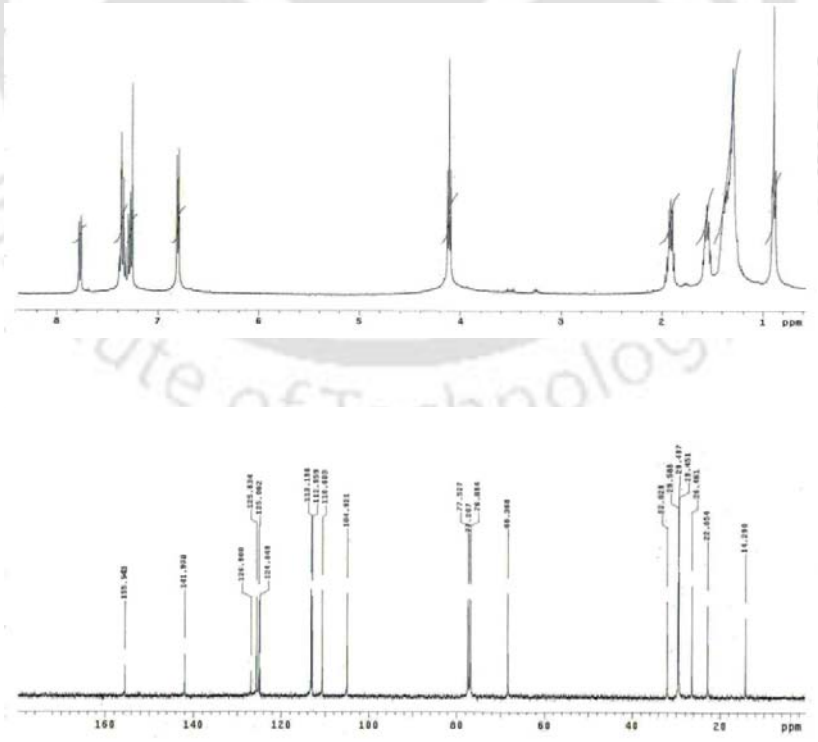

Figure A2.2. ^{1}H (top) and ^{13}C (bottom) NMR spectra of compound **2**.

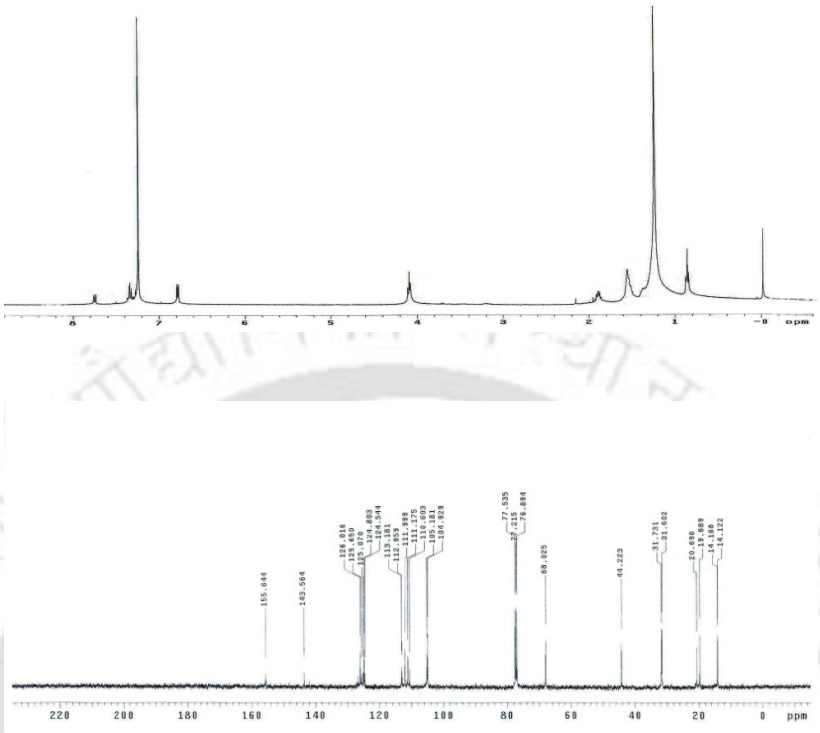

Figure A2.3. ^{1}H (top) and ^{13}C (bottom) NMR spectra of compound **3**.

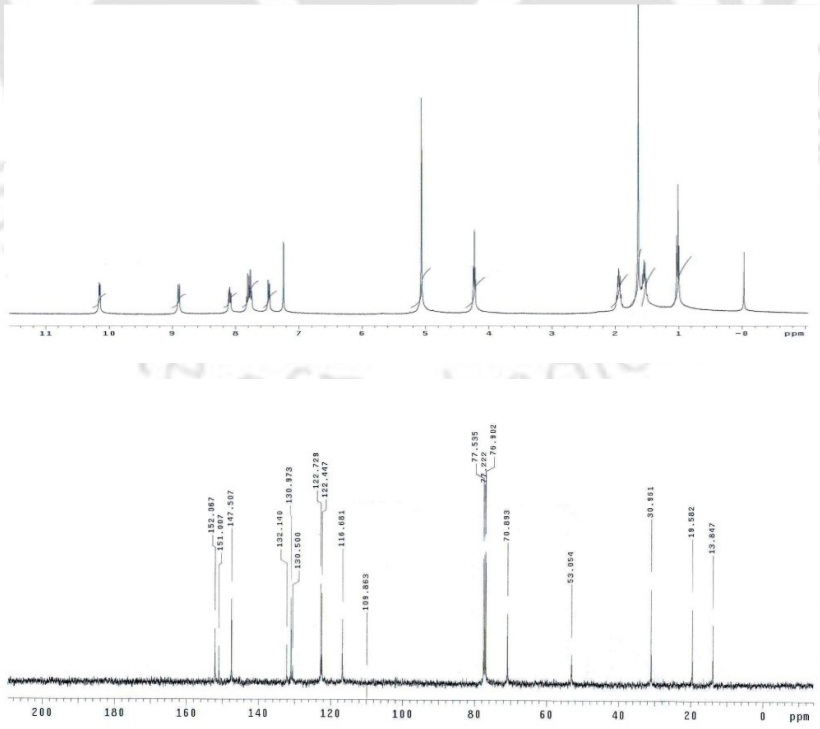

Figure A2.4. ^{1}H (top) and ^{13}C (bottom) NMR spectra of compound **4**.

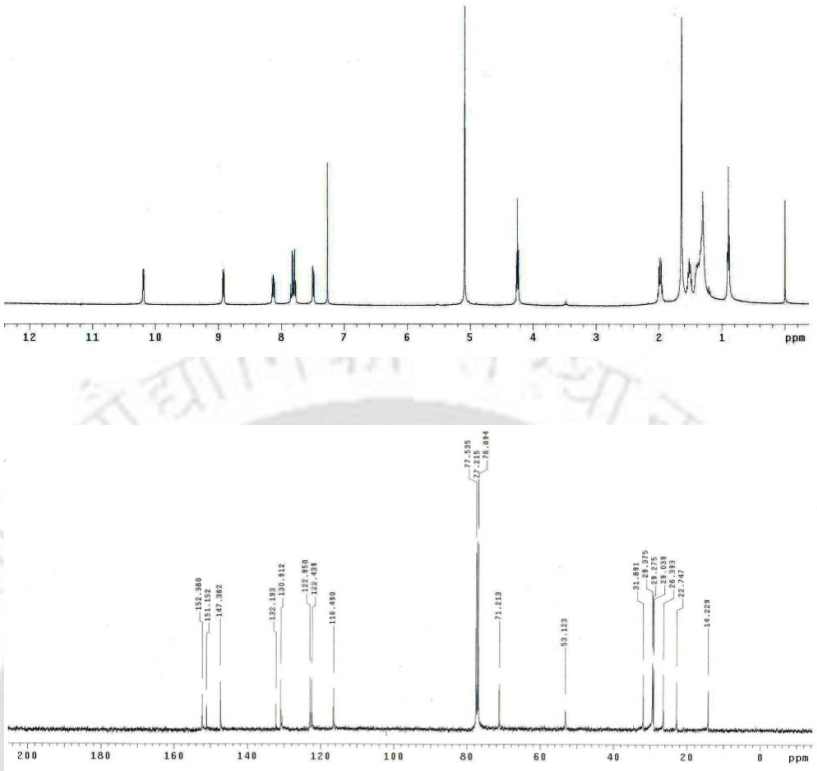

Figure A2.5. ^{1}H (top) and ^{13}C (bottom) NMR spectra of compound **5**.

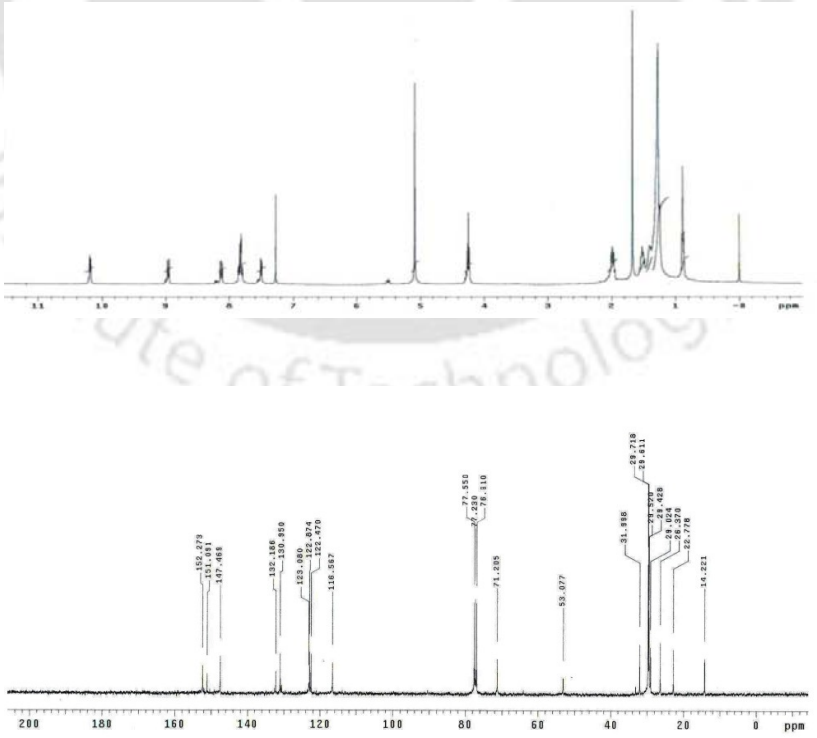

Figure A2.6. ^{1}H (top) and ^{13}C (bottom) NMR spectra of compound **6**.

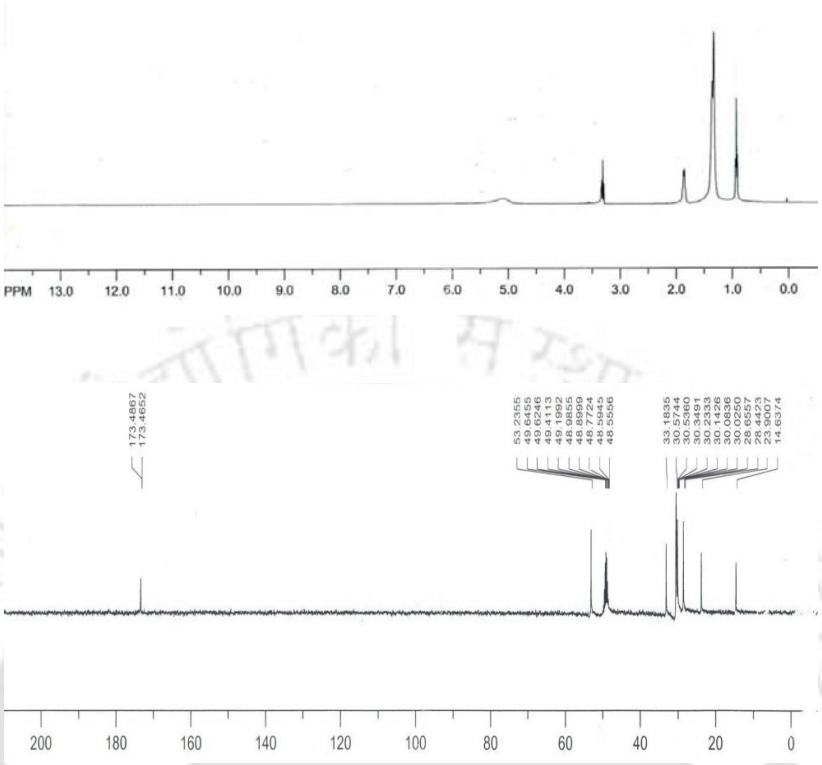

Figure A2.7. ^{1}H (top) and ^{13}C (bottom) NMR spectra of compound **7**.

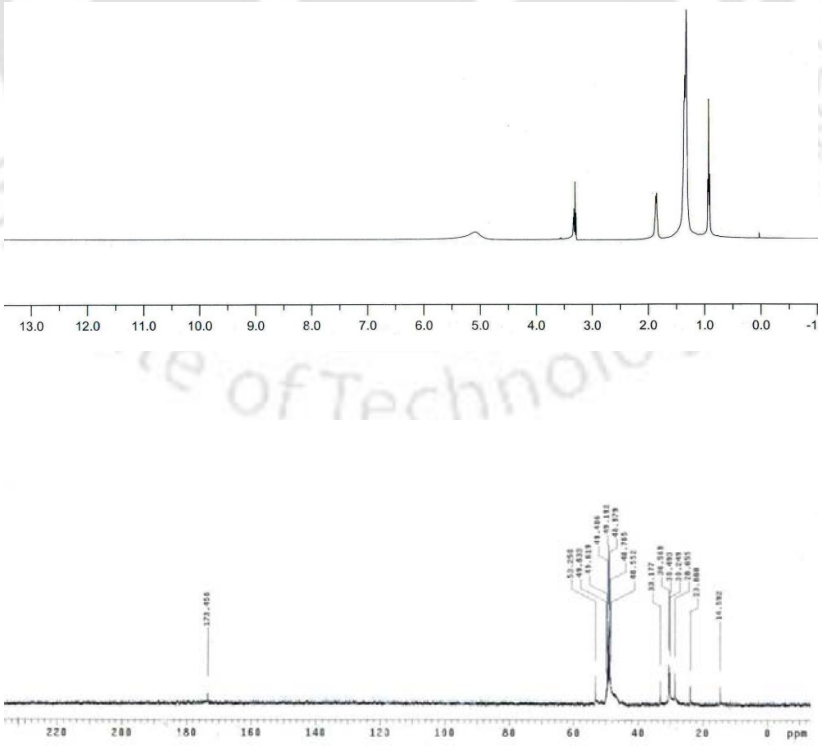

Figure A2.8. ^{1}H (top) and ^{13}C (bottom) NMR spectra of compound **8**.

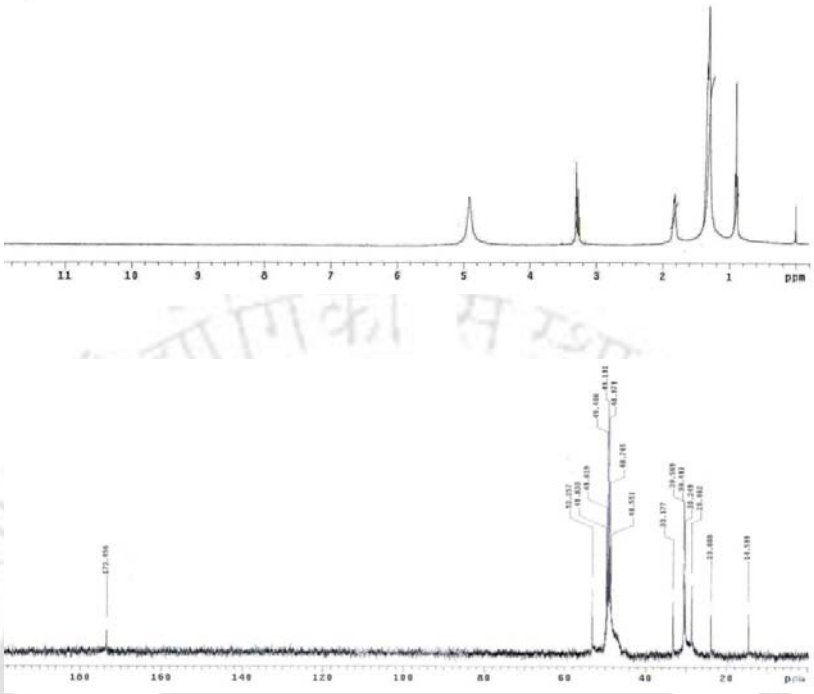

Figure A2.9. ^{1}H (top) and ^{13}C (bottom) NMR spectra of compound **9**.

Chapter 3

Interaction Between 5-(Alkoxy)-naphthalene-1-amine Amphiphile and Protein: A Photophysical Approach

Part I: Photophysical Response of 5-(Alkoxy)naphthalene-1-amine in Presence of Protein

3.1.1. Introduction

Design and development of new fluorescent probes for selective detection of biomolecules may have wide implications in many biological processes like proteomics, medical diagnostics, and pathogen detections.[3.1.1] Biochemists are searching for various ways to detect proteins with high sensitivity and good binding linearity to facilitate both qualitative and quantitative analysis. However, studies aimed at a better understanding of the origin of fluorescence properties of a given fluorophore, in particular the dependence on the environment, are scarcely addressed in the literature. Even less investigated is the mechanism of protein detection by light-up probes. Light-up probes, whose emission intensity increases upon association with biomolecules are useful markers in genomics and proteomics as the binding event to the host molecule may be followed by the appearance of an intense fluorescence emission of the probes.[3.1.2] These light up probes are mainly used for quantification of biomolecules and as stain in gel electrophoresis *viz.* 1-anilino-8-naphthalenesulfonate (1,8-ANS), Nile Red, or the Squaraine dye family (Fig. 3.1.1).[3.1.3] Especially in latter case, the discovery of novel efficient fluorescent probes which can selectively detect or bind one specific protein, are on serendipitous findings[3.1.4] and only few systematic strategies for the rational design of light-up probes or detailed analyses of structure-property relationships are published.[3.1.5]

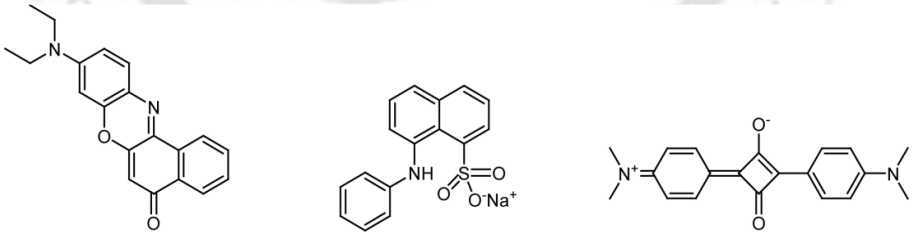

Figure 3.1.1. Structure of some light up probes used for the detection of biomolecules.

Serum albumins are the most widely studied proteins abundant in plasma. Many researchers have studied the structure and properties of serum albumins and their interactions with other proteins, drugs and bioactive small molecules in order to

understand the affect of serum albumin on the photophysical properties of guest molecules.[3.1.6] The specific delivery of ligands by serum albumin originates from the presence of two major and structurally selective binding sites, namely, site I and site II, which are located in three homologous domains that form a heart-shaped protein.[3.1.7] The binding affinity offered by site I is mainly through the hydrophobic interactions, whereas site II involves a combination of hydrophobic, hydrogen bonding, and electrostatic interactions (Fig. 3.1.2).[3.1.8] It has been reported earlier that the molecules possessing higher affinity towards serum albumin and showing preferential binding at site II, exhibits efficient photodynamic therapeutical applications (PDT).[3.1.9] Therefore, discovery of novel and efficient fluorescent probes for the selective binding of protein are on high demand.

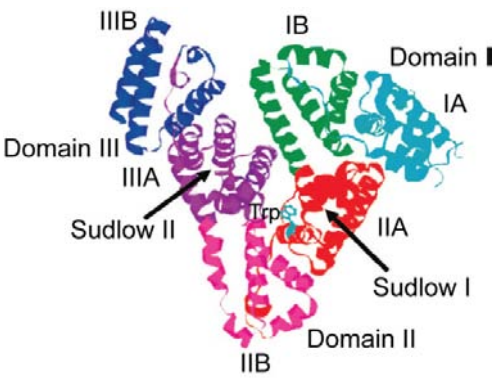

Figure 3.1.2. Crystal structure of HSA (human serum albumin) along with the locations of domain-binding sites. The structure was obtained from the Protein Data Bank (ID code 1ha2).

In this context, the 1st part of chapter 3 discusses about a simple and efficient amphiphilic fluorescent probes [5-(alkoxy)naphthalene-1-amine, (**1-3**) Fig. 3.1.3][2.1] for selective detection of bovine serum albumin (BSA) through non-covalent interactions when used at very low concentration (5 μM). These fluorescent probes possess very attractive photophysical properties, such as absorption in the near-UV region of the spectrum (λ_{max} ~320 nm), well separated from that of the tryptophan (Appendix, Fig. A3.1.1); low fluorescence quantum yield (Φ <0.012 in an aqueous solution) and a large Stokes shift ($\Delta\lambda$ ~10^5 cm^{-1}), allowing unambiguous detection without re-absorption effects and not interfering with background fluorescence of biomolecules. In order to generate the variation in structure and to study their sensing ability for protein, the alkyl chain of compounds has been varied as shown in figure 3.1.3.

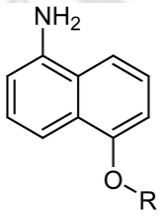

Where, R= C_8H_{17} (**1**), $C_{12}H_{25}$ (**2**) and $C_{16}H_{33}$ (**3**)

Figure 3.1.3. Structure of compounds (**1-3**).

3.1.2. Methods

In order to record the emission spectra of compounds under different experimental conditions, compounds were excited at 320 nm wavelength using slit width of 5 nm. Background intensities of the buffer blanks in which BSA omitted were subtracted from each sample spectrum to cancel out any contribution due to the solvent. The lifetime of the samples were measured using Pico-quant 342 nm LED (light emitting diode) light source while for anisotropy decay, the measurement was carried out using 375 nm lasers at room temperature. The decay curves were analyzed by FAST software using discrete exponential method, provided by Edinburgh instrument along with the fluorescence instrument.

A 1.0 mg/mL protein/enzyme solution was prepared by dissolving the protein/enzyme in the appropriate buffers. Phosphate buffer of pH 7.0 was used for α-amylase, BSA and AMG. As α-amylase was sparingly soluble in buffer solution, the resulted solution was stirred for 20 minutes, followed by centrifugation at 5000 rpm for 20 minutes to collect the supernatant for further analysis. The compound stock solutions were prepared in DMSO because of their poor solubility in water. For interaction study of compounds with protein, a 3.0 mL aqueous solution of compound (5.0 μM) was titrated with different concentrations of protein/enzyme (ranging from 0 to 275 μg/mL), where the total volume of DMSO did not exceed 5%. The presence of 5% DMSO induces no major structural changes to protein/enzyme. Each solution was mixed thoroughly before spectral measurements at room temperature.

3.1.3. Results and Discussion

3.1.3.1. Effect of BSA on Absorption Spectra of Compounds

Absorption and emission spectra of the compound **1** (Fig. 3.1.4A) shows a large Stokes shift of around 10^5 cm^{-1}. Addition of BSA led to decrease in the absorbance at 320 nm, due to the compound, with simultaneous increase in absorbance at 279 nm corresponding to the tryptophan chromophore in BSA forming an isosbestic point at around 290 nm (Fig. 3.1.4B). The decrease in the absorbance of compound suggests a strong interaction between the electronic states of the compound and tryptophan chromophore in BSA.[3.1.6] Since the strength of this electronic interaction is expected to decrease as the cube of the distance separated between compound and BSA, the marked hypochromism indicates a close proximity of compound to BSA.[3.1.10] Even at

low concentrations of BSA, a decrease in absorbance of the compound has been observed, which can be attributed due to the formation of a tight complex with BSA at site I, involving π-stacking and hydrophobic interactions. This interpretation is based on the facts that the site I has a relatively small cavity size of 2.53 Å and tryptophan (Trp-212)[3.1.7] is located only at site I. Half reciprocal analysis (Fig. 3.1.4B, inset) of the absorption data gave an association constant of 3.47 x 10^5 M^{-1} and change in free energy of -15.4 kJ/mol for the complex formation between compound **1** and BSA (Table 3.1.1) using equation 2.7 and 2.8 respectively (Chapter 2). Similar results were also obtained in case of compound **2** and **3** after addition of BSA (Appendix, Fig. A3.1.2).

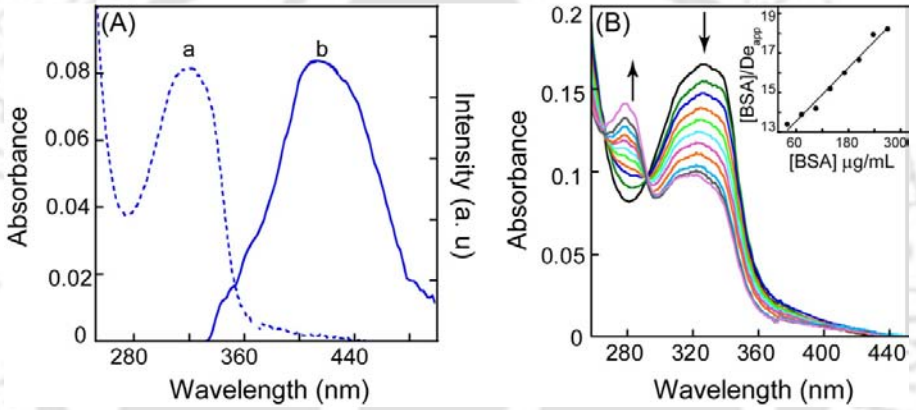

Figure 3.1.4. (A) Absorption (dotted line) and fluorescence (solid line) spectra of compound **1** and (B) Absorption spectra of compound **1** (5 µM) with increasing concentration of BSA (Inset: Half reciprocal plot) ranging from 0 to 275 µg/mL in an aqueous buffer of pH 7.0.

3.1.3.2. Effect of BSA on Intrinsic Fluorescence of Compounds

The compound itself had a very weak fluorescence in absence of protein (Fig. 3.1.4A). On the other hand, the fluorescence spectra of these probes showed a dramatic increase in fluorescence intensity after addition of BSA (Fig. 3.1.5), similar to that when compounds are dissolved in organic solvents (Fig. 3.1.6B), indicates encapsulation of the probe molecules inside the hydrophobic cavity of the protein. The increase in intensity further indicates towards the fact that as more and more binding of the probe to the protein occurs, the non-radiative channels generally present in aqueous solution become less operative.[3.1.11] It is found that the fluorescence quantum yields obtained using equation 2.6 (Chapter 2) in presence of BSA is much higher compared to that obtained in aqueous phase as shown in Table 3.1.1. Thus, the

funneling out of energy *via* non-radiative pathway decreases to a great extent when the probe remains encapsulated within the hydrophobic cavity of the protein. Gradual addition of BSA (from 0 to 275 µg/mL) to the aqueous buffered solution of compounds leads to a 40, 15 and 3-fold increase in fluorescence intensity of **1**, **2** and **3** respectively along with a hypsochromic shift in emission band (Fig. 3.1.5B). The responses of these probes to BSA revealed that compound **1** (C_8) with the smallest alkyl chain length is the most efficient probe, followed by **2** (C_{12}) and **3** (C_{16}) respectively (Fig. 3.1.6A), which can be rationalized in terms of either their decreasing solubility in an aqueous solution or the length of alkyl chain which is not accommodated on site I that prevents a strong interaction with BSA. Similar results were also observed in case of compound **2** and **3** after addition of BSA as shown (Appendix, Fig. A3.1.3) but less prounced in **2** and the least in **3**.

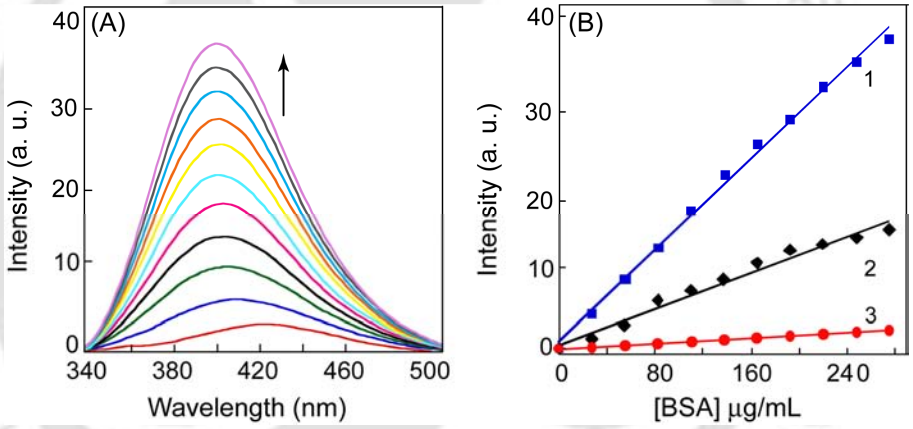

Figure 3.1.5. (A) Emission spectra of compound **1** with increasing concentration of BSA (0 to 275 µg/mL) in an aqueous buffer solution of pH 7.0 and (B) Variation in fluorescence intensity of compounds (**1-3**) as a function of BSA concentration.

However, no significant changes in probes fluorescence intensity as well as emission maxima peak position was observed after addition of same concentration of α-amylase, lysozyme, proteinase K or AMG (Appendix, Fig. A3.1.4 and 5). This difference in behavior of compound towards other proteins/enzymes presuambly reflects differences in their hydrophobic character,[3.1.12] particularly the lack of suitable hydrophobic 'clefts' in order to bind compounds in amylase, lysozyme, proteinase K and AMG. The conventional total protein detection exhibits various responses for different proteins. These differences are related to the amino acid sequence, pI, protein structure and the presence of certain side chains that can dramatically alter the proteins response and their

hydrophobicity. BSA appears to be the most 'hydrophobic' proteins among these proteins/enzymes used (Table 3.1.2) while amylase, lysozyme, proteinase K and AMG, are less 'hydrophobic' proteins and hence have lower binding affinity for the compounds.[3.1.13]

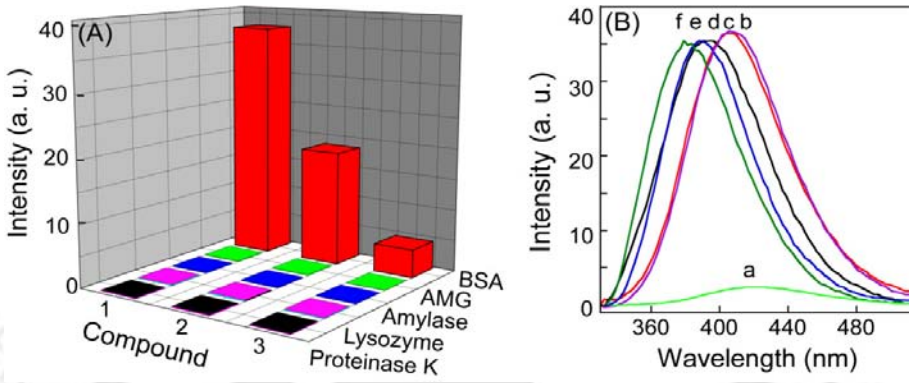

Figure 3.1.6. (A) Fluorescence emission response of compounds (**1**-**3**) toward different proteins/enzymes (275 µg/mL) and (B) Effect of different solvent on the emission spectra of the compound **1**; Where Trace a-f: water, DMSO, ethanol, THF, hexane and toluene.

To shed light on the molecular level interactions between compounds and BSA, it is also necessary to investigate the interactions of these compounds (**1-3**) with free tryptophan amino acid. So, in parallel the control experiments have been done to recognize whether some interactions occurred and to understand the nature of such interactions. However, no significant spectral changes of compounds with free tryptophan were observed (Fig. 3.1.7A and B). This behavior, along with the absorption change observed, indicates that the microenvironment created by the macromolecule induces some changes in the ground as well as in the excited-state of compounds. Control experiments also showed that the addition of BSA to the parent non-amphiphilic compound *i.e.* 5-aminonaphthalene-1-ol under similar experimental conditions does not produce any significant changes in its fluorescence spectral property, suggesting the introduction of an alkyl group (*i.e.* hydrophobicity) is responsible for interactions between amphiphilic compounds and protein.

3.1.2.3. Effect of BSA on Fluorescence Lifetime of Compounds

Fluorescence lifetimes also throw further light on the microenvironment surrounding the excited probe molecules in the proteinous media.[3.1.10,3.1.14] Nanosecond time-resolved fluorescence analysis (Fig. 3.1.8A) showed that the compound **1** alone

exhibits a mono-exponential decay with a lifetime (τ) of 0.25 ns, whereas bi-exponential decay with significantly increased lifetime of 1.21 and 6.11 ns was observed in presence of BSA (Table 3.1.1). On the basis of fluorescence quantum yield and life-time, the non-radiative decay rate constants (k_{nr}) were calculated using equation 2.9 (Chapter 2)[2.7] and found to be 3.95 x 10^9 and 1.29 x 10^8 s^{-1}, respectively for compound **1** alone and its corresponding BSA complex (Table 3.1.1). It is apparent from Table, that in protein environment, the k_{nr} decreased reasonably from that in the aqueous buffered medium. So, the enhancement in lifetimes of fluorophores in presence of BSA is attributed to the decreased non-radiative rates in the protein environment.[3.1.14a] These spectral changes were caused by a complex formation, in which the compound is strongly bound at hydrophobic pockets of the BSA supported by hydrophobic interactions. Similar results were obtained in case of compound **2** and **3** after addition of BSA but less pronounced in **2** and the least in **3** (Table 3.1.1). The lifetime data well matched with the trend, as observed in the case of fluorescence intensity change.

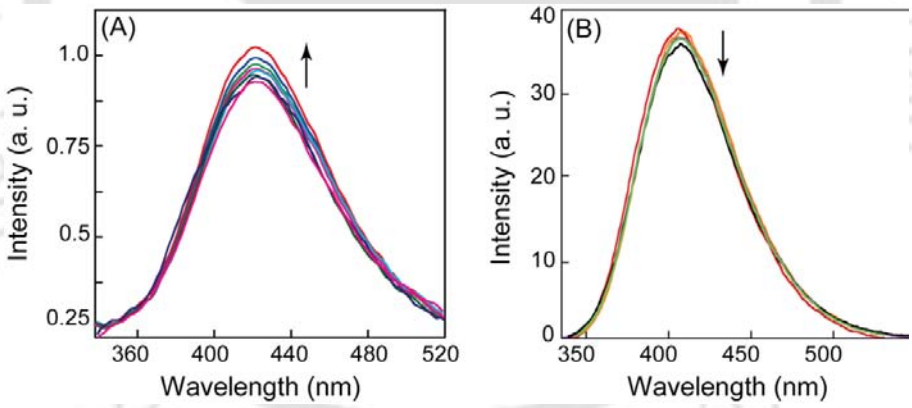

Figure 3.1.7. Emission spectra of (A) Compound **1** with increasing concentration of tryptophan (0 to 275 µg/mL) and (B) 5-aminonaphthalene-1-ol (the parent non-amphiphilic compound) with increasing concentration of BSA from 0 to 275 µg/mL in an aqueous buffer of pH 7.0.

3.1.3.4. Effect of BSA on Steady State Anisotropy of Compounds

As polarization (anisotropy) measurements can give details about an association or binding phenomenon, the technique has been employed to gather additional evidence in support of interactions of the probe with native albumin proteins. [3.1.14a,3.1.15] The restriction imposed on the mobility of the probe in a viscous or organized media can be accessed from the anisotropy values.[3.1.15] An increase in the rigidity of surrounding

environment of a fluorophore results in an increase in fluorescence anisotropy. The variation of fluorescence anisotropy (r) of compounds as a function of protein (BSA) concentration at their respective emission wavelength was displayed in figure 3.1.8B. As mentioned in Table 3.1.1, the fluorescence anisotropy of compounds showed a marked increase on moving from the aqueous phase to the protein environment, revealing that the rotational diffusion of probe molecules is restricted significantly. This also reflects that the protein bind with the probe **1** more strongly compared to **2** and **3**. The increasing concentration of protein caused rapid rise in anisotropy of compounds at the beginning and then levels off gradually suggesting saturation as shown in figure 3.1.8B. The increasing value of steady state anisotropy points towards the fact that considerable restriction is imposed on the mobility of the probe molecules with increasing protein concentration and this can only be possible if protein and probe bind strongly.[3.1.14a]

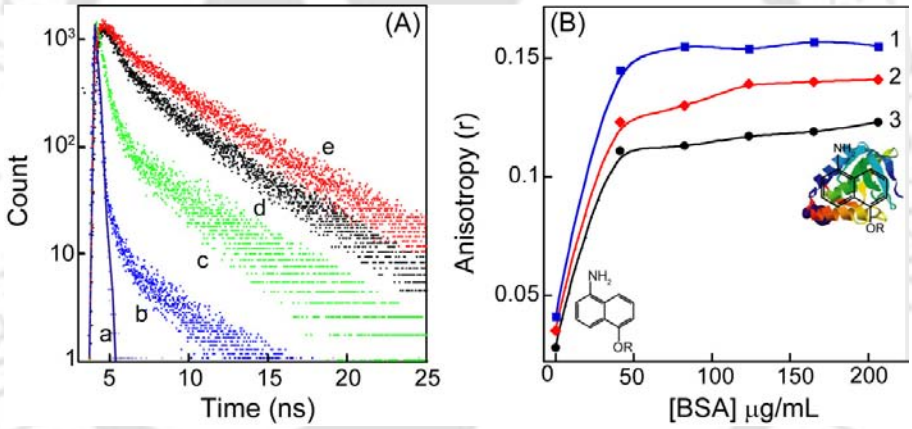

Figure 3.1.8. (A) Time resolved fluorescence spectra of the compounds (5 µM) in absence and presence of BSA (275 µg/mL); Where Trace a: IRF, Trace b-e: compound **1**, **3** + BSA, **2** + BSA and **1** + BSA in an aqueous buffer of pH 7.0 and (B) Variation of fluorescence anisotropy (r) of the compounds (5 µM) as a function of BSA concentration at their respective emission wavelengths.

3.1.3.5. Effect of BSA on Time-resolved Anisotropy Decay of Compounds

Interactions of fluorophores with proteins can lead to the formation of a more stable complex which will tumble more slowly, thus increasing the polarization of the emitted light and reducing the "scrambling" effect. This maximizes the difference in signal between bound and unbound states of the fluorophore with protein. In solution the rotational correlation time of the probe molecules should change in presence of protein or after binding with protein and in order to compare these two effects *i.e.* the lifetime and

the correlation time of the probe molecules the fluorescence anisotropy decay of the compounds in absence and in presence of BSA have been also measured as shown in figure 3.1.9. It is observed that the time-resolved anisotropy data of compound **1** and compound **1**-BSA could be successfully fitted to a single rotational correlation time of 0.91 and 12.9 ns respectively, suggesting the binding of compounds to protein (Table 3.1.1). It's also evident from the data that the correlation time of compounds (**1-3**) alone and in presence of protein are larger than their corresponding lifetime values confirmed the consistency of results obtained in steady state anisotropy measurements.

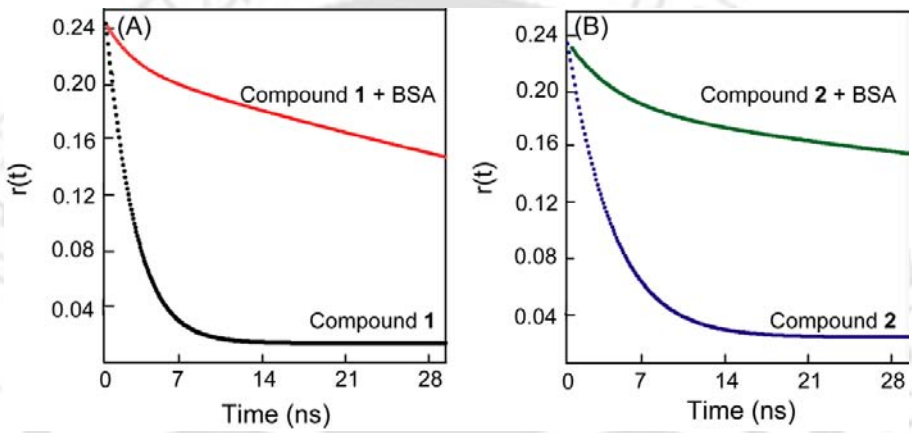

Figure 3.1.9. Anisotropy decay (fit curve) of (A) Compound **1** and (B) Compound **2** alone and in presence of BSA. [Compound] = 5 µM and [BSA] = 275 µg/mL.

Table 3.1.1. Photophysical Properties of Compounds[a] in Absence and Presence of BSA[b].

Sample	Quantum yield (Φ)[c]	τ (ns) τ_1	τ_2	Anisotropy (r)	Correlation time	k_{nr} x 10^8 (s^{-1})	K_a x 10^5 (M^{-1})	ΔG^d (kJ/mol)
1	0.012	0.25	–	0.041	0.91	39.5	–	–
2	0.011	0.15	–	0.035	1.42	65.6	–	–
3	0.009	0.11	–	0.028	1.53	89.1	–	–
1 + BSA	0.22	1.21	6.11	0.155	12.9	1.29	3.47	-15.4
2 + BSA	0.10	1.01	5.61	0.141	7.94	2.10	2.20	-9.76
3 + BSA	0.02	0.27	3.95	0.123	4.19	2.94	2.03	-8.77

[a]5 µM compound; [b]275 µg/mL BSA; [c]Quantum yield relative to 2-aminopyridine standard;[3.1.16] [d]298 K

3.1.3.6. Effect of Denaturation of Protein on Compound-BSA Composites

After finding the binding interaction between compounds and BSA, its also important to see the denaturing effect of the protein on its binding activity and on the overall photophysics of compounds. In the present work, temperature-induced modification of

the protein bound probe has been studied by means of steady-state fluorescence measurements. On gradual increased of temperature (from room temperature to 65 ^{o}C) to the protein-bound compound, the emission profile undergoes a significant change opposite to the observation shown in figure 3.1.5 (Fig. 3.1.10). As seen in figure 3.1.10, the position of emission maxima of compound bound to BSA gradually shifts to red side with increasing temperature from RT to 65^{o}C. The spectral shifts is about 20 nm and this indicates a drastic increase in polarity of the microenvironment of the probe. The peak of the emission maxima of the probe stands at ~420 nm at 65 ^{o}C and this is close to the position of the emission maxima of the probe observed in aqueous buffer. The reverse pattern of fluorescence spectrum with respect to Fig. 3.1.5 suggests with increasing temperature, the protein structure gets disrupted, the probe molecules are no more within the hydrophobic cavity where exposure to water molecules was less. Thus, this observation suggests that the probe molecule binds and remains encapsulated within the hydrophobic interior of protein, and temperature induced denaturation leads to the release or desolvation of the probe molecules and expulsion of it to the bulk aqueous phase (Fig. 3.1.11).

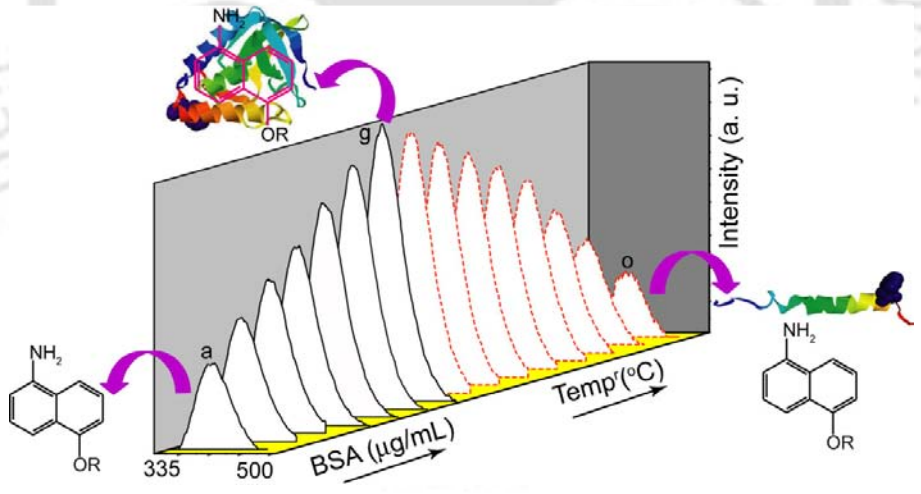

Figure 3.1.10. Emission spectra of compopund **1** (5 µM) with increasing concentration of BSA from 0 to 275 µg/mL (solid black, a-g) and with increasing temperature from RT to 65 oC (dotted red, g-o) in an aqueous buffer of pH 7.0.

Binding of compounds to proteins come from both its non-polar naphthalne amine and the alkyl groups as it has been evident from the earlier performed experiments. It is important to realize that compounds fluorescence may not require complete

immersion of the naphthylamine group in hydrophobic environment inside the protein. It requires only removal of the organic moiety from water, which is an effective quencher of its fluorescence. Thus it can be concluded from the aforementioned results that the compound in presence of BSA, has its naphthylamine group located in such a way that it is mostly or completely occluded from water quenching and therefore fluorescent, while in the aqueous environment, the compounds has its naphthylamine group located such way that it is mostly or completely exposed to water and therefore weak fluorescent. This spectral behavior well point out that the probe binds and remains encapsulated within the protein cavity and temperature induced denaturation leads to greater exposure of the probe to aqueous phase as shown in figure 3.1.11.

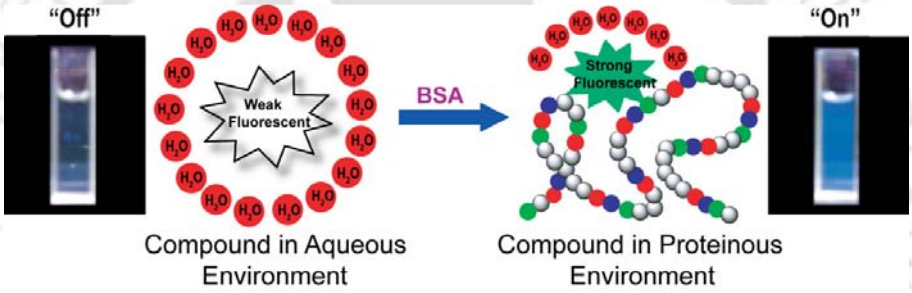

Figure 3.1.11. Schematic illustration showing the effect of microenvironment on the photophysical response of compounds.

Table 3.1.2. Physical Properties of Different Protein/Enzyme.[3.1.17a]

Protein/ Enzyme	Molecular weight (Da)	No. of amino acids	No. of aliphatic side chains (Ala, Ile, Leu & Val)	Aliphatic Index[3.1.17b]
BSA	69323.4	607	Ala-47, Ile-15, Leu-65 & Val-38	77.30
Amylase	55345.1	496	Ala-31, Ile-24, Leu-25 & Val-42	69.33
Proteinase K	28934.9	129	Ala-33, Ile-11, Leu-14 & Val-19	66.52
Lysozyme	14300.1	279	Ala-11, Ile-5, Leu-9 & Val-7	66.59
AMG	12283.3	112	Ala-7, Ile-5, Leu-6 & Val-9	67.86

3.1.4. Conclusions

In conclusion the chapter 3 demonstrates about a novel protein binding amphiphilic fluorophores, which interact non-covalently with protein and provide a dramatic increase in fluorescence intensity. The exclusivity of this molecular system is that it interacts with BSA selectivity and signals the event by 'turn on' fluorescence, while the responses to various other proteins/enzymes are negligible under similar set of

experimental conditions. The selective sensing ability of these probes towards BSA can be explained on basis of proteins hydrophobicity. The photobehavior of compounds are affected by the interplay with BSA but not with tryptophan amino acid suggesting that the microenvironment created by macromolecule induces some change in the excited-state of compounds, while the control experiment between the parent non-amphiphilic compound (5-aminonaphthalene-1-ol) and BSA reveals that the introduction of hydrophobicity do makes a positive contribution to interact with BSA. The steady state anisotropy values point towards the fact that the probe molecule remains bound within the hydrophobic cavity of the protein.

References

[3.1.1] (a) Kodadek, T. *Chem. Biol.* **2001**, *8*, 105; (b) Wang, D.; Gong, X.; Heeger, P. S.; Rininsland, F.; Bazan, G. C.; Heeger, A. J. *Proc. Natl. Acad. Sci. U.S.A.* **2002**, *99*, 49; (c) Pinto, M. R.; Schanze, K. S. *Proc. Natl. Acad. Sci. U.S.A.* **2004**, *101*, 7505.

[3.1.2] Prentø, P. *Biotech. Histochem.* **2001**, *76*, 137.

[3.1.3] (a) Jin, L. T.; Choi, J. K. *Electrophoresis* **2004**, *25*, 2429; (b) Williams, L. R. *Biotech. Histochem.* **2001**, *76*, 127; (c) Cosa, G.; Focsaneanu, K. S.; McLean, J. R. N.; McNamee, J. P.; Scaniano, J. C. *Photochem. Photobiol.* **2001**, *73*, 585; (d) Herr, A. E.; Singh, A. K. *Anal. Chem.* **2004**, *76*, 4727.

[3.1.4] (a) Jisha, V. S.; Arun, K. T.; Hariharan , M.; Ramaiah, D. *J. Am. Chem. Soc.* **2006**, *128*, 6024; (b) Daban, J. R.; Bartolome, S.; Samso, M. *Anal. Biochem.* **1991**, *199*, 169.

[3.1.5] (a) Patonay, G.; Salon, J.; Sowell, J.; Strekowski, L. *Molecules* **2004**, *9*, 40; (b) Rabilloud, T.; Strub, J. M.; Luche, S.; Girardet, J. L.; Dorsselaer, A. V.; Lunardi, J. *Proteome* **2000**, *1*, 1.

[3.1.6] (a) Gentili, P. L.; Ortica, F.; Favaro, G. *J. Phys. Chem. B* **2008**, *112*, 16793; (b) Chakrabarty, A.; Mallick, A.; Haldar, B.; Das P.; Chattopadhyay, N. *Biomacromolecules* **2007**, *8*, 920; (c) Rolinski, O. J.; Martin, A.; Birch, D. J. S.; Biomed. *J. Opt.* **2007**, *12*, 34013; (d) Singh, R. B.; Mahanta, S.; Bagchi A.; Guchhait, N. *Photochem. Photobiol. Sci.* **2009**, *8*, 101.

[3.1.7] (a) He, X. M.; Carter, D. C. *Nature* **1992**, *358*, 209; (b) Dockal, M.; Carter, D. C.; Ruker, F. *J. Biol. Chem.* **1999**, *274*, 29303.

[3.1.8] (a) Lhiaubet-Vallet, V.; Sarabia, Z.; Bosca, F.; Miranda, M. A. *J. Am. Chem. Soc.* **2004**, *126*, 9538; (b) Jimenez, M. C.; Miranda, M. A.; Vaya, I. *J. Am. Chem. Soc.* **2005**, *127*, 10134.

[3.1.9] (a) Szacilowski, K.; Macyk, W.; Drzewiecka-Matuszek, A.; Brindell, M.; Stochel, G. *Chem. Rev.* **2005**, *105***,** 2647; (b) Pandey, R. K.; Constantine, S.; Tsuchida, T.; Zheng, G.; Medforth, C. J.; Aoudia, M.; Kozyrev, A. N.; Rodgers, M. A. J.; Kato, H.; Smith, K. M.; Dougherty, T. J. *J. Med. Chem.* **1997**, *40***,** 2770;

[3.1.10] Cantor, C.; Schimmel, P. R. *Biophysical Chemistry*; part II, W. H. Freeman and company: San Francisco, CA, 1980.

[3.1.11] Barik, A.; Priyadarsini, K. I.; Mohan, H.; *Photochem. Photobiol.* **2003**, *77***,** 597.

[3.1.12] Michael, C.; Puri, N. K. *Biochem. J.* **1992**, *282*, 589.

[3.1.13] (a) Bigelow C. C.; Channon, M. *Handbook of Biochemistry and Molecular Biology*; Ed. Fasman, G. D. CRC Press: Cleveland, 1975; (b) Walker, J. M. *The Proteomics Protocols Handbook*; Humana Press Inc: Totowa, NJ, 2005.

[3.1.14] (a) Mallick, A.; Haldar, B.; Chattopadhyay, N. *J. Phys. Chem. B* **2005**, *109*, 14683; (b) Davis D. M; Birch, D. J. S. *J. Fluoresc.* **1996**, *6*, 23; (c) Moriyama, Y.; Ohta, D.; Hachiya,K.; Mitsui, Y.; Takeda, K. *J. Protein Chem.* **1996**, *15*, 265; (d) Barik, A.; Priyadarsini, K. I.; Mohan, H. J. *Photochem.* **2003**, *77*, 597.

[3.1.15] (a) Lakowicz, J. R. *Principles of Fluorescence Spectroscopy;* Plenum: New York, 1999; (b) Mukherjee, S.; Chattopadhyay, A. *J. Fluoresc.* **1995**, *5*, 237.

[3.1.16] Eaton, D. F.; *Pure Appl. Chem.* **1988**, *60*, 1107.

[3.1.17] (a) Walker, J. M. *The Proteomics Protocols Handbook*; Humana Press Inc: Totowa, NJ, 2005; (b) Ikai, A. J. *J. Biochem.* **1980**, *88*, 1895.

APPENDIX

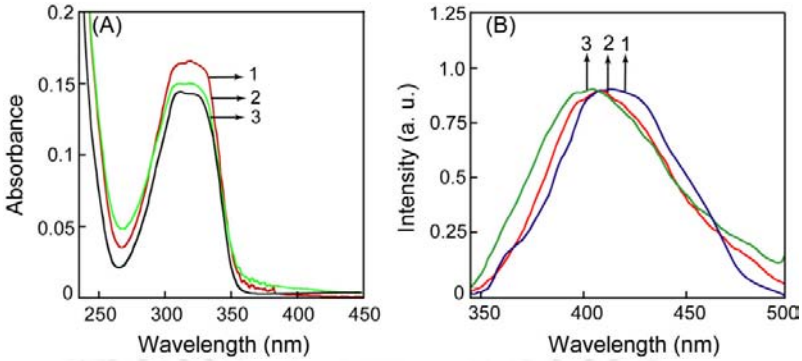

Figure A3.1.1. (A) Absorption spectra and (B) Emission spectra of compounds (**1-3**) in an aqueous buffer of pH 7.

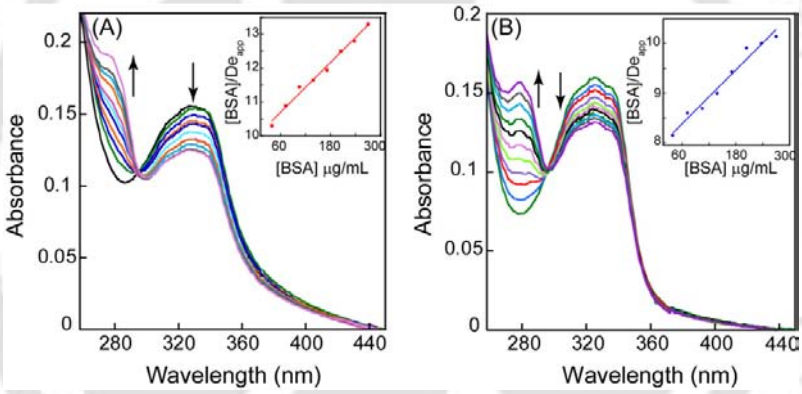

Figure A3.1.2. Absorption spectra of (A) Compound **2** and (B) Compound **3** as a function of BSA concentration (Inset: Half reciprocal plot).

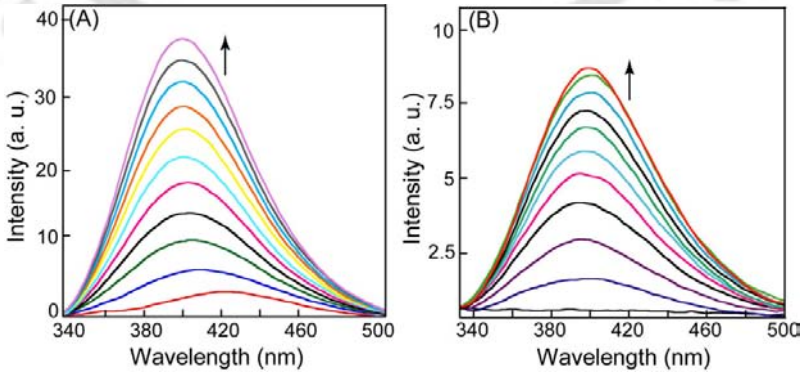

Figure A3.1.3. Emission spectra of (A) Compound **2** and (B) Compound **3** with increasing concentration of BSA (0 to 275 µg/mL) in an aqueous buffer of pH 7.0.

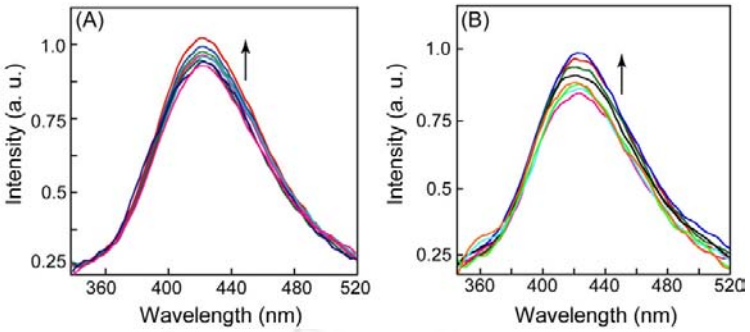

Figure A3.1.4. Emission spectra of compound **1** with increasing concentration of (A) α-amylase and (B) Lysozyme (0 to 275 µg/mL) in an aqueous buffer of pH 7.0.

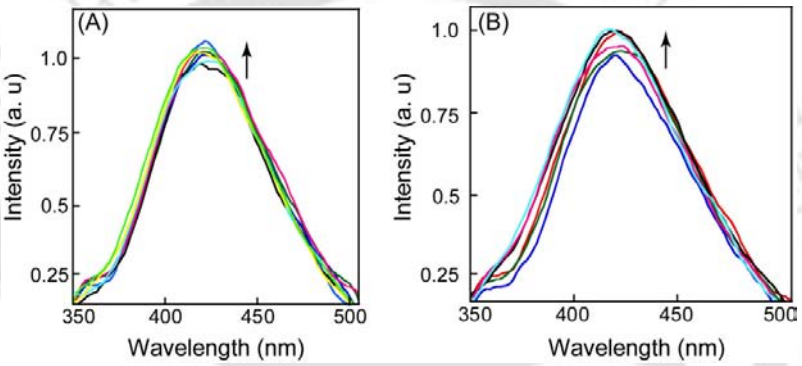

Figure A3.1.5. Emission spectra of compound **1** with increasing concentration of (A) Proteinase K and (B) AMG (0 to 275 µg/mL) in an aqueous buffer of pH 7.0.

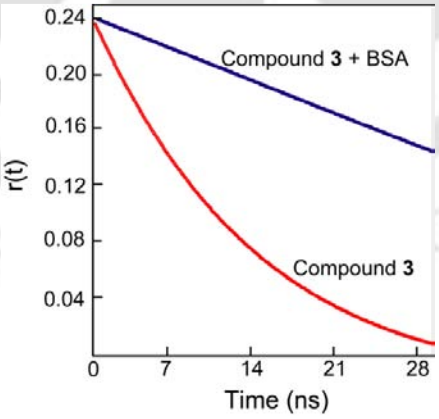

Figure 3.1.6. Anisotropy decay (fit curve) of compound **3** alone and in presence of BSA. Where the [Compound] = 5 µM and [BSA] = 275 µg/mL

Part II: Effect of 5-(Alkoxy)naphthalene-1-amine on the Conformation of Protein

3.2.1. Introduction

Establishing a protein's structure in its native state is a complex proposition. Many physical methods are cumulatively necessary for its elucidation. Moreover, the structure of proteins varies significantly in solution and solid phases. Although many native protein structures are presently known at the level of atomic resolution, a clear understanding of the physical principles of their organization and stabilization in space is still lacking. A useful approach to this problem is studying the denaturation of the native structure by external probes. The commonly used denaturants are urea, guanidine hydrochloride, and ionic amphiphiles or surfactants. Urea and guanidine hydrochloride affect the denaturing process in several ways,[3.2.1] one of which is affecting the water structure[3.2.2] The process is therefore passive, and consequently, the required denaturant concentration is relatively large. Interaction of proteins with amphiphilic molecules can change the conformation of proteins in the bulk and at the interface.[3.2.3] Therefore, understanding of interaction between amphiphiles and proteins in the bulk and at the interface, formation of protein-amphiphile complexes and displacement of protein molecules from the interface by amphiphilic molecules is important from scientific as well as practical viewpoints. In electrophoresis, proteins are classically treated with SDS to denature the native tertiary and quaternary structures, allowing the separation of proteins according to their molecular weight (Fig. 3.2.1).[3.2.4]

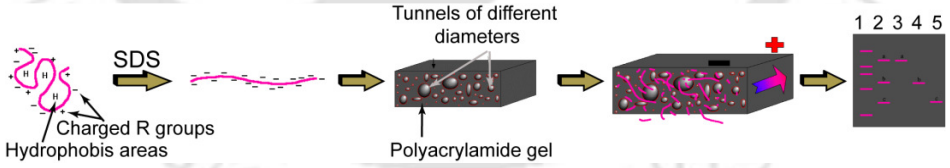

Figure 3.2.1. Use of SDS in gel electrophoresis to denature the native tertiary and quaternary structures of protein.

The 2nd part of chapter 3 describes the effect of 5-(alkoxy)naphthalene-1-amine amphiphile[2.1] [(**1-3**), Fig. 3.1.3] on the conformation of bovine serum albumin (BSA), when used at higher concentration (40 μM). The synthesis of compounds has been described in chapter 2. In order to generate the variation in structure and to study their effect on the conformation of BSA, the alkyl chain length of compounds has been varied.

3.2.2. Methods

A 10 mM phosphate buffer of pH 7.0 was prepared in double-distilled water for all the experiments. A stock solution of BSA (10 μM) was prepared in an aqueous solution of 10 mM phosphate buffer of pH 7.0, while compounds stock solution were prepared in DMSO because of their lower solubility in water. In a 3.0 mL aqueous buffer solution of BSA (10 μM), different concentrations of compounds were varied (0 to 40 μM), so that the total volume of DMSO did not exceed 15%. The presence of 15% DMSO induces no major BSA structural changes (Appendix, Fig. 3.2.1).

3.2.3. Reuslts and Discussion

3.2.3.1. Effect of Compounds on Absorption Spectra of BSA

UV–visible absorption spectroscopy is a very simple method to explore the structural change and to know the complex formation in solution.[3.2.5] Figure 3.2.2A shows the UV–visible absorption spectra of BSA, with increasing concentrations of the compound **1** in an aqueous phosphate buffer of pH 7.0. Addition of compound led to the increase in absorbance of BSA at 280 nm, with simultaneous increase in absorbance of the compound at 320 nm along with a red shift of absorption maxima to 324 nm (Fig. 3.2.2B) upon complexation with BSA. A reasonable explanation for the two evidences may come from the complex formation between BSA and compounds.[3.2.6] Similar results were also obtained in case of compound **2** and **3** (Appendix, Fig. A3.2.2).

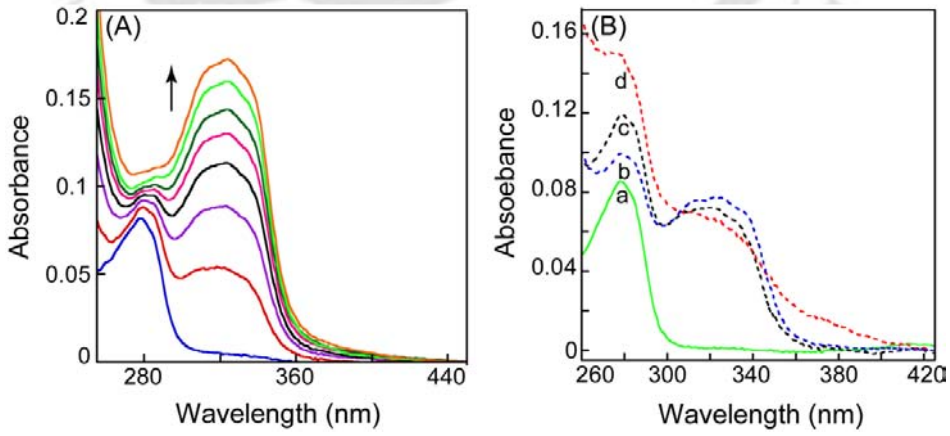

Figure 3.2.2. (A) Absorption spectra of BSA (3 μM) with increasing concentrations of the compound **1** (0-20 μM) in phosphate buffer of pH 7.0 (Inset: Plot of the absorbance of BSA at 280 nm as a function of

compound **1** concentration) and (B) Absorption spectra of BSA alone (a) and BSA with compound **1** (b)**, 2** (c) and **3** (d).

3.2.3.2. Quenching of Intrinsic Fluorescence of BSA by Compounds

Proteins fluorescence was a sensitive tool to investigate the conformation of protein when its environment and structure gets change. Fluorescence quenching can be dynamic, resulting from collisional encounters between the fluorophore and the quencher, or static, resulting from the formation of a ground state complex between the fluorophore and the quencher.[3.2.6] Type of fluorescence quenching (like dynamic, collisional or static) provide information about the changes of the molecular microenvironment in a vicinity of chromophore molecules. Static and dynamic quenching can be distinguished by their different binding constants dependence on temperature and viscosity, or preferably by lifetime measurements.

Tryptophan fluorescence is widely used as a tool to monitor changes in proteins structure and to make inferences regarding local structure and dynamics.[3.2.7] There are two tryptophans in BSA: Trp-134 is in domain I in the 8th helix of D129-R144, which is well exposed, and Trp-212 is in domain II, in the 2nd helix of E206-F221, and is buried inside the protein structure.[3.2.8] Thus, intrinsic fluorescence of BSA is mainly due to sole tryptophan residues (Trp-134 and 212) in the hydrophobic cavity of domain I and II. The fluorescence spectrum of BSA presents strong emission maximum at 345 nm, when excited at 295 nm in an aqueous buffer solution.[3.2.9] Excitation wavelength of 295 nm was chosen to avoid the contribution from the tyrosine residues in proteins. The compounds (**1**-**3**) were almost non-fluorescent or possess a very weak emission under the present experimental conditions. The addition of compounds to BSA leads to a significant change in the fluorescence spectrum of BSA, indicating the binding of compounds to BSA. Steady-state fluorescence experiments shows that compound (**1**-**3**) can markedly influence the emission properties of BSA. Figure 3.2.3A shows the steady-state fluorescence spectrum of BSA in presence of different concentrations of compound **1** (0-40 μM) at pH 7.0. Similar trends were also observed in case of BSA after addition of compound **2** and **3** (Appendix, Fig. A3.2.3).Figure depicts that the increasing concentrations of compounds caused a progressive reduction in fluorescence intensity accompanied by a large red shift in λ_{max} of BSA by 34, 23 and 18 nm upon complexation with compound **1**, **2** and **3** respectively (Fig. 3.2.3B).

function of compound **1** concentration) and (B) Absorption spectra of BSA alone (a, solid line) and BSA with compound **1** (b, blue)**, 2** (c, black) and **3** (d, red).

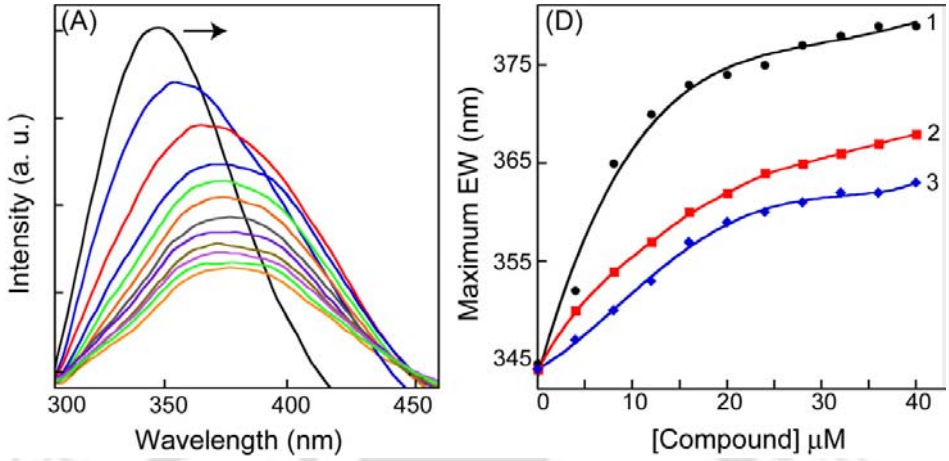

Figure 3.2.3. (A) Fluorescence spectra of BSA (10 µM) with increasing concentration of compound **1** from 0 to 40 µM in 10 mM phosphate buffer of pH 7.0 and (B) Variation in fluorescence emission wavelength of BSA as a function of compounds concentration.

The apparent maximum emission wavelength of BSA at about 345 nm indicates that the tryptophan residues present in the native protein are on the surface and exposed to the aqueous environment. This red shift of emission maximum along with reduction in fluorescence intensity indicates that the interaction of BSA with compound changes the environment of tryptophan with probable increase in hydrophilicity from hydrophobic or less hydrophilic environment. The structure of hydrophobic sub-domain where tryptophan placed was not compact and the segment of polypeptide changed its conformation to a more extended state after addition of compounds.[3.2.10] Shifts in emission wavelength as well as intensity of tryptophan residues in protein are generally observed upon unfolding.[3.2.11] The tryptophan emission of a native protein can be greater or smaller than the emission of free tryptophan in an aqueous solution. The emission maximum is usually shifted from shorter to longer wavelengths upon protein unfolding, which corresponds to the fluorescence maximum of tryptophan in an aqueous solution.[3.2.11] The emission maximum of tryptophan can vary greatly between proteins and its emission spectrum should reflect the average environment of the tryptophan. The variations in tryptophan emissions are consequences of the protein conformational change. Trp-134 is more exposed to the hydrophilic environment while Trp-212 lies in the hydrophobic core.[3.2.8] Because of its higher exposure; Trp-134 is more likely to be quenched in the native state.

BSA gets unfolded with increasing concentration of compounds as a result structure of proteins loosens, forming pores or pathways for compounds to reach the buried tryptophan (Fig. 3.2.8).

The increase in restriction in the environment around the protein tryptophan is also shown in figure 3.2.3B, where emission maximum is plotted as a function of compounds (**1**, **2** and **3**) concentration. At the ultimate saturation condition in our experiment, where compounds molar concentration was 40 μM, the emission maximum of native BSA shifted from 345 to 379, 368 and 363 nm in presence of compound **1**, **2** and **3** respectively. The difference in way of interactions of compounds with albumin molecule is not surprising because it is expected that the protein-compound interactions will be strongly influenced by the amphiphilic nature; that is, the hydrophobic chain length and the charge or nature of the hydrophilic group.[3.2.12] All the three compounds have a common polar head group with only variation in alkyl chain length. The complex-formation processes in solution are clearly evidenced for BSA with compounds, as the steady-state fluorescence spectra in figure 3.2.3 suggest.

A gradual quenching of the fluorescence intensity of tryptophan has been observed with increasing concentration of compounds at pH 7.0. It is possible to estimate the quenching of tryptophan fluorescence in the presence of compounds using the Stern-Volmer equation. On the basis of relationship between quenching of excited states and quencher concentration, the Stern-Volmer equation is given by[3.1.15a]

$$F_o/F = 1 + K_{SV}[Q] \qquad (3.2.1)$$

Here, F_o and F are the relative fluorescence intensity in absence and presence of quencher, respectively and [Q] is the concentration of the quencher. K_{SV} is the Stern-Volmer quenching constant which measures the efficiency of quenching. In many instances, the fluorophore can be quenched both by collision and by complex formation with the same quencher. When in this case, the Stern–Volmer plot exhibits an upward curvature, concave towards the y-axis at high quencher concentration, and F_o/F is related to [Q] by the following form of modified Stern–Volmer equation: [3.1.15a]

$$F_o/F = (1 + K_D[Q])\,(1 + K_S[Q]) \qquad (3.2.2)$$

$$F_o/F = 1 + K_{app}[Q] \qquad (3.2.3)$$

Where, K_D and K_S are the dynamic and static quenching constants, respectively. The first factor on the right-hand side in equation 3.2.2 describes the “dynamic” quenching, resulting from encounters between quencher and fluorophore during the excited state and

the second factor describes the "static" quenching, that is quenching by the formation of a complex between quencher and fluorophore predating the excitation. If there is a departure from linearity, due to the term in $[Q]^2$ being appreciable, it is certain that both ground-state complexes and excited-state interactions contribute to the quenching, which accounts for the upward curvature observed at high [Q] when both static and dynamic quenching occur for the same fluorophore. The apparent quenching constant (K_{app}) is calculated at each quencher concentration. A plot of K_{app} versus [Q] yields a straight line with an intercept of $K_D + K_S$ and a slope of $K_S K_D$. The static and dynamic quenching constants can be obtained from the solutions of the quadratic equation. [3.1.15a]

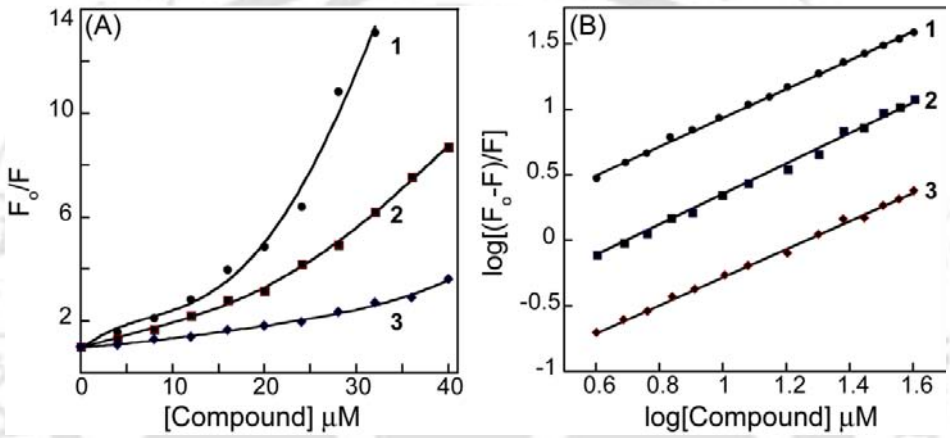

Figure 3.2.4. Stern–Volmer plots of the (A) BSA-compound composites and (B) Plot of log[(F_o - F)/F] vs. log[compound] for BSA-compound composites at pH 7.0.

Table 3.2.1. Quenching Parameters for Different BSA-Compound Composites.

Sample	K_D[a] (M^{-1})	K_S[b] (M^{-1})	K_A[c] (M^{-1})	n[d]
BSA + Compound **1**	10.4 x 10^4	6.94 x 10^4	38.2 x 10^3	1.08
BSA + Compound **2**	7.79 x 10^4	4.89 x 10^4	19.1 x 10^3	1.00
BSA + Compound **3**	4.64 x 10^4	1.95 x 10^4	5.89 x 10^3	1.02

[a,b]Stern-Volmer dynamic and static quenching constant; [c]Binding constant and [d]Number of binding sites

Figure 3.2.4A shows the Stern-Volmer plots of F_o/F versus compound concentration (i.e. quencher), having substantial upward curvature, deviating from the linearity. The upward curvature due to quenching of BSA fluorescence reflects the contribution of static quenching to the dynamic quenching of the fluorophore by compounds. The upward-curving Stern-Volmer plots could be analyzed in terms of both static and dynamic quenching constants as shown in equation 3.2.2. The dynamic and static Stern-Volmer quenching constants K_D and K_S of BSA with compounds are listed in Table 3.2.1.

Furthermore, if high concentrations of compound caused denaturation, an abrupt upward curvature would result.[3.2.13] In the modified Stern-Volmer plots, straight lines are obtained (Fig. 3.2.5), indicating either that only a single tryptophan residue is accessible, or that the exposed residues are equally available to the quencher. Apparently, the binding of BSA to compounds cause a dramatic conformational change that result in exposure of the previously shielded tryptophan residue. Changes in accessibility due to conformational changes have been reported for several other proteins.[3.2.14] The quenching of BSA fluorescence by compounds **2** and **3** also shows a positive deviation of Stern-Volmer plots from linearity, which indicates the denaturation of BSA and the exposure of buried tryptophan (Fig. 3.2.4A). Considerable fluorescence remained even at high compound concentration, which indicates that compound **2** and **3** quenches the fluorescence of BSA with less effectiveness than **1**. Table 3.2.1, also shows that the dynamic and static Stern–Volmer constant decreases with increasing the alkyl chain length of compounds. These aforementioned results indicate that the changes of the environment of tryptophan residues depend on the aliphatic chain length of compounds. The data provided in Table 3.2.1 support the fact that BSA fluorescence was strongly quenched by compound **1**, but was poorly quenched by **2** and **3**. The change in the fluorescence parameters of BSA (*e.g.* emission maximum wavelength, emission intensity and lifetime etc.) shows that the environment of tryptophan residues present in BSA are highly affected during the interactions with compounds.

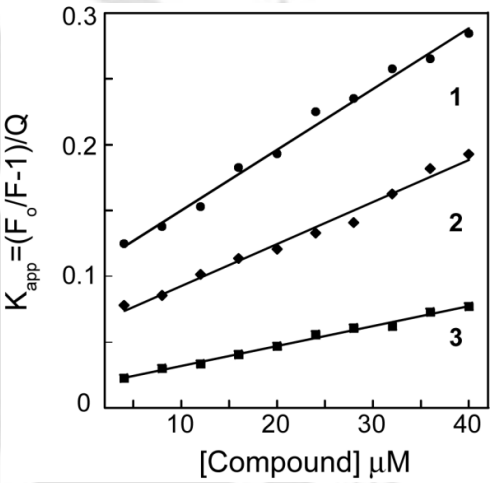

Figure 3.2.5. The modified Stern-Volmer plot of K_{app} versus concentration of compounds.

For the quenching process, under the assumption that BSA has the same and independent binding sites, the following equation was employed for the determination of binding constant or association constant (K_A) and the number of binding sites (n):[3.2.15]

$$\log[(F_o - F)/F]) = \log K_A + n\log[Q] \qquad (3.2.4)$$

Binding constant and the number of binding sites can be calculated by plotting $\log[(F_o - F)/F]$ versus log[compound] as shown in figure 3.2.4B. From the slope of the linear fitting plots, number binding sites (n) and from the intercept ($\log K_A$), the binding constants K_A,

were calculated and listed in Table 3.2.1. The obtained values of n indicate that in each case the probe is located in only one binding site. The table also shows that compared to compound **3** and **2**, **1** exhibits relatively more affinity for BSA (Table 3.2.1), which may be responsible for its higher quenching effectiveness. The association constants calculated for different BSA-compound composites also suggest lower binding affinity compared to the other strong protein-compound complexes with binding constants ranged from 10^6 to10^8 M^{-1}. However lower binding constants (10^3 to 10^5 M^{-1}) were also recently reported for several other protein-compound complexes.[3.2.16]

3.2.3.3. Steady State Anisotropy of BSA in Presence of Compounds

As polarization (anisotropy) measurements can give details about an association or binding phenomenon, the technique has been employed to gather additional evidence in support of the interaction between BSA and compound.[3.1.15a] An increase in the rigidity of the surrounding environment of a fluorophore results in an increase in the fluorescence anisotropy. In order to gets information regarding the conformational changes in the protein structure in presence of compounds the steady state anisotropy of BSA has been performed as defined by equation 2.3 (Chapter 2). The anisotropy values were averaged over an integration time of 10 s and a maximum number of three measurements were made for each sample. All anisotropy values of BSA in presence of compound are the mean values of three individual determinations. The measurements of the polarized steady state fluorescence of BSA make it possible to analyze the rotation of the entire protein molecule, while the contribution from the rotation of the domain containing the tryptophan and the rotation of the tryptophan group with respect to the nearby surroundings are considered to be negligible. As shown in figure 3.2.6A, the anisotropy of BSA found to increase with increasing concentration of compounds. The increasing value of anisotropy of BSA indicates the loosening of the globules *i.e.* the denutaration of protein, which reduces the rotational diffusion coefficient for the protein molecules.

3.2.3.4. Fluorescence Lifetime decay of BSA in the Presence of Compounds

Time-resolved fluorescence study was also carried out to investigate the quenching mechanism of BSA fluorescence by compounds. There are two lifetime components in native BSA, one (τ_1 = 5.8 ± 0.2 ns) contributing 75 % of the total fluorescence and the other (τ_2 = 1.2 ± 0.2 ns) contributing the rest of the fluorescence.[3.2.17] The one with a

longer lifetime was assigned to Trp-134 and the other was assigned to Trp-212. The relative contribution of each component was dependent on the folding/unfolding conditions due to the protein's multiple local configurations and changes in the extent of solvent accessibility. Thus, the information of the protein conformational behavior can be obtained from the emission spectra of tryptophan in the bioconjugates. Fluorescence lifetime serves as a sensitive parameter for exploring the local environment around a fluorophore, and it is sensitive to excited-state interactions.[3.2.18] It also contributes to the understanding of the interactions between the probes and the proteins.[3.1.14a] The fluorescence lifetime of the tryptophan residues in proteins is a complex function of its interactions with the local environment and the solvent. To explain the variation of large red shift and increase in the K_{SV} values of BSA-compound composites with the variation of alkyl chain length, the time-resolved fluorescence experiment with BSA in absence and presence of compounds have been performed. The fluorescence lifetime decay profiles of the native BSA, BSA-compound (**1, 2** and **3**) composites, are shown in figure 3.2.6B. The best fits for BSA were obtained using a bi-exponential function, which is typical for tryptophan in proteins. The two time constants of BSA alone in buffer are 6.01 and 1.22 ns respectively which are in good agreement with the above-mentioned values. But in presence of compounds fluorescence lifetimes of the tryptophan residues in BSA decreased differently. A decrease in lifetime of BSA (τ_1 and τ_2) from 6.01 and 1.22 to 4.83 and 0.77, 5.36 and 0.87 and 5.62 and 0.91 ns results due to the addition of compound **1**, **2** and **3** respectively. Typical decay profiles of BSA in compounds (**1, 2** and **3**) environments are shown in figure 3.2.6B. The fluorescence lifetimes and the various statistical parameters used to check the goodness of fit are given in Table 3. A glance at Table 3.2.2 reflects that two of the lifetime values τ_1 and τ_2 are observed to be lower in presence of the compounds than those measured for native BSA in an aqueous buffered solution. So, τ_1 and τ_2 components may be assigned to the not free (bound to compound) probe molecule in amphiphilic environments. Instead of placing too much emphasis on the magnitude of individual decay constants in such biexponential decays, the mean fluorescence lifetime defined by equation 2.2 (Chapter 2) has been chosen as an important parameter for exploiting the behavior of BSA molecule bound to compounds. The mean lifetime values of BSA in an amphiphilic environments calculated using equation 3 are tabulated in Table 3.2.2. Interestingly, the decay parameters are affected by the compounds environment, with the mean lifetime of BSA (τ_m) changing from 5.04 ns in

buffer to 2.76, 3.49 and 3.74 ns in presence of 40 μM of compound **1**, **2** and **3** respectively. The occurrence of dynamic quenching of BSA fluorescence was further supported by the measurements of fluorescence lifetime of BSA as a function of compounds concentration (Appendix, Fig. A3.2.4), which shows that the mean lifetime of BSA decreases with increasing concentration of compounds. Thus, the decrease in fluorescence lifetime was a clear consequence of the significant interactions between compounds and BSA. It is clear from the lifetime measurements of BSA in presence of compounds that fluorescence decay of BSA is faster with decreasing chain length of compounds. Out of these compounds, the lifetime of BSA was found to be shorter in presence of compound **1** compared to **2** and **3**, which is also consistent with comparatively higher K_{SV} values obtained for the compound **1** than **2** and **3** respectively showing the same trend as observed in fluorescence intensity change.

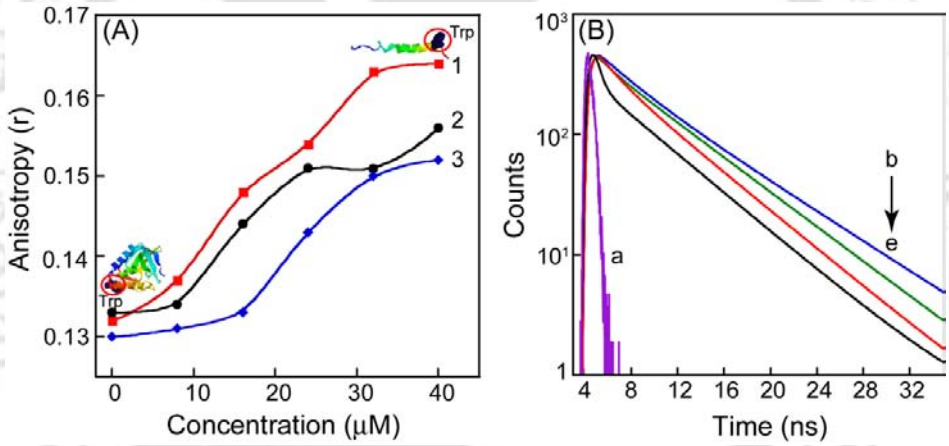

Figure 3.2.6. (A) Fluorescence anisotropy of BSA (10 μM) as a function of compounds concentrations ranging from 0 to 40 μM in an aqueous buffer of pH 7.0. (B) Time resolved fluorescence quenching decays of BSA in prresence of compounds; where Trace a: IRF, Trace b: BSA alone and Trace c-e are BSA-compound composite with compound **3, 2** and **1** respectively.

From the lifetime data of the fluorophore (tryptophan in BSA), the degree of exposure of the probe to aqueous phase can be predicted. The closer are the lifetime values in the amphiphilic environment and the aqueous environment, the greater is the degree of exposure of the probe to the aqueous environment. Table 3.2.2 reveals that all of the lifetime components of BSA in presence of compounds are lower than the corresponding values of BSA in buffer medium. This indicates that in native BSA the polarity of the microenvironment is lower than that in the compound environment; *i.e.* BSA resides in

the more polar region in BSA-compound composites than that in native BSA in an aqueous buffer environment, resulting in a concomitant decrease in the lifetime values. Thus, it can be concluded that the addition of compounds increases the hydrophilicity around the Trp-134, results in the deformation of secondary structure of protein and hence the red shift of emission spectrum along with the reduction in fluorescence intensity. At a 40 μM concentration of compounds, the emission maximum of BSA exhibits no further red shift and no reduction in fluorescence intensity, suggesting the saturation of tryptophan environments in protein.

Table 3.2.2. Fluorescence Lifetime (τ) of BSA and Different BSA-Compound Composites

Sample	λ_{max}[a] (nm)	τ_1 (ns)	τ_2 (ns)	α_1	α_2	τ_m (ns)	χ^2
Native BSA[b]	345	6.01	1.22	0.016	0.004	5.04	1.001
BSA + Compound **1**[c]	379	4.83	0.77	0.013	0.013	2.76	1.003
BSA + Compound **2**	368	5.36	0.87	0.014	0.010	3.49	1.002
BSA + Compound **3**	363	5.62	0.91	0.014	0.009	3.74	1.001

[a]λ_{exc} = 290 nm; [b][BSA] = 10 μM and [c][Compound] = 40 μM

3.2.3.5. Distance Measurement Using Resonance Energy Transfer Between Compounds and BSA

Fluorescence resonance energy transfer (FRET) technique has emerged as a successful tool to determine the spatial distance between two points (a donor and an acceptor) in proteins and FRET distances between two points have been extensively used to study protein folding pathways, conformational changes upon compound binding, protein-protein interactions, and monomer-dimer equilibrium.[3.2.19] According to Förster's theory, the efficiency of FRET depends mainly on the following factors: (i) the extent of overlap between the donor emission and the acceptor absorption, (ii) the orientation of the transition dipole of donor and acceptor, and (iii) the distance between the donor and the acceptor.[3.2.20] In a proteinous environment the proximity of a guest molecule to the tryptophan moiety is often determined through FRET study. For this purpose the donors (BSA) was excited at 295 nm where the absorbance of the acceptors (compound) were negligible. On gradual addition of compounds, fluorescence intensity of the tryptophan residues present in BSA decreased along with red shift of the emission spectra (Fig. 3.2.3A). This indicates an efficient energy transfer from the tryptophan residues present in BSA to compounds. By Förster's theory, the efficiency of energy transfer (E) is related to the distance r between donor and acceptor as defined by equation 3.2.5,

$$E = R_o^6 / (R_o^6 + r^6) \qquad (3.2.5)$$

Where r is the distance between acceptor and donor and R_o is the critical distance when the transfer efficiency is 50% and is given by the following equation

$$R_o = 0.211\ [\kappa^2 n^{-4} \Phi_D J(\lambda)]^{1/6} \qquad (3.2.6)$$

Where n is the refractive index of the medium, κ^2 is the orientation factor, and Φ_D is the quantum yield of the donor. The spectral overlap integral (J) between the donor emission spectrum and the acceptor absorbance spectrum was approximated by,

$$J(\lambda) = \int F_d(\lambda)\, \varepsilon_a(\lambda)\, \lambda^4 d\lambda \,/\, \int F_d(\lambda) d\lambda \qquad (3.2.7)$$

Where $F_d(\lambda)$ and $\varepsilon_a(\lambda)$ represent the fluorescence intensity of the donor and the molar extinction coefficient of the acceptor, respectively, at the wavelength λ. The value of J can be evaluated by integrating the overlapped portion of the spectra in figure 3.2.7A. If both the donor and acceptor are tumbling rapidly and free to assume any orientations, then the dipole orientation factor, κ^2, equals 2/3.[3.2.21] In the present case, n = 1.36 and Φ_D = 0.118.[3.2.21,3.2.22] The energy transfer data were obtained by measuring the change in donor fluorescence. The donor fluorescence intensity (F_d) was measured in the absence and presence (F_a) of acceptor. The efficiency of transfer (E) was calculated using equation 3.2.8.

$$E = 1 - F_a/F_d \qquad (3.2.8)$$

In absence of compounds, intrinsic fluorescence of tryptophan in BSA (3 μM) displayed typical emission spectrum with emission maxima around 345 nm, while 5-(alkoxy)naphthalene-1-amine shows a broad and intense absorption in the UV region at 320 nm. The absorption spectrum of compounds (3 μM) extensively overlaps the fluorescence emission of the tryptophan in BSA (Fig. 3.2.7A). Binding of compounds to BSA results in the red shift of the emission maxima of tryptophan emission spectrum; however, compounds decreased the fluorescence intensity of tryptophan in a concentration dependent manner. Taking together, the result indicates that the quenching of the tryptophan fluorescence was due to a non-radiative energy transfer between tryptophan and compounds. Figure 3.2.7A shows the overlap absorption spectra of compound **1** with the fluorescence spectrum of BSA. Compound **1** shows larger overlapping compared to **2** and **3** (Appendix, Fig. A3.2.5), which indeed enhance the resonance energy transfer (Table 3.2.3) between compound **1** and BSA than **2** and **3**, even though there is not too much differences in their molar extinction coefficient values (Table 3.2.3).

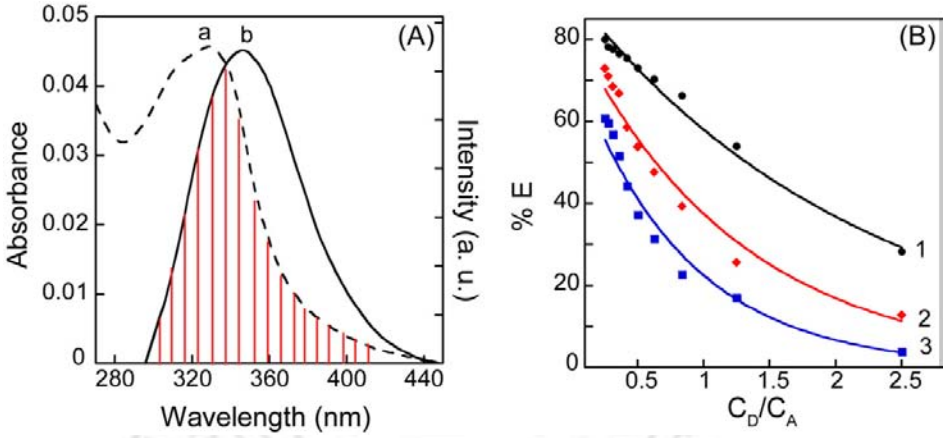

Figure 3.2.7. (A) The overlap of the fluorescence spectra of BSA (b, solid line) and the absorption spectra of compound **1** (a, dotted line) and (B) Dependence of the efficiency of quenching of BSA by the compound, $E = 1 - F/F_o$ as a function of the BSA to compound ratio (C_D/C_A).

Table 3.2.3. Energy Transfer Parameters for Different BSA-Compound Composites.

Sample	ε^a ($M^{-1}cm^{-1}$)	J ($M^{-1}cm^{-1}nm^4$)	R_o(nm)	r (nm)	E
BSA + Compound **1**	1.43×10^4	3.04×10^{14}	2.72	2.15	0.80
BSA + Compound **2**	1.50×10^4	3.19×10^{14}	2.74	2.16	0.72
BSA + Compound **3**	1.56×10^4	3.32×10^{14}	2.76	2.18	0.61

[a]At 320 nm wavelength

The larger overlap between emission spectrum of BSA and absorbance spectrum of compound **1** compare to **2** and **3** indicates that **1** should show more fluorescence-quenching effect than those of **2** and **3** (Table 3.2.3). This indeed was the observation as shown in figure 3.2.3, where fluorescence of BSA was quenched more in the presence of compound **1** than **2** and **3** (Appendix, Fig. A3.2.3). Efficient FRET in BSA suggests that the probe molecule resides closer to the tryptophan moiety of the proteins. Following Sengupta *et al*.[3.2.23] and other workers results,[3.2.24] it can be concluded that the probe is located near to Trp-134 rather than Trp-212 in BSA. As shown in Table 3.2.3 the distance between compounds and tryptophan residuee in BSA found are far lower than 7 nm obeying the conditions of Förster energy transfer theory.[3.2.25] To determine the relative proximity of the probe molecule to tryptophan residues in BSA environments, the energy transfer efficiency (Table 3.2.3) has been determined which is mainly dependent upon the extent of overlap between the emission of donor and the absorption of acceptor and the distances between the donor and acceptor molecules maintaining 1:1 situation of donor:

acceptor concentration defined by the equation 3.2.8 (Fig. 3.2.7B). All distances reported are the averages of three identical experiments (Table 3.2.3).

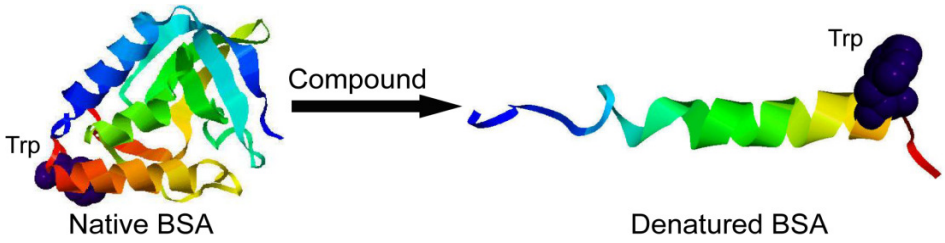

Figure 3.2.8. Schematic model showing the effect of compounds on tryptophan environment in protein.

3.2.4. Conclusions

The mechanism of binding of compounds with BSA has been investigated using UV-visible, steady-state and lifetime fluorescence measurements. The BSA fluorescence exhibits appreciable bathochromic shift along with a reduction in fluorescence intensity and fluorescence lifetime upon binding with compounds. The fluorescence quenching efficiency of compounds seems to be dependent on the length of the hydrocarbon chain, which decreases with decreasing chain length of compounds from C_8 to C_{16}. The aforementioned results indicate that compounds binds near Trp-134 in the sub-domain IA of the native BSA and is accessible to Trp-212 when BSA is get unfolded. The data well supports the idea that BSA loses its structure incrementally during its interactions with compounds, also supported by increased anisotropy value of BSA as a function of compounds concentration. Variation in emission maxima along with anisotropy value of tryptophan residues in BSA showed that the interactions of BSA with compound decreases with increasing hydrocarbon chain length. The above observation indicates that the reduction in fluorescence of BSA is due to change in environment of tryptophan from less hydrophilic to more hydrophilic along with the energy transfer from tryptophan residues to the probe in each case. The analysis of quenching data using Stern-Volmer equation reveals that both dynamic and static quenching mechanisms were operating in all BSA-compound composites. The number of binding sites of all BSA-compound composites was also estimated and found to be one which indicates that in each case probe is located near only one binding site. The calculated quenching rate constants and binding constants were also shown to depend on the alkyl chain length.

References

[3.2.1] (a) Nozaki, Y.; Reynolds, J. A.; Tanford, C. *J. Biol. Chem.* **1974**, *249*, 4452; (b) Ramos, C. H. I.; Baldwin, R. L. *Protein Sci.* **2002**, *11*, 1771; (c) Timasheff, S. N. *Annu. Rev. Biphys. Biomol. Struct.* **1993**, *22*, 67; (d) Bostrom, M.; Williams, D. R. M.; Ninham, B. W. *Biophys. J.* **2003**, *85*, 686; (e) Russo, A. T.; Rosgen, J.; Bolen, D. W. *J. Mol. Biol.* **2003**, *330*, 851; (f) Schellman, J. A. *Biophys. J.* **2003**, *85*, 108.

[3.2.2] Das Gupta, P. K.; Moulik, S. P. *J. Phys. Chem.* **1987**, *91*, 5826.

[3.2.3] (a) Gelamo, E. L.; Silva, C. H.; Imasato, H.; Tabak, M. *Biochim. Biophys. Acta* **2002**, *1594*, 84; (b) Chakraborty, T.; Chakraborty, I.; Ghosh, S. *Langmuir* **2006,** *22,* 9905; (c) Kotsmar, C. S.; Pradines, V.; Alahverdjieva, V. S.; Aksenenko, E. V.; Fainerman, V. B.; Kovalchuk, V. I.; Kragel, J.; Leser, M. E.; Noskov, B. A.; Miller, R. *Adv. Colloid Interface Sci.* **2009**, *150*, 41.

[3.2.4] Reynolds, J. A.; Herbert, S.; Polet, H.; Steinhardt, J. *Biochemistry* **1967**, *6*, 937.

[3.2.5] Hu, Y. J.; Liu Y.; Wang, J. B.; Xiao, X. H.; Qu, S. S. *J. Pharm. Biomed. Anal.* **2004**, *36*, 915.

[3.2.6] Yue, Y. Y.; Chen, X. G.; Qin, J.; Yao. X. J. *Dyes Pigments* **2008**, 79, 176.

[3.2.7] (a) Tian, J.; Liu, J.; Tian, X.; Hu, Z.; Chen, X. *J. Mol. Struct*. **2004**, *69*, 1197; (b) Chen, Y.; Barkley, M. *Biochem.* **1998**, *37*, 9976; (c) Gensch,T. *Photochem. Photobiol. Sci.* **2004**, *3*, 531; (d) Albani, J. R. *J. Fluor.* **2007**, *17*, 406.

[3.2.8] Sun, C.; Yang, J. *Biophys. J.* **2005**, *88*, 3518.

[3.2.9] Vanderkooi, J. M.; Calhoun, D. B.; Englander, S. W. *Science* **1987**, *236*, 568.

[3.2.10] Yuan, T.; Weljie, A. M.; Vogel, H. J. *Biochemistry* **1998**, *37*, 3187.

[3.2.11] (a) Eftink, M. R. *Methods Biochem Anal.* **1990**, *35*, 117; (b) Burstein, E. A. *Luminescence of Protein Chromophores. In Model Studies: Science and Technology Results*, Vol. 6: Biophysics, VINITI, Moscow 1976.

[3.2.12] Wu, D.; Xu, G.; Sun, Y.; Zhang, H.; Mao, H.; Feng, Y. *Biomacromolecules* **2007**, *8*, 708.

[3.2.13] Eftink, M. R.; Ghiron, C. A. *Biochemistry* **1977**, *16*, 5546.

[3.2.14] (a) Weber, J.; Senior, A. E. *Biochemistry* **2000**, *39*, 5287; (b) Wells, T. A.; Nakazwa, M.; Manabe, K.; Song, P. S. *Biochemistry* **1994**, *33*, 708.

[3.2.15] Bi, S.; Ding, L.; Tian, Y.; Song, D.; Zhou, X.; Liu, X.; Zhang, H. *J. Mol. Struct*. **2005**, *703*, 37.

[3.2.16] (a) He, W.; Li, Y.; Xue, C.; Hu, Z.; Chen, X.; Sheng, F. *Bioorg. Med. Chem*. **2005**, *13*, 1837; (b) Dufour, C.; Dangles, O. *Biochim. Biophys. Acta* **2005**, *1721*, 164; (c) Kragh-Hansen, U. *Dan. Med. Bull*. **1990**, *37*, 57; (d) Nsoukpoe-Kossi, C. N.; Sedaghat-Herati, M. R.; Ragi, C.; Hotchandani, S.; Tajmir-Riahi, H. A. *Int. J. Biol. Macromol.* **2007**, *40*, 484.

[3.2.17] Patel, A. B.; Srivastava, S.; Phadke, R. S. *J. Biol. Chem*. **1999**, *274*, 21755.

[3.2.18] Das, P.; Mallick, A.; Haldar, B.; Chakrabarty, A.; Chattopadhyay, N. *J. Chem. Phys.* **2006**, *125*, 044516/1-6.

[3.2.19] (a) Panda, D.; Roy, S.; Bhattacharyya, B. *Biochemistry* **1992**, *31*, 9709; (b) Deniz, A. A.; Laurence, T. A.; Beligere, G. S.; Dahan, M.; Martin, A. B.; Chemla, D. S.;. Dawson, P. E.; Schultz, P. G.; Weiss, S. *Proc. Natl. Acad. Sci.* U.S.A. **2000**, *97*, 5179; (c) Mukhopadhyay, J.; Kapanidis, A. N.; Mekler, V.; Kortkhonjia, E.; Ebright, Y. W.; Ebright, R. H. *Cell* **2001**, *106*, 453.

[3.2.20] Rohatgi Mukherjee, K. K. *Fundamentals of Photochemistry*, Wiley Eastern, New Delhi, 1986.

[3.2.21] Förster, T. *Discuss. Faraday Soc.* **1959**, *27*, 7.

[3.2.22] Sen, T.; Haldar, K. K.; Patra, A. *J. Phys. Chem. C* **2008,** *112,* 17945.

[3.2.23] (a) Guharay, J.; Sengupta, B.; Sengupta, P. K. *Proteins: Struct. Funct. Genet.* **2000**, *43*, 75; (b) Sengupta, B.; Sengupta, P. K. *Biochim. Biophys. Res. Commun.* **2002**, *299*, 400; (c) Sengupta, B.; Sengupta, P. K. *Biopolymer* **2003**, *72*, 427.

[3.2.24] (a) Sen, P.; Roy, D.; Sahu, K.; Mondal, S. K.; Bhattacharya, K. *Chem. Phys. Lett.* **2004**, *395*, 58; (b) Baughter, J. F.; Grossweiner, L. I.; Lewis, *J. Chem. Soc., Faraday Trans II* **1974**, *70*, 1389.

[3.2.25] Cui, F. L.; Fan, J.; Ping, L. J.; Hu, Z. *Bioorg. Med. Chem.* **2004**, *12*, 151.

APPENDIX

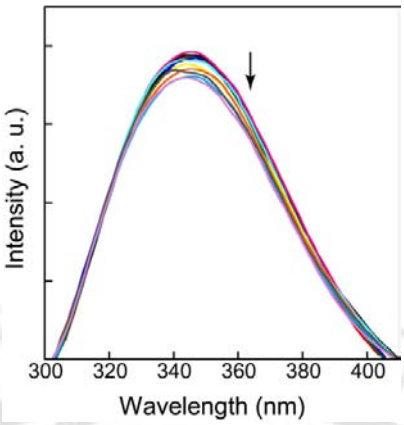

Figure A3.2.1. Emission spectra of BSA with increasing amount of DMSO from 0 to 15% in an aqueous solution.

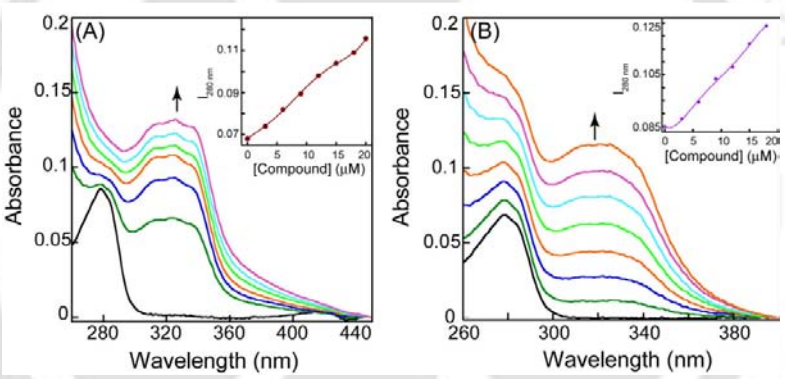

Figure A3.2.2. Absorption spectra of BSA with increasing concentration of (A) Compound **2** and (B) Compound **3** in an aqueous buffer solution. Inset shows the absorbance of BSA at 280 nm as a function of compounds concentration.

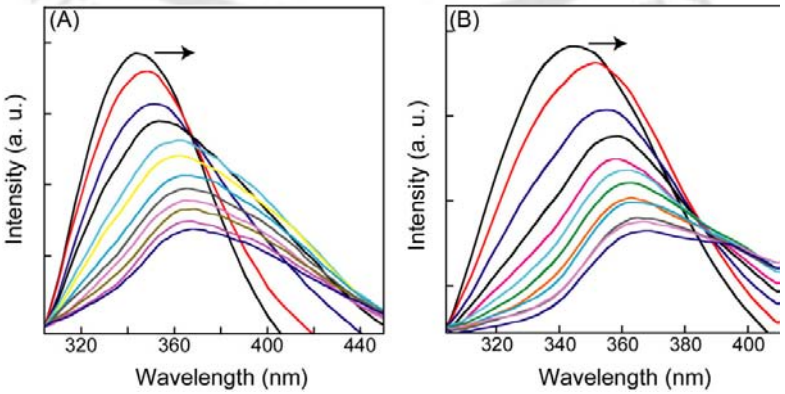

Figure A3.2.3. Fluorescence spectra of BSA with increasing concentration of (A) Compound **2** and (B) Compound **3** in 10 mM phosphate buffer of pH 7.0.

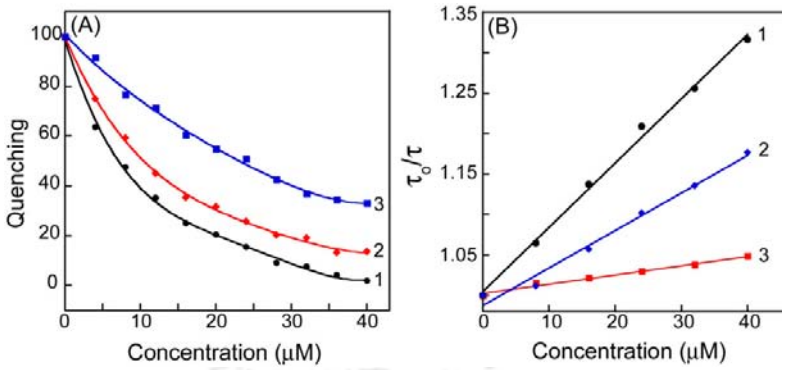

Figure A3.2.4. (A) Quenching of fluorescence intensity of BSA as a function of compounds concentration and (B) Lifetime decay of BSA as a function of compounds concentrations. Where τ_o and τ are the mean lifetime of BSA in absence and presence of compounds.

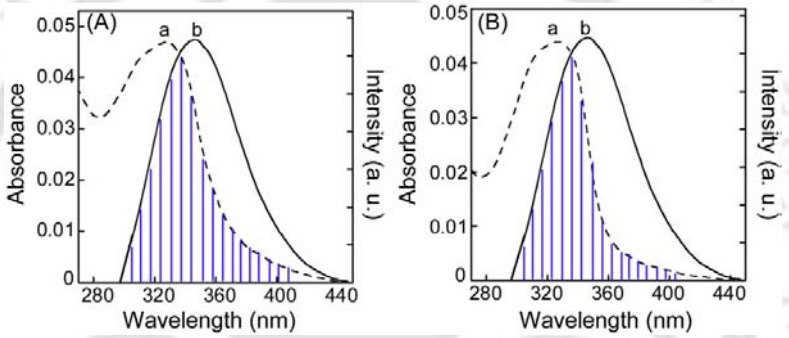

Figure A3.2.5. Overlapping fluorescence spectra of BSA (b, solid line) with absorption spectra of (A) Compound **2** (a, dotted line) and (B) Compound **3** (a, dotted line). [BSA] = 3 μM and [compound] = 3 μM.

Chapter 4

Role of N-Methyl-8-(Alkoxy)quinolinium Iodide Amphiphile in Suppression of Protein-Protein Interactions

4.1. Introduction

A wide range of human pathologies are associated with the conversion of polypeptide chains from their soluble states into well-organized fibrillar aggregates having extensive β-sheet structure.[4.1] Recent findings indicate that soluble oligomers of proteins which are precursors in the pathway leading to insoluble amyloid fibrils are the toxic species.[4.2] Also, in most cases where protein aggregation and disease associated phenotypes were separated in time, fibrous proteinacious inclusions were observed well after the onset of the behavioural or neuropathological symptoms.[4.3] Clearly, the soluble aggregates formed early in the aggregation pathway seem to play a major role in the neurodegenerative diseases. Such disorders, which may collectively be grouped as "protein deposition diseases," include neurodegenerative conditions, such as Alzheimer's disease, Parkinson's disease and the spongiform encephalopathies. They also include systemic amyloidoses, such as light chain and lysozyme amyloidoses, familial amyloid polyneuropathy and dialysis-related amyloidosis, as well as localized amyloidoses, including type II diabetes and aortic medial amyloidosis. Overall, more than 40 human protein deposition diseases have been described so far, each having a distinct clinical profile and each associated with the aggregation of a single dominant peptide or protein.

Some of the protein deposition disorders result from the aggregation of unstructured peptides, intrinsically disordered proteins or unfolded fragments of otherwise folded proteins. Many of the polypeptide chains undergoing aggregation in protein deposition diseases are, however, globular proteins—that is, they normally adopt under physiological conditions a cooperative and persistent fold in which well-defined secondary and tertiary structures are present. Examples include immunoglobulin light chains, transthyretin, β2-microglobulin, lysozyme (Fig. 4.1), various forms of ataxins, superoxide dismutase and prolactin.[4.1] In these highly evolved states, the propensity of proteins to aggregate is generally very low.[4.4] Nevertheless, such folded proteins, and indeed many similar proteins that are not

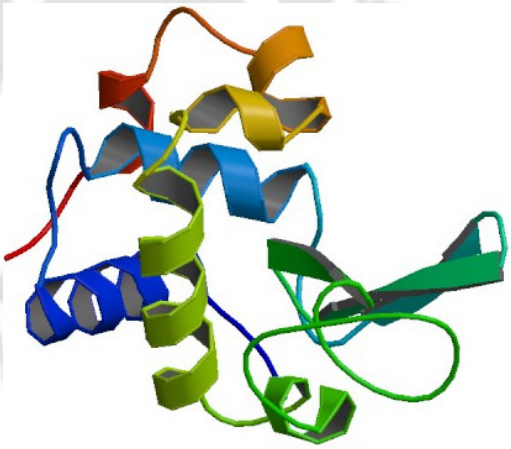

Figure 4.1. Ribbon Drawing of lysozyme. The structure was obtained from the Protein Data Bank (ID code 1HEM).

associated with disease, have been shown in vitro to undergo amyloid fibril formation readily under solution conditions that promote their partial unfolding, such as at low pH,[4.5] high pH,[4.6] high temperature,[4.7] high pressure,[4.8] and in the presence of co-solvents.[4.9]

Protein aggregation is a multi-step process with several intermediates; hence varied approaches at different stages are being used to block the growth of protein oligomers either in vitro or in vivo.[4.10] One of the promising strategies to prevent protein aggregation is to stabilize their native state by small molecules.[4.11] As the native structure of protein undergoes partial unfolding before aggregation, stabilization of the native state may increase the activation energy barrier, thereby slowing the aggregation kinetics and moving away from amyloidgenic state.[4.12] Hen egg white lysozyme (HEWL) has been used as a model protein to study fibril formation in vitro[4.13] as its structure and folding mechanisms have been extensively characterized as shown in figure 4.1.[4.14] These features make lysozyme an interesting model for the study of amyloid aggregation. HEWL can be converted to amyloid fibrils under environmental conditions of high pH[4.6] or low pH and elevated temperatures.[4.13,4.15] The fibrils formed from HEWL share similar characteristics to other amyloids and are toxic to cultured cells. Thus, inhibition or reversion of amyloid aggregation may represent a possible therapeutic strategy for the prevention and treatment of amyloid diseases.[4.16]

There is a great deal of interest for developing small molecule inhibitors of protein misfolding and aggregation due to a growing number of pathologic states known as amyloid disorders. In this context small molecules which bind to and stabilize the monomeric protein have invited attention owing to their ability to significantly slow down or inhibit aggregation and amyloid formation should be considered in strategies aimed at the development of novel therapeutic agents. In searching for alternative ways to reduce amyloid fibrils or inhibit amyloid formation, the fourth chapter of the thesis describes the inhibitory effect of cationic amphiphiles *viz.* N-methyl-8-(alkoxy)quinolinium iodide [(**4-6**), (Fig. 4.2)] on aggregation behavior of hen egg white lysozyme (HEWL) at alkaline pH using congo red (CR) and thioflavin T (ThT) binding assays along with the atomic force

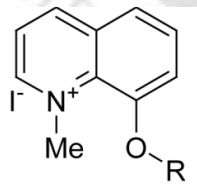

Where, R= C_4H_9 (**4**), C_8H_{17} (**5**) and $C_{12}H_{25}$ (**6**)

Figure 4.2. Structure of compounds (**4-6**).

microscopy (AFM). The synthetic procedure of the compounds has been described in chapter 2. In this study, the cation (head group) of the amphiphile was preserved but the aliphatic counterpart (tail group) was altered, to generate a variation in the structure and their subsequent effect as an inhibitor for amyloid formation as shown in figure 4.2.

4.2. Methods

4.2.1. Sample Preparation

Stock of HEWL and N-methyl-8-(alkoxy)quinolinium iodide were freshly prepared in deionised water and DMSO. Aggregation was induced by dissolving the HEWL solutions of 1 mg/mL (70 μM) by in a 50 mM phosphate buffer of pH 12.2, while the concentration of compounds used for inhibitory effect on HEWL aggregation was 30 and 60 μM. To assess the effect of inhibitors, control samples which contained no inhibitor but were identical otherwise were run in parallel. All experiments were performed at room temperature (RT).

4.2.2 Congo Red Binding Assay

After overnight incubation of HEWL (70 μM) either alone or in presence of amphiphilic compounds (30 and 60 μM) in 50 mM phosphate buffer of pH 12.2 was mixed with a freshly prepared aqueous solution of CR (20 μM). Emission spectrum of CR in presence of HEWL under different experimental conditions was measured using excitation wavelength of 490 nm and slit width of 5 nm.

4.2.3 Thioflavin T Binding Assay

Time dependent kinetics of HEWL amyloid formation was monitored by thioflavin T (ThT) binding assay. After overnight incubation (~12 h), 70 μM of HEWL in 50 mM phosphate buffer of pH 12.2, either alone or in presence of compound (30 and 60 μM) was transferred to a freshly prepared aqueous solution of ThT diluted with 20 mM, glycine-glycine buffer of pH 8.5, in such a way so that the molar concentration of ThT was twofold excess over HEWL in the assay medium. The protein was typically ~10 μM in the assay medium after dilution. The samples were excited at 450 nm and subsequent fluorescence emission between 470 and 550 nm using slit width of 5 nm was recorded at different time intervals.

4.2.4 Atomic Force Microscope

HEWL samples incubated under different experimental conditions were diluted 2 fold in incubating buffer and added to freshly cleaved mica. After a few minutes, these were rinsed with deionised water to remove unabsorbed sample and dried at room temperature. AFM measurements were performed on Picoplus microscope (Molecular Imaging, USA) under non contact or MAC MODE.

4.3. Results and Discussion

4.3.1. Binding of Compounds with HEWL

Proteins fluorescence was a sensitive tool to investigate the interaction with ligands or other compounds. Protein fluorescence is mainly due to the presence of tryptophan (Trp) and is widely used as a tool to monitor changes in proteins structure and to make inferences regarding local structure and dynamics.[4.17] Hence, in order to investigate the interactions between amphiphilic compounds and HEWL steady state fluorescence spectroscopy has been employed. Binding of compounds with HEWL samples incubated overnight with compounds were ascertained by comparing tryptophan emission spectra of compounds bound HEWL with unbound one. The fluorescence spectrum of HEWL presents strong emission at 345 nm, when excited at 295 nm in an aqueous buffer solution of pH 7.0. Excitation wavelength of 295 nm was chosen to avoid the contribution from the tyrosine residues in proteins and compounds (**4**-**6**) were non-fluorescent under the present experimental conditions. The overnight incubation of HEWL with compounds leads to a significant change in its fluorescence spectrum, indicating significant interaction of compounds with HEWL (Fig. 4.3). Figure depicts that the overnight incubation of HEWL with compounds at pH 7.0 results in diminished fluorescence intensity accompanied by blue shift in λ_{max} of HEWL by ~8 nm upon

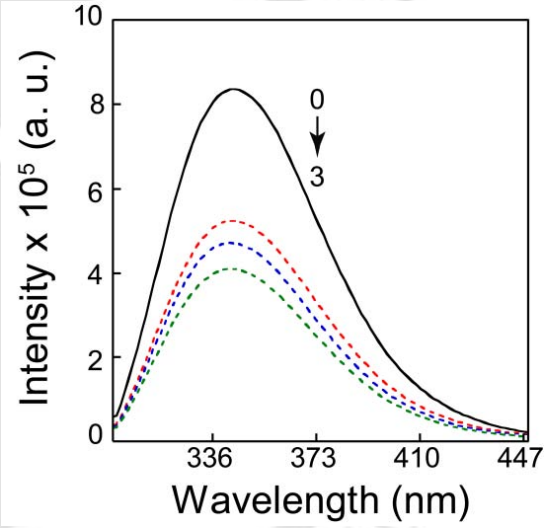

Figure 4.3. Emission spectra of HEWL in absence (solid line) and presence of different compounds (dotted line) in phosphate buffer of pH 7.0.

complexation with compounds. The blue shift in the HEWL–compound composites arises due to the change in the environment of tryptophan from a solvent exposed region to a relatively more non-polar environment in presence of compounds,[4.18] confirmed the binding of compounds with HEWL.

4.3.2. Congo Red Absorbance Assay

As protein starts to aggregate, the spectral properties of congo red (CR) exhibits a considerable red shift along with a increase in absorbance maxima.[4.19] Hence, CR absorbance property has been used to investigate the inhibitory effect of compounds on HEWL aggregation process (Fig. 4.4) at alkaline pH. When the protein starts to aggregate the solutions of CR suspension changed from an orange-red to a rose color. The result shown in figure 4.4 demonstrates that spectral correlate of the color change. There is a hyperchnomicity and a shift of the absorbance maximum of CR when protein starts to aggregate as the time progress. The absorbance of CR at ~514 nm in presence of HEWL incubated with and without compounds has been plotted as a function of incubation time (Fig. 4.4D) along with the change in wavelength maxima as a function of time (Appendix, Fig. A4.1). The HEWL sample alone exhibited a greater absorbance difference and wavelength maxima, which is indicative of a strong binding affinity between CR dye and HEWL, thus, signifying a higher degree of aggregate formation. The control sample of HEWL without compounds shows a shift of CR wavelength maxima from 490 to 514 nm, while in presence of compound **4**, **5** and **6** the shift was from 490 to 514, 512 and 510 nm respectively (Appendix, Fig. A4.1). The results also revealed that the change in CR absorbance and wavelength maxima with HEWL was found to depend on the compound concentrations tested (Fig. 4.4D). It also inferred from the figure that in presence of compound **4** the change in absorbance and wavelength maxima of CR samples with HEWL is the least followed by **5** and **6** compared with the control sample having no compound indicating the fact that compounds ability to arrest the growth of HEWL aggregate decreases with decreasing alkyl chain length indicating the significance contribution of their hydrophobicity in the antiaggregant process. The absorbance spectra of CR in presence of compounds (the control sample) have been also examined to check their effect on dye and found that compounds by themselves did not alter the CR spectral property at the concentrations examined. Thus lower absorbance of CR samples with

HEWL in presence of compounds at alkaline pH could be attributed to attenuation of fibrillation.

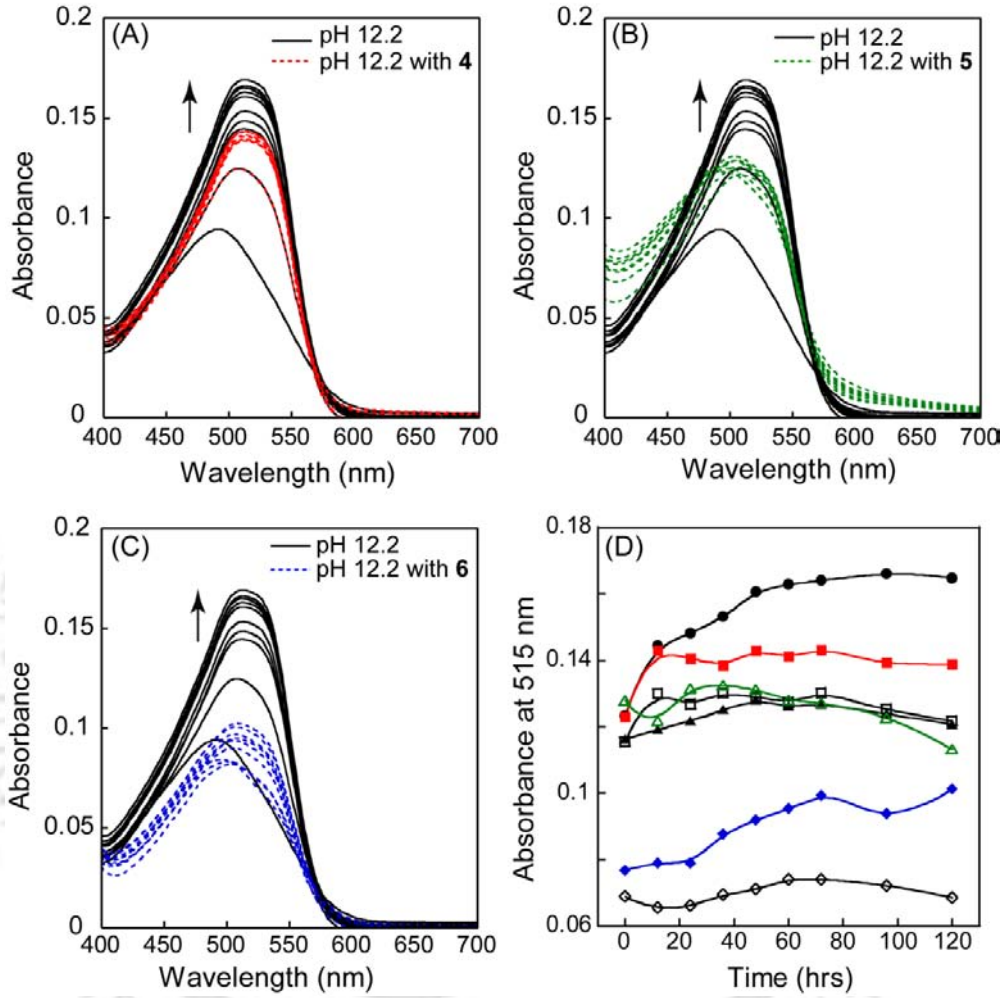

Figure 4.4. CR absorbance in presence of HEWL under different experimental conditions: (A) Without (solid line) and with compound **4** (dotted line), (B) Without (solid line) and with compound **5** (dotted line), (C) Without (solid line) and with compound **6** (dotted line) and (D) Plot of CR absorbance in presence of HEWL at different concentration of compounds as a function of incubation time. Lysozyme without compound at pH 12.2 (●), lysozyme at pH 12.2 with 30 (■) and 60 µM (□) of compound **4**, 30 (▲) and 60 µM (Δ) of compound **5**, 30 (♦) and 60 µM (◊) of compound **6**.

4.3.3. Congo Red Fluorescence Assay

Congo red also shows a fluorescent activity when bound to amyloid fibrils or in amyloidogenic conditions, which tends to be used as a sensitive diagnosis tool for amyloidosis.[4.20] It is believed that it hydrogen bonds to the beta pleated sheet structure of amyloid with the dye molecules aligned in a very regular manner. Hence, the inhibitory

effect of these compounds, on aggregation behavior of HEWL was also examined *via* CR fluorescence measurements as shown in figure 4.5. It evident from figure 4.5D the CR fluorescence intensity in presence of HEWL at pH 12.2 by itself increased dramatically in the first 60 h and then reached a plateau. In contrast, the pH 7.0 samples revealed a relatively low fluorescence intensity that remained fairly invariant with time (Fig. 4.5D). The results also revealed that the reduction level of HEWL aggregation was dependent upon the compound concentrations tested (30 and 60 µM). For instance, after incubation for 120 h, the percentages of the maximum CR fluorescence intensity in presence of HEWL samples incubated with 30 and 60 µM of compounds **4**, **5** and **6** were 88 and 83, 62 and 51 and 51 and 21 respectively (Appendix Fig. A4.3).

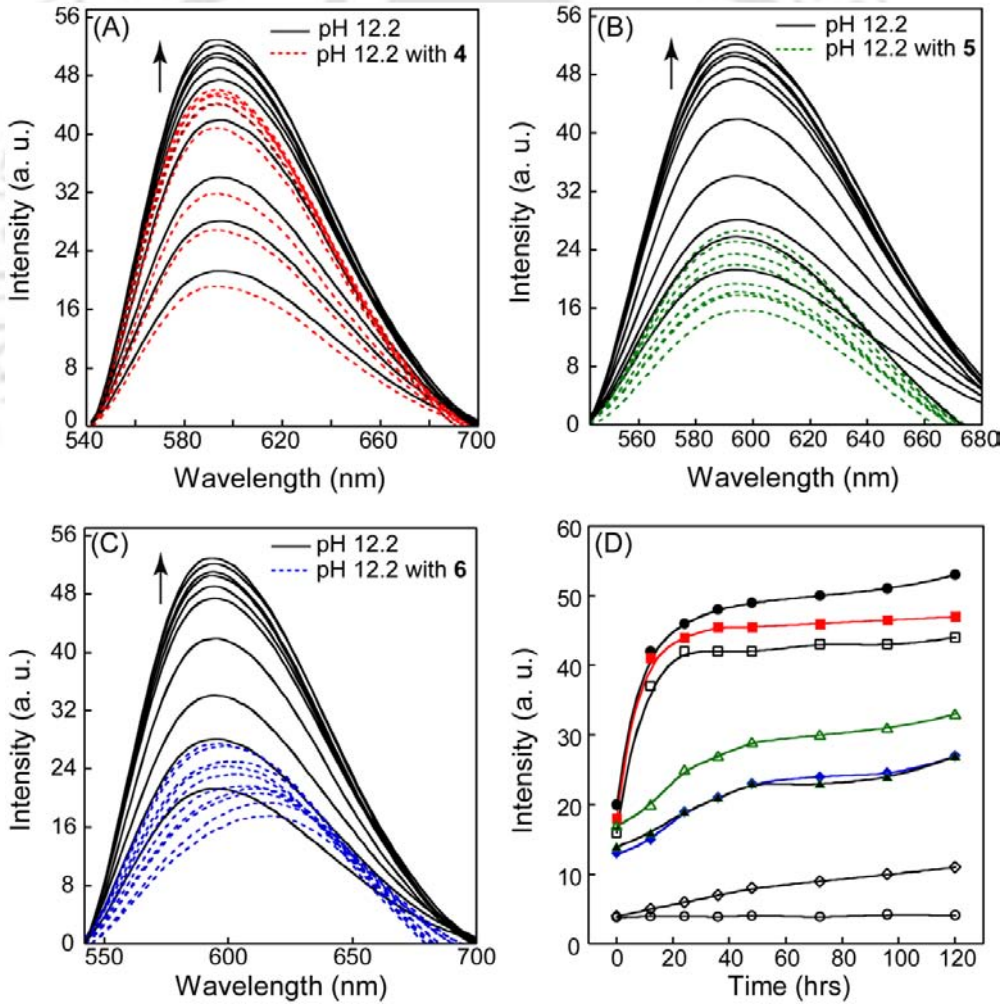

Figure 4.5. CR fluorescence in presence of HEWL under different experimental conditions: (A) Without (solid line) and with compound **4** (dotted line), (B) Without (solid line) and with compound **5** (dotted line), (C) Without (solid line) and with compound **6** (dotted line) and (D) Plot of CR fluorescence intensity in

presence of HEWL at different concentration of compounds as a function of incubation time. Lysozyme without compound at pH 12.2 (●) and pH 7.0 (○), lysozyme at pH 12.2 with 30 (■) and 60 μM (□) of compound **4**, 30 (▲) and 60 μM (Δ) of compound **5**, 30 (♦) and 60 μM (◊) of compound **6**.

The data also showed that HEWL sample incubated with compound **6** had a significantly smaller final CR fluorescence intensity than that of sample having compound **5** and **4** in the same concentration range, implying that considerably smaller amount of aggregate was present in HEWL samples in presence of compound **6** and **5** as compared with that of compound **4**. Notably, it has been also found that compounds by itself unable to quench the CR fluorescence at the concentrations examined in this study (Appendix, Fig. A4.2). Therefore, the reduction in CR fluorescence observed in the samples could be attributed to the arrest of aggregation of HEWL by the addition of compounds.

4.3.4. Thioflavin T Fluorescence Assay

ThT binds to beta sheets, such as those in amyloid oligomers and undergoes a characteristic blue shift of its emission spectrum.[4.21] It has been claimed that ThT will not undergo this blue shift upon binding to precursor monomers or small oligomers,[4.22] or to unaggregated material with a high beta sheet content,[4.23] and that blue shift is only observed if amyloid fibrils are present. Hence, in order to ascertain the amyloid characteristics of the aggregates formed, the binding of ThT with HEWL has been examined as a function of incubation time for a period of ~120 h (Fig. 4.6). As expected, a higher intensity and a gradual rise in ThT fluorescence for the sample of pH 12.2 have been observed with the progression of time due to the amyloidogenic conditions. It is therefore likely that amyloid-like aggregates are being formed on prolonged exposure of HEWL at alkaline pH. In figure 4.6D, the results also revealed that the reduction level of HEWL aggregation was dependent upon the compound concentrations tested (30 and 60 μM) similar that observed in case of CR binding assay in the previous section. For instance, after incubation for 120 h, the percentages of maximum ThT fluorescence intensity in presence of HEWL samples incubated with 30 and 60 μM compounds **4**, **5** and **6** were 97 and 90, 80 and 63, and 63 and 53 respectively (Appendix Fig. A4.3). Notably, it has been found that compounds are unable to quench ThT fluorescence at the concentrations examined in this study (Appendix, Fig. A4.2), indicating the reduction in ThT fluorescence observed in the HEWL samples incubated with compounds **5** and **6** could be attributed to attenuation of fibrillation. This indicates that the presence of either

compound **5** or **6** is effective in preventing the formation of amyloid-like aggregates of HEWL on exposure to alkaline pH.

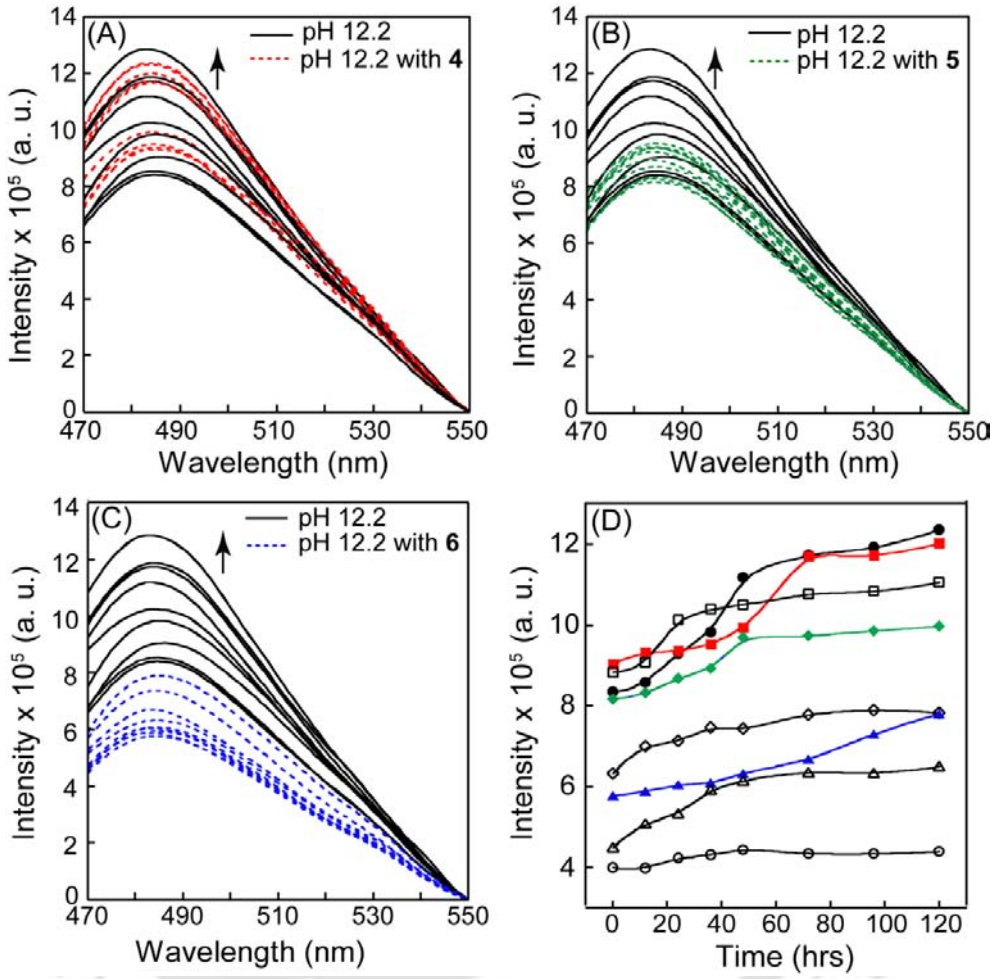

Figure 4.6. ThT fluorescence in presence of HEWL under different experimental conditions: (A) Without (solid line) and with compound **4** (dotted line), (B) Without (solid line) and with compound **5** (dotted line), (C) Without (solid line) and with compound **6** (dotted line) and (D) Plot of ThT fluorescence intensity at different concentration of compounds as a function of incubation time. Lysozyme without compound at pH 12.2 (●) and pH 7.0 (○), lysozyme at pH 12.2 with 30 (■) and 60 µM (□) of compound **4**, 30 (♦) and 60 µM (◊) of compound **5**, 30 (▲) and 60 µM (Δ) of compound **6**.

4.3.5. Atomic Force Microscope Imaging

To further confirm the presence of amyloid fibrils of HEWL and to observe the morphology of aggregated protein under different experimental conditions, atomic force microscopy was employed. In figure 4.7, panel A, B, D, E and F displays the representative micrographs of HEWL alone at pH 7.0 and at pH 12.2, HEWL at pH 12.2

with 60 μM of compound **4**, **5** and **6.** In panel A, the monomeric HEWL appears at neutral pH as expected, while in panel B the amorphous aggregates of HEWL with heterogeneity in size and shape appears at alkaline pH, along with some ordered aggregates resembling amyloid fibrils (panel C) after 240 hrs of incubation in absence of any additives. These differences in morphology of aggregates suggest that protein can exist as a mixture of amorphous or fibrillar forms under similar experimental conditions. Similarly, in presence of compound **4** at pH 12.2, HEWL showed a heterogeneous mixture of amorphous aggregates in panel D similar to panel B, indicating that HEWL oligomerisation is not completely arrested in prior presence of compound **4**. These results are also consistent with the enhanced fluorescence intensity of CR and ThT in samples having HEWL alone and with compound **4**. Neither the ordered fibrillar of HEWL nor large amorphous aggregates were observed in presence of compound **5** and **6** (panel E and F), resembled with low fluorescence intensity of CR and ThT, clearly demonstrating the inhibitory effect of compounds on HEWL aggregation.

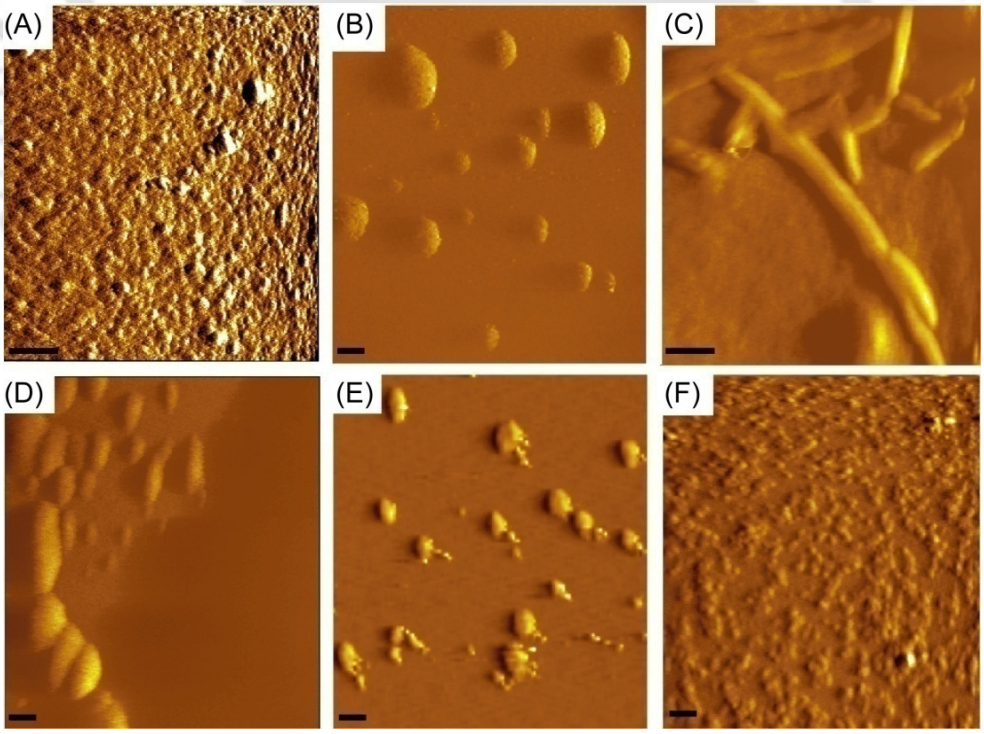

Figure 4.7. AFM images of HEWL at specified times under different experimental conditions: (A) Native lysozyme at pH 7.0, (B) Lysozyme incubated at pH 12.2, (C) Lysozyme incubated at pH 12.2, (D) Lysozyme incubated with compound **4** (60 μM) at pH 12.2, (E) Lysozyme incubated with compound **5** (60 μM) at pH 12.2, (F) Lysozyme incubated with compound **6** (60 μM) at pH 12.2. The images have taken after 240 hrs of incubation time and the scale bar denotes 100 nm.

4.3.6 Mechanism of Inhibition

Increased in CR and ThT fluorescence intensity after binding with HEWL at pH 12.2 (Fig. 4.5 and 4.6) compared with the control at pH 7.0 suggests a significant unfolding of the protein at alkaline pH and formation of aggregates. CR and ThT are known to show an enhanced fluorescent activity with the growth of aggregates. It is possible that hydrophobic regions of the protein are exposed in this process and act as a driving force for the aggregation process latter stabilized by intermolecular disulfide linkages.[4.6] In order to understand the inhibitory effect of amphiphilic compounds on HEWL aggregation was either due to cationic head group or as a consequence of aliphatic tail group, some additional control experiments with the neutral counterpart of the compound [8-(alkoxy)quinoline] and the parent non-amphiphilic compound (8-hydroxyquinoline) independently have been pursued (Appendix, Fig. A4.4). The control samples were unable to arrest the growth of HEWL aggregates under identical experimental conditions, depicting the fact that the cationic head group as well as the aliphatic tail group of the compound is indispensable for inhibition of aggregation process and removal of either head group or the hydrocarbon chain from the compound obliterates its ability to do the same. The lower potency of compound **4** (with four methylene group) relative to **5** (with eight methylene group) and **6** (with twelve methylene group) suggests the role of hydrophobic interactions involving the length of the aliphatic chain do make a positive contribution to the antiaggregant process. Thus the amphiphilic nature (both cationic head and aliphatic tail group) of the compound may influence the interaction of compounds with the solvent and the protein as well. It is apparent that increasing the exposure of hydrophobic surfaces mirrors the growth of HEWL aggregates by lowering the energy barrier for nucleation. It is therefore quite likely that amphiphilic compounds will favorably bind to these available hydrophobic regions in HEWL thereby not only diminishing their exposure to polar solvent but also halting the aggregation. It could be presumed from our results that the compound could directly bind to the partially unfolded protein and this binding can assist in stabilizing the protein, as its functional groups are more exposed to the environment and it can inhibit fibril formation by interfering with protofibril or globular aggregates and subsequently fibril formation as shown in figure 4.8.

One type of non-covalent interactions through which compounds may be affecting the protein stability would be through the formation of aromatic-π interactions.[4.24] The results

from this selection also correlate well with the previously described selections with both antibodies and peptides, where aromatic residue rich sequences are strongly favored.[4.25] Lysozyme has a high percentage of aromatic amino acids with six tryptophan residues. As the protein undergoes partial unfolding, the aromatic residues are more exposed and, therefore, aromatic-π interaction between the head group of the compound and those exposed aromatic residues could take place ultimately resulting in protein stabilization. Additionally, if these aromatic residues are involved in oligomer-oligomer interactions, presence of aromatic-π interactions could also slow down the rate of fibril formation.[4.26]

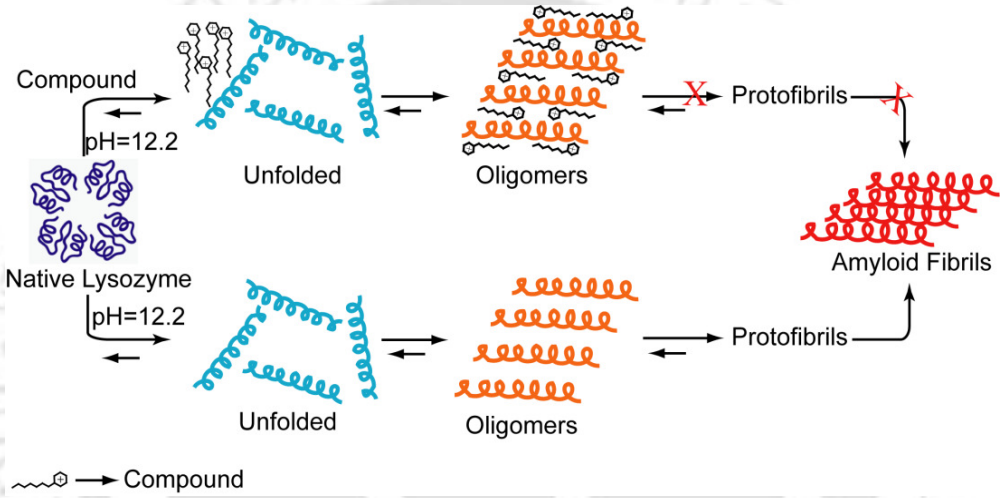

Figure 4.8. Schematic illustration showing the role of compounds in arresting the growth of aggregates.

4.4. Conclusions

In conclusion this work demonstrates the potential of quinolinium based cationic amphiphiles in suppression of HEWL aggregation at alkaline pH *via* CR and ThT binding assay experiments along with AFM techniques. It could be deduced from the aforementioned results that compounds could directly bind to the partially unfolded protein and the binding can assist in stabilizing the protein. The control experiments also depict the fact that the cationic head group as well as the aliphatic tail group of compound is indispensable for inhibition of aggregation process and removal of either head group or the hydrocarbon chain from the compound obliterates its ability to do the same. Compounds **5** and **6** appear more potent in halting the growth of aggregates compared with **4** in μM concentration range. The current results are informative and can provide an aid in designing potential targets for molecular therapeutics in the prevention or retardation of amyloid formation implicated in pathological diseases.

References

[4.1] (a) Selkoe, D. J. *Nature* **2003***, 426,* 900; (b) Westermark, P.; Benson, M. D.; Buxbaum, J. N.; Cohen, A. S.; Frangione, B.; Ikeda, S.; Masters, C. L; Merlini, G.; Saraiva, M. J.; Sipe, J. D.; Amyloid: toward terminology clarification. Report from the Nomenclature Committee of the International Society of Amyloidosis. *Amyloid* **2005**, *12*, 1; (c) Chiti, F.; Dobson, C. M. *Annu. Rev. Biochem.* **2006**, *75*, 333.

[4.2] (a) Walsh, D. M.; Klyubin, I.; Fadeeva, J. V.; Cullen, W. K.; Anwyl, R.; Wolfe, M. S.; Rowan, M. J.; Selkoe, D. J. *Nature* **2002**, *416*, 535; (b) Bucciantini, M.; Giannoni, E.; Chiti, F.; Baroni, F.; Formigli, L.; Zurdo, J.; Taddei, N.; Ramponi, G.; Dobson, C. M.; Stefani, M. *Nature* **2002**, *416*, 507; (c) Lambert, M. P.; Barlow, A. K.; Chromy, B. A.; Edwards, C.; Freed, R.; Liosatos, M.; Morgan, T. E.; Rozovsky, I.; Trommer, B.; Viola, K. L. *Proc. Natl. Acad. Sci. USA* **1998**, *95*, 6448.

[4.3] Caughey, B.; Lansbury Jr., P. T. *Annu. Rev. Neurosci.* **2003**, *26*, 267.

[4.4] Bemporad, F.; Calloni, G.; Campioni, S.; Plakoutsi, G.; Taddei, N.; Chiti, F. *Acc. Chem. Res.* **2006**, *39*, 620.

[4.5] (a) Guijarro, J. I.; Sunde, M.; Jones, J. A.; Campbell, I. D.; Dobson, C. M. *Proc. Natl. Acad. Sci. USA* **1998**, *95*, 4224. (b) McParland, V. J.; Kad, N. M.; Kalverda, A. P.; Brown, A.; Kirwin-Jones, P.; Hunter, M. G.; Sunde, M.; Radford, S. E. *Biochemistry* **2000**, *39*, 8735.

[4.6] Kumar, S.; Ravi, V. K.; Swaminathan, R. *Biochim. Biophys. Acta* **2009**, *1794*, 913.

[4.7] (a) Litvinovich, S. V.; Brew, S. A.; Aota, S.; Akiyama, S. K.; Haudenschild, C.; Ingham, K. C. *J. Mol. Biol.* **1998**, *280*, 245; (b) Fändrich, M.; Fletcher, M. A.; Dobson, C. M. *Nature* **2001**, *410*, 165.

[4.8] (a) Ferrão-Gonzales, A. D.; Souto, S. O.; Silva, J. L.; Foguel, D. *Proc. Natl. Acad. Sci. USA* **2000**, *97*, 6445; (b) De Felice, F. G.; Vieira, M. N. N. Meirelles, M. N. L.; Morozova-Roche, L. A.; Dobson C. M. Ferreira, S. T. *FASEB J.* **2004**, *18*, 1099.

[4.9] (a) Chiti, F.; Webster, P.; Taddei, N.; Clark, A.; Stefani, M.; Ramponi, G.; Dobson, C. M. *Proc. Natl. Acad. Sci. USA* **1999,** *96*, 3590; (b) Schmittschmitt, J. P.; Scholtz, J. M. *Protein Sci*., **2003,** *12*, 2374.

[4.10] (a) Rochet, J. C. *Exp. Rev. Mol. Med.* **2007**, *9*, 1; (b) May, B. C.; Govaerts, C.; Cohen, F. E. *Neurology* **2006**, *66*, 118.

[4.11] Johnson, S. M.; Wiseman, R. L.; Sekijima, Y.; Green, N. S.; Adamski-Werner, S. L.; Kelly, J. W. *Acc. Chem. Res.* **2005,** *38,* 911.

[4.12] Hammarstrom, P.; Wiseman, R. L.; Powers, E. T.; Kelly, J. W. *Science* **2003**, *299*, 713.

[4.13] (a) Morozova-Roche, L. A.; Zurdo, J.; Spencer, A.; Noppe, W.; Receveur, V.; Archer, D. B.; Joniau, M.; Dobson, C. M. *J. Struct. Biol.* **2000**, *2*, 339; (b) Makin, O. S.; Serpell, L. C. *FEBS J.* **2005**, *23*, 5950; (c) Krebs, M. R.; Wilkins, D. K.; Chung, E. W.; Pitkeathly, M. C.; Chamberlain, A. K.; Zurdo, J.; Robinson, C. V.; Dobson, C. M. *J. Mol. Biol.* **2000**, *3*, 541; (d) Vernaglia, B. A.; Huang, J.; Clark, E. D. *Biomacromoclecules* **2004**, *5*, 1362.

[4.14] (a) Frare, E.; Mossuto, M. F.; Polverino de Laureto, P.; Dumoulin, M.; Dobson, C. M.; Fontana, A. *J. Mol. Biol.* **2006**, *3*, 551; (b) Greaves, T. L.; Drummond, C. J. *Chem. Rev.* **2008**, *1*, 206; (c) Rogers, R. D.; Seddon, K. R. *Science* **2008**, *302*, 792.

[4.15] Cao, A.; Hu, D.; Lai, L. *Protein Sci.* **2004**, *2*, 319.

[4.16] (a) De Felice, F. G.; Vieira, M. N. N.; Saraiva, L. M. *FASEB J.* **2004**, *18*, 1366; (b) De Felice, F. G.; Ferreira, S. T. *Cell Mol. Neurobiol.* **2002**, *22*, 545; (c) De Felice, F. G.; Houzel, J. C.; Garcia-Abreu, J.

FASEB J. **2001**, *15*, 1297; (d) Kisilevsky, R.; Szarek, W. A.; Ancsin, J. B. *Am. J. Pathol.* **2004**, *164*, 2127; (e) Lee, E. N.; Cho, H. J.; Lee, C. H.; Lee, D.; Chung, K. C.; Paik, S. R. *Biochemistry* **2004**, *43*, 3704; (f) Raghu, P.; Reddy, G. B.; Sivakumar, B. *Arch. Biochem. Biophys.* **2002**, *400*, 43.

[4.17] Lakowicz, J. R. Principles of Fluorescence spectroscopy, 2nd ed.; Kluwer Academic/Plenum Publishers: New York, 1999.

[4.18] Kumagai, I.; Sunada, F.; Takeda, S.; Miura, K. *J. Biol. Chem.* **1992**, *267*, 4608.

[4.19] (a) Khurana, R.; Gillespie, J. R.; Talapatra, A.; Minert, L. J.; Ionescu-Zanetti, C.; Millett, I.; Fink, A. L. *Biochemistry* **2001**, *40*, 3525; (b) Shashilov, V. A.; Lednev, I. K. *J. Am. Chem. Soc.* **2008**, *130,* 309.

[4.20] Lillie, R. D. *Conn's Biological Stains*, Williams & Wilkins, Baltimore, MD., U.S.A.

[4.21] LeVine III, H. *Methods in Enzymology* **1999**, *309*, 274.

[4.22] LeVine III, H. *Prot. Sci.* **1993***, 2*, 404.

[4.23] LeVine III, H. *Amyloid Int. J. Exp. Clin. Invest*. **1995**, *2*, 1.

[4.24] Tsou, I.; Tatko, C. D.; Waters, M. L. *J. Am. Chem. Soc.* **2002**, *124*, 14917.

[4.25] Bucciantini, M.; Giannoni, E.; Chiti, F.; Baroni, F.; Formigli, L.; Zurdo, J. S.; Taddei, N.; Ramponi, G.; Dobson, C. M.; Stefani, M. *Nature* **2002**, *416*, 507.

[4.26] Johnson, R. M.; Hecht, K.; Deber, C. M. *Biochemistry* **2007**, *32*, 9208.

APPENDIX

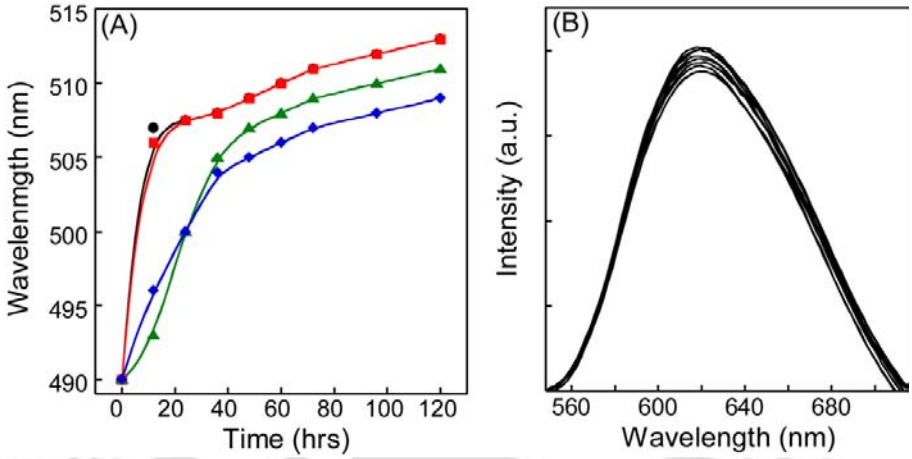

Figure A4.1. (A) Change in the absorbance maxima wavelength of CR in presence of HEWL under different experimental conditions as a function of time. HEWL without compound at pH 12.2 (●), HEWL at pH 12.2 with 30 of compound **4** (■), compound **5** (▲) and compound **6** (♦) and (B) Emission spectra of CR with HEWL at pH 7.0 under different interval of time.

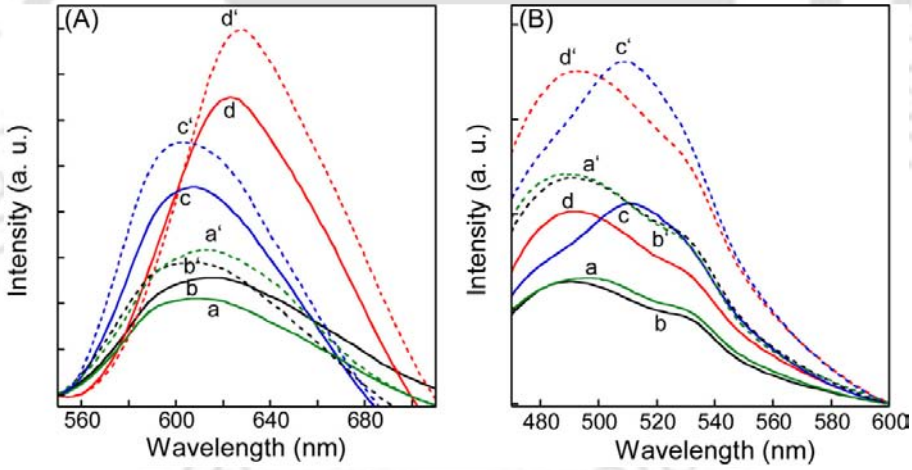

Figure A4.2. Emission spectra of (A) Congo red and (B) Thioflavin T in presence of different concentration of compounds at pH 12.2. Where without compound at 0 hrs (b) and at 24 hrs (b`), with compound **4** at 0 hrs (d) and at 24 hrs (d`), with compound **5** at 0 hrs (c) and at 24 hrs (c`), with compound **6** at 0 hrs (a) and at 24 hrs (a`).

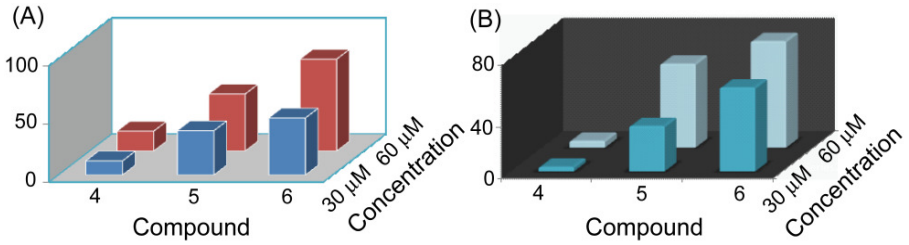

Figure A4.3. Inhibition percentage of HEWL aggregation by compounds estimated by (A) Congo red and (B) Thioflavin T binding assay.

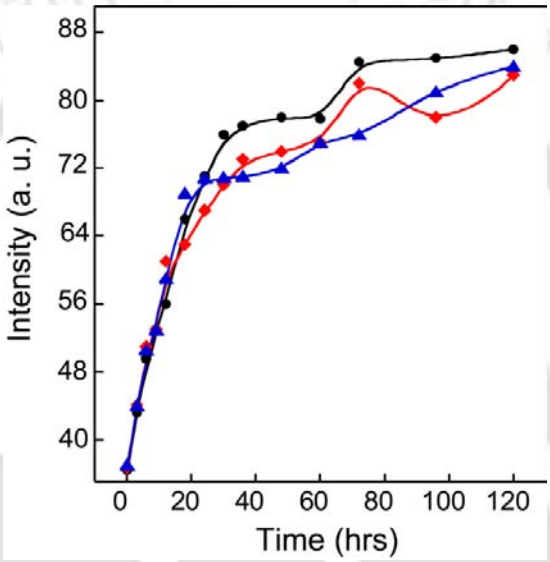

Figure A4.4. Intensity of CR fluorescence in presence of the parent compound (8-hydroxyquinoline) and neutral counterpart of the compound [8-(alkoxy)quinoline]. HEWL alone at pH 12.2 (●), HEWL at pH 12.2 with 8-hydroxyquinoline (♦) and 8-(alkoxy)quinoline (▲).

Chapter 5

Role of 2-(Alkyl)malonic Acid Amphiphile as an Inhibitor of Metalloenzyme

5.1 Introduction

A metalloenzyme is protein having a metal ion as cofactor[5.1] and that has a strong link with the protein part, where the metal is embedded within the molecule. The metal ion is usually coordinated by nitrogen, oxygen or sulfur atoms belonging to amino acids in the polypeptide chain and/or a macrocyclic ligand incorporated into the protein. The metal ion has been placed in environment where its selected function is both kinetically and thermodynamically favorable. Amino acids in their peptide linkage in proteins possess groups with the ability to bind to the metal resulting in coordinate-covalent bonds. The free amino and carboxyl groups in a protein can bind to the metal and this may bind the protein to a specific, active conformation.[5.2] The fact that metals bind to several ligands is important in that metals play a role in bringing remote parts of the amino acid sequence together and help establish an active conformation of the enzyme (Fig. 5.1).

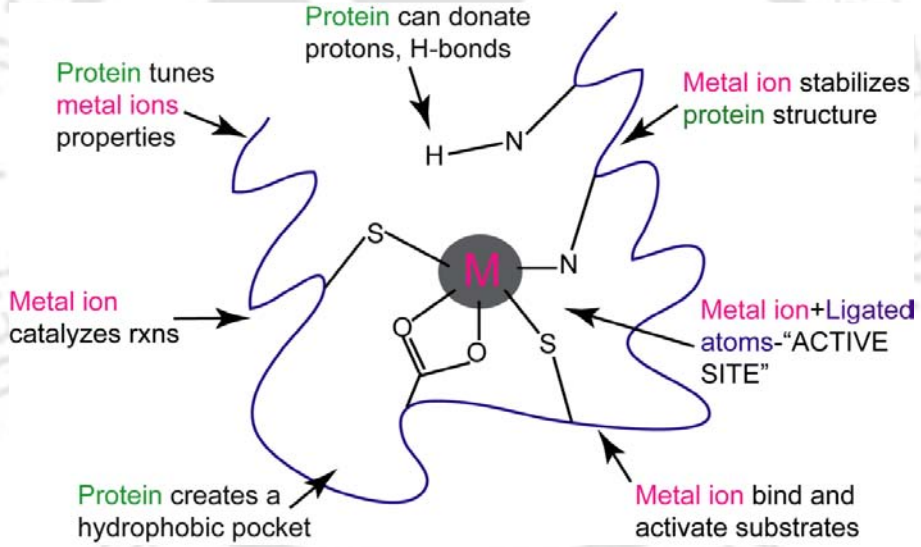

Figure 5.1. General structure of a metalloenzyme showing the role of metal ion.

The metal is usually in the form of an ion, and its main role is to function in enzymatic reactions. Metalloproteins have many different functions in cells, such as enzymes, transport and storage proteins, and signal transduction. Approximately one-third of the known enzymes have metals as part of their structure, require that metals be added for activity, or are further activated by metals.[5.3] The metal sometimes plays a direct role in the generation of active sites, binding and activation of substrates (Fig. 5.1). Some common examples of metalloenzymes include amylases, polymerases, hemoglobins,

cytochromes, phosphotransferases, alcohol dehydrogenase, arginase, ferredoxin, and cytochrome oxidase etc.[5.4]

Enzyme inhibitors are molecules that bind to enzymes and decrease their activity. Since blocking an enzyme's activity can kill a pathogen or correct a metabolic imbalance, many drugs are enzyme inhibitors. They are also used as herbicides and pesticides. Many drug molecules are enzyme inhibitors, so their discovery and improvement is an active area of research in biochemistry and pharmacology. A medicinal enzyme inhibitor is often judged by its specificity (its lack of binding to other proteins) and its potency (its dissociation constant, which indicates the concentration needed to inhibit the enzyme). A high specificity and potency ensure that a drug will have few side effects and thus low toxicity. The binding of an inhibitor can stop a substrate from entering the enzyme's active site and/or hinder the enzyme from catalyzing its reaction. Inhibitor binding is either reversible or irreversible. Irreversible inhibitors usually react with the enzyme and change it chemically. These inhibitors modify key amino acid residues needed for enzymatic activity. In contrast, reversible inhibitors bind non-covalently and different types of inhibition are produced depending on whether these inhibitors bind the enzyme, the enzyme-substrate complex, or both.[5.5]

Malonic acid and its derivatives are an important class of bioactive molecules and they have been used to study the topography of the active center of dicarboxylate transporter in intact rat liver mitochondria.[5.6] These compounds were shown to act as inhibitors of succinate transport[5.7] and fatty acid biosynthesis. The compounds were also tested for their ability to induce interferon-gamma (IFNγ) in cultures of human peripheral blood leukocytes, for the treatment of obesity,[5.8] as a lubrication performance in polar base oils and for methyl oxidation in the animal body.[5.9] Malonic acid itself forms uncharged mono-malonato complexes with divalent cations.[5.10] Substituted malonic acid have been investigated and successfully used as chelating units in magnesium selective ionophores.[5.11] From an extensive bibliographic search in the Cambridge Structural Database, it was found that an overwhelming majority of the magnesium complexes showed an octahedral

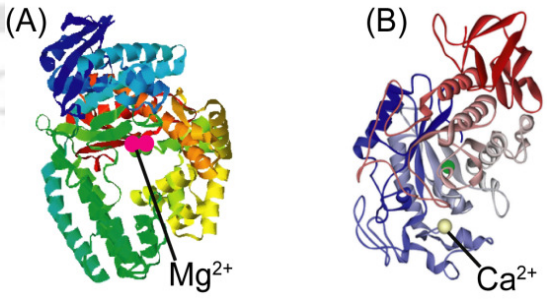

Figure 5.2. Structure of (A) *Taq* polymerase and (B) α-amylase (From PDB 3*KTQ* and 1*SMD*).

co-ordination of magnesium by the ligand atoms. Alkyl substituted malonic acids have also been used as metal extraction reagents for quantitative extraction of metals.[5.12] The strong metal binding ability of these compounds suggests that they hold considerable promise as potential inhibitors of metalloenzymes like polymerase and amylase which require Mg^{2+} and Ca^{2+} ion, respectively, for their structural stability and enzymatic activity (Fig. 5.2).[5.13]

DNA polymerases enzyme has long been recognized as a significant therapeutic target for infectious microorganisms and a number of compounds showing promising inhibitory activity towards the enzyme have been synthesized and characterized.[5.14] The choice of the polymerase enzyme as a therapeutic target assumes special significance owing to the emergence of antibiotic resistant strains, which is a constant challenge in modern healthcare and therapy of infectious diseases. Additionally, polymerase antagonists have been the centre of attraction owing to their potential application as antiproliferative agents against tumor cells.[5.15] Chemotherapy plays a key role in the treatment of many tumors. In this context, DNA polymerases represent important cellular targets in the development of anticancer and antiviral agents.[5.16] α-amylase is a glycoprotein[5.17] which breaks down long-chain carbohydrates such as starch, ultimately yielding maltotriose and maltose from amylose, or maltose, glucose and limit dextrin from amylopectin. It is produced mainly in the pancreas and the glands that make saliva. When the pancreas is diseased or inflamed, amylase is released into the blood. The excessive amylase in the blood may be implicated in digestive tract problems.[5.18] Currently, there is considerable interest in developing inhibitors for digestive enzymes such as α-amylase and other intestinal glucosidases as they can significantly influence breakdown of ingested starch and other carbohydrates and regulate absorption of glucose into the bloodstream. Such inhibitors could impact control of blood glucose levels and have significant implications in the treatment of type 2 diabetes.

It is quite clear from the aforementioned facts that there is an increasing demand in developing potent inhibitors of metalloenzymes and in this context synthesis of novel antagonistic amphiphilic compounds and evaluation of their inhibitory effect on candidate metalloenzymes assumes great significance. Such an endeavor would eventually lead to the generation of potent agents for effective therapy of infectious diseases and cancer. In chapter 5, experiments have been performed to explore the potential of 2-alkykylmalonic acid[2.3,2.4] [(**7-9**), Fig. 5.3] as an inhibitor of metalloenzyme for which *Taq* DNA

polymerase and α-amylase have been chosen as model enzymes (Fig. 5.2). The current investigation reports the effect of substituted malonic acid compounds in chelating magnesium and calcium and its subsequent inhibitory effect on *Taq* polymerase in polymerase chain reaction (PCR), and α-amylase in starch digestion process. Steady-state and nanosecond time-resolved fluorescence studies of α-amylase and its composites with amphiphilic compounds have been also described to understand the conformational changes associated with removal of metal ion from the active sites of the enzyme along with starch digestion study by UV-visible spectroscopy. A possible mechanism of enzyme inhibition mediated through the strong metal chelating property of the amphiphiles has been also suggested.

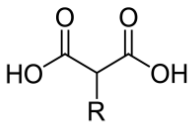

Where, R= C_8H_{17} (**7**), $C_{12}H_{25}$ (**8**) and $C_{16}H_{33}$ (**9**)

Figure 5.3. Structure of compounds (**7-9**).

5.2. Methods

5.2.1 Polymerase Chain Reaction (PCR) Studies

The potency of compounds *viz.* 2-octylmalonic acid (**7**), 2-octadecylmalonic acid (**8**) and 2-hexadecylmalonic acid (**9**) as magnesium chelators and potential inhibitors of *Taq* DNA polymerase enzyme was ascertained by performing polymerase chain reaction (PCR). A 23.0 mM stock solution of the compounds (**7**, **8** and **9**) was prepared in ultra-filtered water (pH ~9.0). Experiments were performed to study the effect of saturation of compounds with magnesium chloride as follows: In one set of experiment (Set A), varying concentrations of compounds (4.5, 3.6, 2.7, 1.75 and 0.83 mM) were pre-incubated overnight at room temperature with 1.5 µL of a 25.0 mM stock solution of magnesium chloride. In a parallel set of experiment (Set B), varying concentrations of compounds were pre-incubated overnight at room temperature with 1.5 µL of ultra filtered water instead of magnesium chloride. Reaction mixtures from set A and B were subsequently included in a PCR reaction mixture. Genomic DNA from *Escherichia coli* MTCC 433 was isolated using the bacterial genomic DNA isolation kit (Sigma, USA) and used as template DNA. The oligonucleotide primers used for PCR amplification included the universal primers specific for the domain *Bacteria* and the sequences of the forward and reverse primers were 8F: 5' AGAGTTTGATCCTGGCTCAG 3' and 1492R: 5' GGTTACCTTGTTACGACTT 3'. PCR amplification was carried out in a total reaction volume of 25.0 µL, which contained contents of the reaction mixtures obtained from set

A or set B, 2.0 µL of template DNA sample (50 ng), 2.5 µL of PCR buffer (60 mM Tris-HCl pH 8.5, 1.5 mM $MgCl_2$, 25.0 mM KCl, 10.0 mM 2-mercaptoethanol, 0.1% Triton X-100), 200.0 µM of each deoxynucleoside triphosphate (dNTP), 1.0 unit of *Taq* DNA polymerase (Sibenzyme, Novosibirsk, Russia) and 50.0 pmol each of forward and reverse primer. Template DNA was initially denatured at 94 °C for 2.0 min. Subsequently, a total of 35 amplification cycles were carried out in a programmable thermal cycler (Gene Amp Gold PCR System, Applied Biosystems, USA). Each cycle consisted of denaturation for 1.0 min at 94 °C, primer annealing for 1.0 min at 55 °C and extension for 1.0 min at 72 °C. The last cycle was followed by a final extension at 72 °C for 10 min. PCR products were analyzed by agarose (1%) gel electrophoresis.[5.19]

5.2.2. Enzymatic Starch Digestion Studies

The potency of compounds as calcium chelators and potential inhibitors of α-amylase (from hog pancreas, Fluka) was ascertained by performing starch digestion studies. As porcine α-amylase is likely to lose its activity at pH ~9.0, a 23.0 mM stock solution of compounds (**7**, **8** and **9**) was prepared in 1:1 (v/v) mixture of ultra-filtered water and DMSO. In one set of experiment (Set A), the enzyme solution (1.0 mg/mL in 10.0 mM phosphate buffer of pH 7.0) was pre-incubated overnight at room temperature with equal amounts of DMSO (v/v) instead of amphiphilic compounds solution to check the effect of DMSO on enzymatic activity. In a parallel set of experiment (Set B), varying concentrations of compounds (4.5, 3.6, 2.7, 1.75 and 0.83 mM) were pre-incubated overnight at room temperature with 100.0 µL of a 1.0 mg/mL of enzyme solution prepared in 10.0 mM phosphate buffer of pH 7.0. For the starch digestion kinetics studies, 100.0 µL of the pre-incubated enzyme solution with DMSO (Set A) was added to 36.0 mL of the starch solution having a starch concentration of 0.05 mg/mL. An equivalent amount of pre-incubated enzyme solution with compound (Set B) was added to 36.0 mL of starch solution having concentration of 0.05 mg/mL to compare the kinetics of starch digestion by the enzyme in presence of the compounds. Aliquots (2.0 mL) from each of the reaction mixtures were withdrawn at regular time intervals and to each of these 10.0 µL of iodine solution (Gram's iodine, HiMedia) were added and the UV-visible spectra of the solutions were subsequently recorded. For kinetics data, the absorbance at 580 nm was plotted as a function of time.

5.3. Results and Discussion

5.3.1 Effect of Compounds on the Enzymatic Activity of *Taq* DNA Polymerase

Figure 5.4 depicts the results obtained from PCR in presence of compounds **7**, **8** and **9**. It is evident from the figure that when varying concentrations of the compound **7** (4.5, 3.6, 2.7, 1.75 and 0.83 mM) were pre-incubated with 1.5 uL of 25.0 mM of magnesium chloride (experiment set A), the PCR reaction was completely inhibited at high concentrations of **7** (Lanes b-d). However, when the concentration of **7** was as low as 1.75 and 0.83 mM (Lanes e-f), the PCR reaction was positive as evidenced from the presence of amplicons in the lanes. A plausible explanation for these results is as follows: In the experiment set A, decreasing concentrations of the compound **7** was incubated with 1.5 μL of 25.0 mM magnesium chloride for saturation of the compound. The concentration of magnesium chloride (1.5 mM) used was suboptimal for complete saturation when higher concentrations of **7** (4.5, 3.6 and 2.7 mM) was used during pre-incubation. Hence, the compound still retained additional magnesium ion binding ability at these concentrations. Consequently in the PCR reaction, the compound was able to sequester magnesium ions from the active site of the enzyme *Taq* polymerase as well as additional magnesium ions present in the PCR buffer (1.5 mM magnesium is present in the buffer). In the context of DNA polymerase activity, the role of the metal ion (magnesium in case of *Taq* polymerase) in mediating the nucleotidyl transfer has been well established. Two magnesium ions present in the active site of *Taq* polymerase are in contact with the conserved aspartate residues of the enzyme (Fig. 5.2). Further, one of the metal ions is involved in activation of the 3'-OH of the DNA primer for attack of the nucleotide α-phosphate, while the other metal ion presumably stabilizes the displaced pyrophosphate moiety.[5.17,5.20] Thus, the role of the magnesium ions is pivotal in the nucleotidyl transfer mechanism and synthesis of the new DNA strand. Further, the structure of the amphiphile **7** suggests that it is a potent magnesium chelator as similar compounds based on malonic acid have been shown to have a high propensity to bind magnesium ion.[16] Hence, the detrimental effect of compound **7** in PCR can be accounted in terms of its inherent magnesium chelating property and subsequent inhibitory effect on *Taq* polymerase activity. It may also be mentioned that collectively the results obtained from set A clearly indicate that the inhibition of the polymerase enzyme which in turn stalled the PCR reaction is a function of the effect of saturation of the compound **7** with magnesium chloride and is determined by the concentration of the compound used. When lower

concentration of **7** (1.75 and 0.83 mM) was used in the experiments, the compound was fully saturated by magnesium during the pre-incubation step. Subsequently, this rendered the compound **7** ineffective to further chelate magnesium ions that were complexed with *Taq* polymerase enzyme or present in the PCR buffer. Hence, as expected a positive PCR reaction ensued and amplicons of the expected size of 1485 bp were obtained (Lanes e-f).

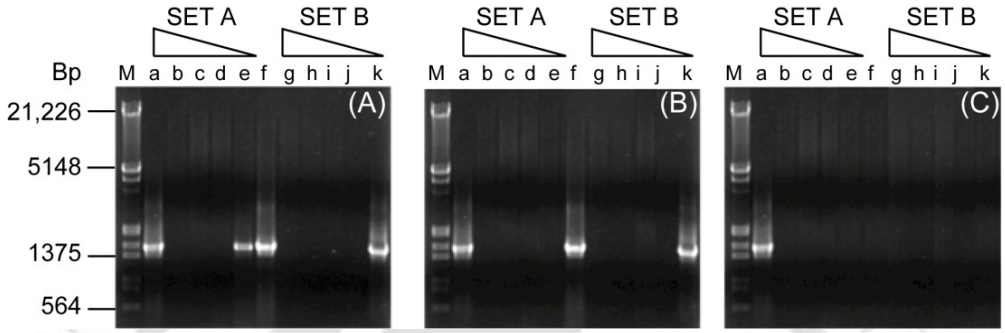

Figure 5.4. Agarose gel electrophoresis of amplicons obtained from PCR reaction mixtures containing (A) Compound **7**, (B) Compound **8** and (C) Compound **9**. Lane a: Amplicon obtained from control PCR reaction using ultrafiltered water (pH~9.0) and without compound; Lanes b-f: Amplicons obtained from experiment set A; Lanes g-k: Amplicons obtained from experiment set B. Arrow indicates an amplicon of 1485 bp.

The effect of saturation of compounds with magnesium chloride and corresponding inhibition of polymerase activity in PCR is further corroborated by the results obtained in experiment set B. It is clear from figure 5.4A that there was considerable inhibition of the PCR reaction when compound **7** was used at varying concentrations without any saturation step. A complete inhibition of the PCR reaction could be observed when **7** was used at concentrations ranging from 4.5 to 1.75 mM (Lanes g-j). It can be construed that at these concentrations **7** is able to effectively bind magnesium and reduce its accessibility for the enzyme. As a result the enzyme activity is hampered and the progress of the PCR reaction is significantly affected. At the lowest concentration of **7** (0.83 mM) the compound is unable to chelate magnesium sufficiently enough so as to inhibit the enzyme and halt the reaction. Hence, under these conditions PCR reaction yields a positive amplicon (Lane k). The magnesium chelating ability of amphiphilic compounds and the consequential inhibition of *Taq* polymerase in PCR reaction are clearly established.

It may be noted that a high pH of ~9.0 was chosen for the PCR study so as to ensure that all the malonic acid ($H_2\mathbf{L}$) head groups are in the malonate ($\mathbf{L}^{2-}$) form, so as to exert

stronger metal chelating properties.[5.21] At this pH, the precipitation of magnesium hydroxide was not observed. This precipitation was probably prevented since all the malonic acid ($H_2\mathbf{L}$) is essentially in the malonate ($\mathbf{L}^{2-}$) form. Furthermore, the stability constant of the Mg-complex is high, which facilitates the formation of the magnesium (II) malonate complex.[5.22] The possible role of the high pH being a cause of inhibition of the enzyme activity was negated by the fact that a positive amplicon was obtained in a control reaction when ultra-filtered water of pH ~9.0 was used to set up a conventional PCR reaction in the absence of the amphiphiles (Fig. 5.4A, Lane a).

5.3.2. Characterization of the Compound-metal Complex

When the compound **8** was used in a similar experimental setup, amplicons could only be obtained in presence of the lowest concentration of compound **8** used in experiment set A and B (Fig. 5.4B, Lanes f and k). The PCR reaction was completely inhibited at high concentrations of **8** (Fig. 5.4B, Lanes b-e). Thus the presence of the compound **8** resulted in the inhibition of enzyme in same manner as **7**, discussed above. When the compound **9** was used in a similar experimental setup, amplicons could not be obtained from any of the PCR experimental samples except for the control reaction (Fig. 5.4C). Thus the presence of the compound **9** resulted in complete inhibition of the enzyme independent of its concentration. Further, when the compound **9** was used, a precipitate was observed in all the tubes (at all concentrations) following PCR. Both compounds (**8** and **9**) are capable of forming complex with magnesium. However, in case of compound **9** an insoluble complex was observed which precipitated out of the reaction mixture, possibly because of the hydrophobicity. In order to study the formation compound-metal complex SEM followed by EDX (energy dispersive X-ray) analysis have been carried out, which revealed the presence of magnesium in the precipitate (Fig. 5.5A).

Further, FT-IR analysis of the precipitate obtained from the reaction mixture indicated the formation of magnesium-compound [Mg**L**] complex when compared with the result obtained with pure pre-formed complex (Fig. 5.5B). The peak at around 1720 cm^{-1} in spectra *a* is due to the carboxylic acid, while in spectra *b* and *c* the peak at around 1600 cm^{-1} is due to the carboxylate ion that can form hydrogen bond and account for the formation of complex between the compounds and magnesium. Collectively, these results clearly indicated that the compound **9** possessed strong magnesium binding ability and the complex formed thereof fell out of solution leading to dramatic depletion of

magnesium ions in the reaction mixture which eventually caused complete inhibition of the PCR.

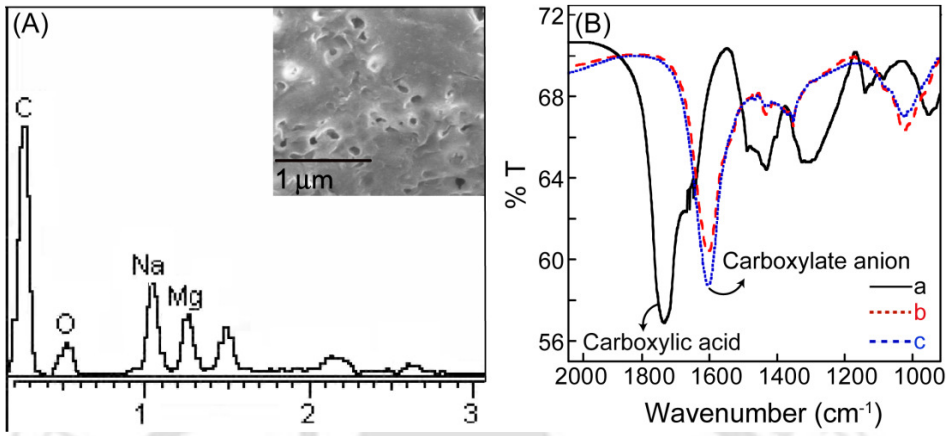

Figure 5.5. (A) EDX and Inset: SEM image of the precipitate from PCR reaction in presence of compound **9**; and (B) FT-IR spectra of the compound **9** before and after PCR reaction. Where, a: compound **9**, b: preformed Mg-complex, c: precipitate obtained from PCR reaction.

5.3.3. Effect of Compounds on the Enzymatic Activity of *α*-amylase

The inhibitory effect of amphiphilic compounds on the activity of *α*-amylase was studied by following UV-visible absorption of starch-iodine solution[5.23] in the presence of pure enzyme only and in presence of the enzyme-compound composites separately. Figure 5.6A and B represents the time-dependent decrease in absorbance of the starch-iodine complex in the presence of pure enzyme and compound-enzyme composites. It is evident from figure 5.6A that in case of pure enzyme a systematic decrease in the absorbance of starch-iodine solution was observed with time, indicating rapid digestion of starch by *α*-amylase. However, in case of the compound **7**-enzyme composites, hydrolysis of starch was completely abolished as no significant change in absorbance of the starch-iodine solution could be observed (Fig. 5.6B).

This indicated a profound inhibition of enzyme activity by compounds and the inhibition was unequivocally observed irrespective of the alkyl chain length of amphiphilic compounds. From figure 5.6C it is clear that the kinetics of starch digestion by pure α-amylase in buffer as well as in buffer-DMSO mixture (1:1) was comparable. Hence the activity of the enzyme was retained in presence of DMSO. Further, from figure 5.6C, the inhibitory effect of compounds on the activity of *α*-amylase was apparent as the typical

decrease in the absorbance of starch-iodine solution was not observed in case of the enzyme-compound composites.

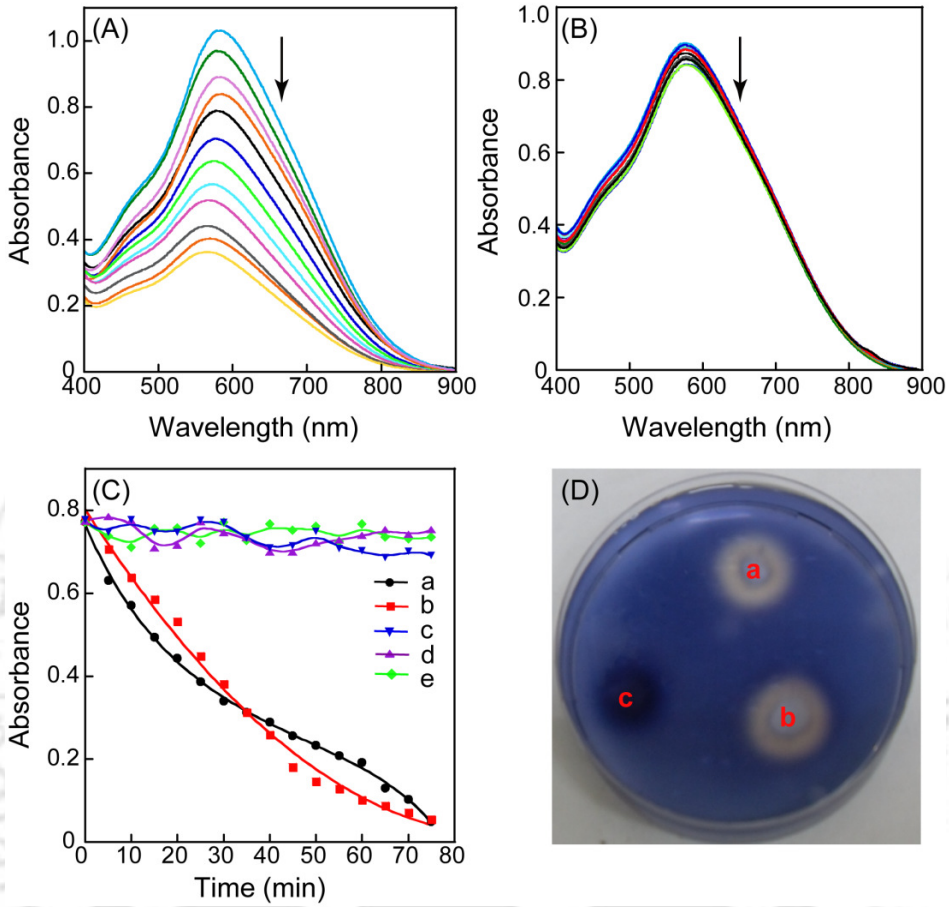

Figure 5.6. UV-visible spectra of the starch digestion by (A) α-amylase; (B) α-amylase-compound **7** composite; (C) Comparative kinetics study of starch digestion by pure α-amylase in buffer (a), pure α-amylase in buffer DMSO mixture (b), α-amylase-compound **7** (c), α-amylase-compound **8** (d) and α-amylase-compound **9** (e) as followed by the absorbance at 580 nm and (D) Starch agar plate assay for enzymatic activity of pure α-amylase in buffer (a), pure α-amylase in 1:1 mixture of buffer and DMSO (b) and α-amylase-compound **7** composites (c).

The enzymatic activity of amylase by varying the concentration of compounds has been also studied as shown in figure 5.7. Interestingly, unlike *Taq* DNA polymerase, the activity of amylase was inhibited even at a very low concentration of compounds (0.83 mM) which is comparable to the known inhibitors of amylase reported in the literature.[5.24] This indicates that a very low concentration of the compound was sufficient to chelate the metal from the enzyme which resulted in the loss of activity. The starch agar plate test has

been also persuaded in order to further ascertain the enzymatic activity of the enzyme-compound composite vis-à-vis the pure enzyme. The clear zone obtained around the wells in starch agar plate indicates amylase activity. The results of such tests are shown in figure 5.6D, where zone *a* and *b* are due to amylase only in buffer and buffer-DMSO mixture, respectively. It is also evident from the figure that enzyme-compound composite failed to produce any zone (zone *c*), indicating the ability of the compounds to act as a potent inhibitor of amylase. As clear from the figure, the zone of activity associated with the amylase in buffer-DMSO mixture was same as that of pure enzyme in buffer, indicating the enzyme retained its activity in presence of DMSO. Collectively, the starch agar tests corroborate earlier results.

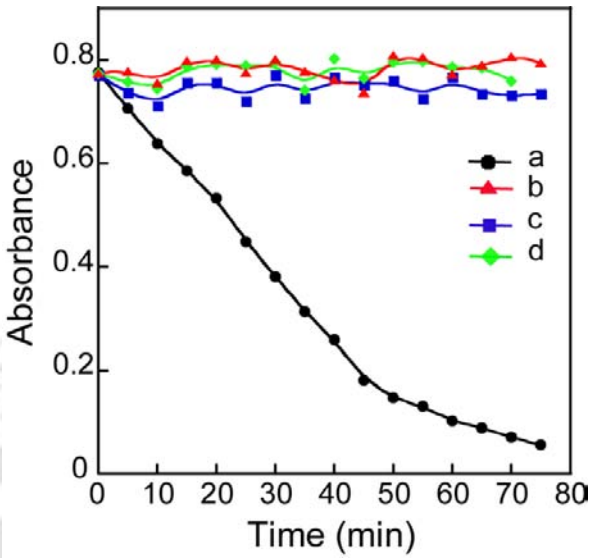

Figure 5.7. Comparative kinetics of starch digestion by amylase in presence of different concentration of compound **7**. Trace: a amylase and b-d: amylase + compound **7** (4.5, 2.7 and 0.83 mM)

5.3.4. Role of Chelating and Amphiphilic Nature of Compounds in Enzyme Inhibition

In order to gain further insight on the mechanism of enzyme inhibition caused by amphiphilic compounds some additional experiments have been pursued. The acid group of the compound which is responsible for chelating metal ion was modified to corresponding ester by reaction with ethanol. The modified amphiphilic compound failed to inhibit amylase activity. The control samples with only diethyl malonate and only malonic acid were also unable to inhibit the enzyme under identical experimental conditions (Fig. 5.8A-C). These experiments clearly established the fact that the malonic acid head group as well as the amphiphilic nature of the compound is indispensable for the inhibition of enzyme *i.e.* the removal of either chelating head group or the hydrocarbon chain from the compound obliterates its ability to inhibit the enzyme. Essentially interactions of the enzyme with the amphiphilic compounds lead to the

removal of metal ion from the active sites of the enzyme, which possibly results in disruption of the native conformation of the enzyme and concomitant loss of activity.[5.25] Conventionally, binding of the inhibitor with enzyme molecule is generally regarded as a critical step for manifestation of enzyme inhibition. However, literature reports suggest that metal chelators can also play the role of potent enzyme inhibitors by selectively removing metal ions from the active site of such enzymes.[5.26] Further, addition of Ca^{2+} to the enzyme solution incubated with compound was unable to recover the enzymatic activity (Fig. 5.8D), supporting the fact that the inhibition was irreversible in nature. Irreversible inhibition of enzyme by metal chelation has also been reported earlier for M17 leucine aminipeptidase.[5.27]

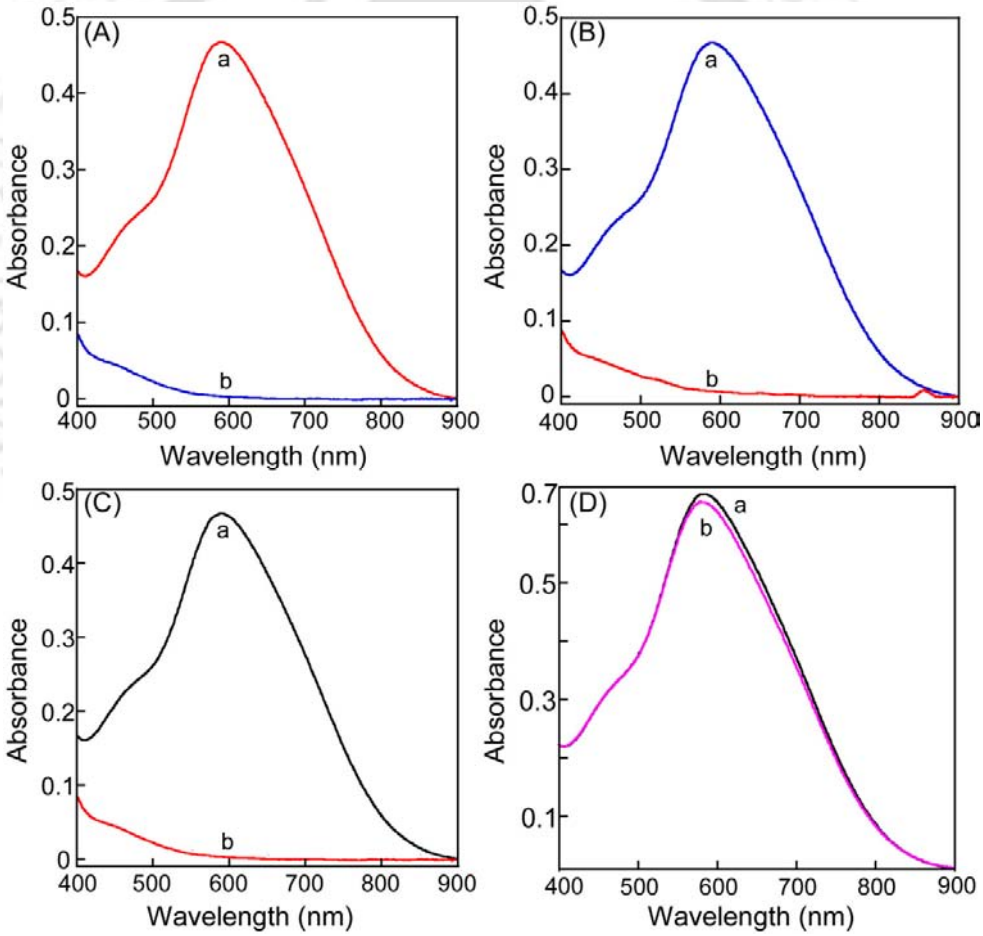

Figure 5.8. UV-visible spectra of starch digestion by (A) α-amylase-2-octyl diethyl malonate; (B) α-amylase-diethyl malonate; (C) α-amylase-malonic acid composites at zero minutes (a) and after 90 minutes (b) in an aqueous buffer DMSO mixture (1:1) and (D) Addition of $CaCl_2$ to the solution of amylase-compound **7** composites. The concentrations of the enzyme, 2-alkyldiethyl malonate, diethyl malonate and malonic acid used were 1 mg/mL and 4.5 mM.

In order to verify the possible structural changes of the protein in presence of compounds, the steady state fluorescence anisotropy (r) of pure enzyme and enzyme-amphiphile composites has been measured at room temperature. Table 5.1 shows the variation of the fluorescence anisotropy (r) of amylase upon interactions with compounds. The anisotropy of pure amylase increases from 0.068 in native solution to 0.085, 0.102 and 0.113 upon interactions with compounds **7**, **8** and **9** respectively, which suggests the increased rigidity of the surrounding environment of the fluorophore. From the results indicated in Table 5.1 it can also be observed that the value of anisotropy for enzyme-compound composites are more than the pure enzyme, indicating the loosening of the globules, which reduces the rotational diffusion coefficient for the enzyme molecules and leads to an increase in anisotropy. This was further supported by steady state and lifetime fluorescence measurements, as described in the next section.

5.3.5. Probing Molecular-level Interaction of Compounds with α-amylase

To get a molecular insight of the nature of compound-amylase interactions fluorescence spectroscopy has been employed. In proteins, tryptophan (Trp) fluorescence is widely used as a tool to monitor changes in its structures and to draw inferences regarding local structure and dynamics.[5.28] α-amylase contains both tyrosine and tryptophan residues and the change in its conformation or microenvironment caused by metal ions or inhibitors can be detected by fluorescence spectroscopy. The wavelength of emission maximum for Trp depends on its microenvironment. Specifically, a low polarity, hydrophobic microenvironment is characterized by λ_{max} ~331 nm, while for Trp in an aqueous phase λ_{max} is 350 to 353 nm. Effect of amphiphiles on the photophysical properties of the enzyme were studied by steady state and lifetime fluorescence measurements. The fluorescence spectrum of amylase exhibits strong emission with maximum at 340 nm, when excited at 290 nm. Excitation wavelength of 290 nm was taken to avoid the contribution from the tyrosine residues. A 10 nm blue shift in λ_{max} of amylase relative to that of Trp in an aqueous phase suggests that the Trp residues in amylase are located in hydrophobic environment. As shown in figure 5.9A, the presence of compounds caused a reduction in fluorescence intensity accompanied by a blue shift in λ_{max} by 5 nm, upon complexation with the enzyme. This blue-shift of emission maximum along with decrease in intensity indicates that interaction of compounds with the enzyme changes the polarity of microenvironment of Trp residues with probable increase in hydrophobicity in its

vicinity and this phenomenon is seen when the protein is in either native or structurally disrupted states.[5.29]

To explain the variation of blue shift and decrease in the intensity of amylase-compound composites compared to the pure amylase, the time-resolved fluorescence experiment with α-amylase in absence and presence of compounds has been performed. The fluorescence lifetime decay profiles of the pure amylase and amylase-compound composites are shown in figure 5.9B. The fluorescence lifetimes and the various statistical parameters used to check the goodness of fit are given in Table 5.1.

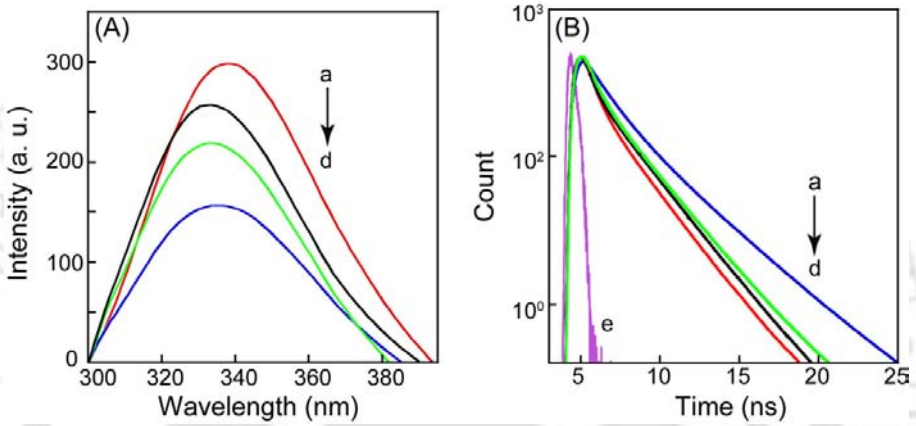

Figure 5.9. (A) Steady state fluorescence emission spectra and (B) Time resolved fluorescence spectra of pure α-amylase and α-amylase-compound composites 1:1 in buffer DMSO mixture. Where, Trace a-d: α-amylase only, α-amylase+**9**, α-amylase+**8** and α-amylase+**7** and Trace e: IRF. The concentration of the amylase and compounds used were 1 mg/mL and 4.5 mM.

The two time constants of amylase alone in buffer DMSO mixture (1:1) are 4.52 and 1.57 ns, while in presence of compounds the fluorescence lifetime of the Trp residues have decreased significantly. A decrease of lifetime from 4.52 (τ_1) to 2.98 and from 1.57 (τ_2) to 0.62 ns results due to the addition of compound **7**. Thus, the decrease of fluorescence lifetime was a clear consequence of the significant interactions between compounds and enzyme. It is clear from the lifetime measurements that fluorescence decay of amylase has significant impact due to presence of compounds. Therefore, metal ions-induced fluorescence quenching of amylase is attributed to the complex formation between amphiphiles and metal ion, and this binding perturbs the microenvironment around the Trp residues and causes the fluorescence quenching of enzyme. Removal of metal ion has significant impact on the polarity of microenvironment of Trp residue as indicated by

change for the maximum emission wavelength of Trp after addition of compounds. The aforementioned results indicate that the Trp residues in the enzyme is positioned in the vicinity of Ca^{2+} binding sites and removal of the divalent cation by amphiphilic compounds probably induces a change in the conformation of the active site in the protein and abolishes its activity. In corroboration with these results, the data shown in the present study also indicates that the metal ion not only plays an essential role in the catalytic mechanism but also has a great impact on the structural features of the enzyme.

Based on the cumulative results obtained for compound-amylase interactions, the following mechanism for amphiphile mediated enzyme inhibition has been proposed. α-amylase consists of a single polypeptide chain of about 475 amino acid residues, has two -SH groups and four disulfide bridges and contains a tightly bound Ca^{2+}.[5.30] α-amylases have long been known to require at least one Ca^{2+} ion per enzyme molecule for maintaining their tertiary structure and catalytic activity.[5.28,5.13] Ligands that bind Ca^{2+} ion in α-amylase belong to domains A and B of the enzyme (Fig. 5.2) and the active sites cleft is located between these two domains. Essentially the Ca^{2+} ion appears to stabilize the active site cleft by inducing an ionic bridge between domains A and B. The divalent metal ion is octahedrally coordinated by four amino acid residues of the enzyme *viz.* Asn-100, His-201, Asp-159 and Asp-167 from the domain A and B, while its coordination sphere is completed by water molecule as shown in figure 5.10.

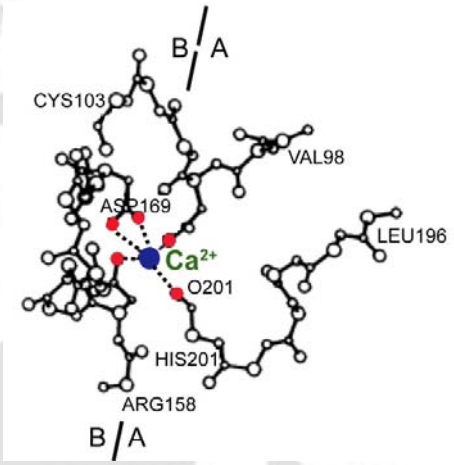

Figure 5.10. Stereo view of the Calcium binding site in α-amylase: Asn-100 and His-201 belong to domain A, Asp-159 and Asp-167 to domain B.[5.13b]

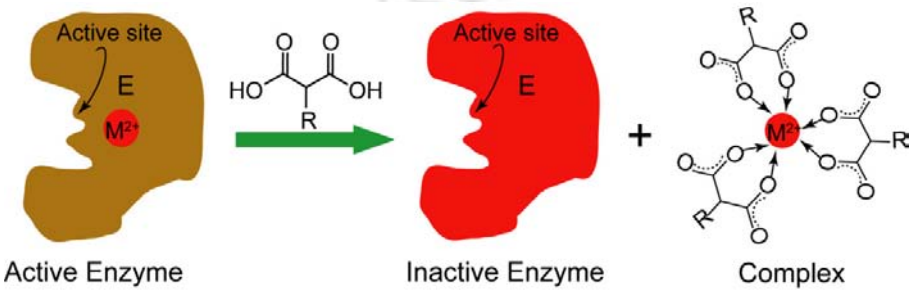

Figure 5.11. Schematic model showing the extraction of metal from the active sites of the enzyme by the compound (where, R = C_8H_{17}, $C_{12}H_{25}$ or $C_{16}H_{33}$).

Table 5.1. Anisotropy (r) and Fluorescence Lifetime (τ) Parameters of Pure α-amylase[a] and α-amylase-Compound[b] Composites.

Sample	λ_{em} (nm)[c]	Anisotropy (r)	τ_1 (ns)	τ_2 (ns)	α_1	α_2	χ^2
α-amylase[d]	340	0.068	4.52	1.57	0.011	0.012	1.001
α-amylase + **7**	335	0.085	2.98	0.62	0.012	0.019	1.000
α-amylase + **8**	335	0.102	3.13	0.51	0.014	0.018	1.003
α-amylase + **9**	335	0.113	3.27	0.69	0.014	0.028	1.002

[a][amylase] = 1 mg/mL, [b][compound] = 4.5 mM, [c]λ_{ex} = 290 nm and [d]1:1 mixture of buffer and DMSO

5.4. Conclusions

The present studies have systematically shown the effect of amphiphilic compounds in chelating the metal from the active sites of *Taq* polymerase and α-amylase enzyme and their subsequent inhibitory effect in polymerase chain reaction (PCR) and enzymatic assay of starch-iodine complex. Evidences for the formation of magnesium-compound complex during the process of enzyme inhibition have been provided based on the results of IR spectroscopy and EDX analysis, while the complexation of compounds with calcium ion in α-amylase was demonstrated by UV-visible and fluorescence spectroscopy. In the present case of enzymatic process, it is essentially the disruption of the native three dimensional structures of the enzymes due to the removal of metal ion from its active sites by compounds which was responsible for the loss of its activity. The native structure of the enzyme gets disrupted was further supported by steady state anisotropy measurements in presence of compounds. These amphiphilic compounds hold considerable promise as small molecule inhibitors of metal-dependent enzymes such as DNA polymerase and α-amylase. The strong structural homology amongst DNA polymerases could further motivate investigations to ascertain the inhibitory effect of these compounds against other polymerases and as well as other metalloenzymes.

References

[5.1] Shriver, D. F.; Atkins, P.W. *Inorganic Chemistry* 3rd ed., Oxford University Press, 1999.

[5.2] Messerschmidt, A; Huber, R.; Wieghardt, K.; Poulos, T. *Handbook of Metalloproteins,* Wiley, 2001.

[5.3] Waldron, K. J.; Robinson, N. J. *Nat. Rev. Microbiol.* **2009**, *7*, 25.

[5.4] Orten, J. M.; Otto, W. N. *Human Biochemistry*, St. Louis: The C.V. Mosby Co., 1975.

[5.5] Berg, J.; Tymoczko, J.; Stryer , L. *Biochemistry,* W. H. Freeman and Company, 2002.

[5.6] (a) Pratt, W. B.; Ruddon, R.W.; Ensminger, W. D. *The Anticancer Drugs*; Oxford University Press: Oxford, UK, 1994; (b) Heinemann, V.; Hertel, L. W.; Grindey, G. B.; Plunkett, W. *Cancer Res.* **1988**, *48*, 4024; (c) Ross, D. D.; Chen, S. R.; Cuddy, D. P. *Cancer Res.* **1990**, *50*, 2658; (d) Lister, T. A.; Rohaniter, A. Z. S. *Semin. Hematol.* **1982**, *19*, 172.

[5.7] Beaupoil-Abadie, B.; Raffali, M.; Cozzone, P.; Marchis-Mouren, G. *Biochim. Biophys. Acta* **1973**, *297*, 436.

[5.8] (a) Banks, P. A.; Freeman, M. L. *Am. J. Gastroenterol.* **2006**, *101*, 2379; (b) Owyang, C. *Pancreatitis*; Goldman, L.; Eds.: Ausiello D.; Cecil Medicine; 23rd ed. Philadelphia, Pa: Saunders Elsevier; 2007.

[5.9] (a) Pungitore, C. R.; Leon, L. G.; Garcia, C.; Martin, V. S.; Tonn, C. E.; Padron, J. M. *Bioorg. Med. Chem Lett.* **2007**, *17*, 1332; (b) Tami, C.; Puig, M.; Reepmeyer, J. C.; Ye, H.; D'Avignon, D. A.; Buhse, L.; Verthelyi, D. *Biomaterials* **2008**, *29*, 4808.

[5.10] (a) Vinson, J. A.; Kharrat, H. A.; Shuta, D. *The Open Nutraceuticals Journal* **2009**, *2*, 88; (b) Obiro, W.C.; Zhang, T.; Jiang, B. *Bri. J. Nutr.* **2008**, *100*, 1.

[5.11] Sholtz, K. F.; Bondarenko, D. I.; Mamaev, D. V. *FEBS Lett.* **1993**, *327*, 54.

[5.12] Sholts, K. F.; Mamaev, D. V.; Bondarenko, D. I.; Lagutina, L. S. *Biokhimiya* **1990**, *55*, 1832.

[5.13] Mitsubishi Chemical Industries Co., Ltd., Japan. Jpn. Kokai Tokkyo Koho 1984; (b) Buisson, G. Duee, E.; Haser, R.; Payan, F. *EMBO J.* **1987**, 6, 3909.

[5.14] (a) Karl, B. Z. *Physiol. Chem.* **1941**, *269*, 135; (b) Gelles, E.; Nancollas, G. H. *J. Chem. Soc.* **1956**, 4847; (c) Nair, V. S. K.; Nancollas, G. H. *J. Chem. Soc.* **1961**, 4367.

[5.15] (a) Miiller, M.; Rouilly, M.; Rusterholz, B.; MajZurawska, M.; Hu, Z.; Simon, W. *Mikrochim. Acta* **1988**, *III*, 283; (b) Rouilly, M.; Badertscher, M.; Pretsch, E.; Suter, G.; Simon, W. *Anal. Chem.* **1988**, *60*, 2013; (c) Erne, D.; Stojanac, N. D.; Ammann, P.; Hofstetter, E.; Pretsch, W.; Simon, H. *Chim. Acta* **1980**, *63*, 2271.

[5.16] Aggett, J.; Timperley, M. H. *Anal. Chim. Acta* **1969**, *47*, 551.

[5.17] (a) Doublie, S.; Sawaya, M. R.; Ellenberger, T. *Structure* **1999**, *7*, R31; (b) Kuhl, A.; Svenstrup, N.; Ladel, C.; Otteneder, M.; Binas, A.; Schiffer, G; Brands, M.; Lampe, T.; Ziegelbauer, K.; Rubsamen-Waigmann, H.; Haebich, D.; Ehlert, K. *Antimicrob. Agents Chemother.* **2005**, *49*, 987.

[5.18] Svenstrup, N.; Kuhl, A.; Ehlert, K.; Habich, D. *Bioorg. Med. Chem. Lett.* **2008**, *18*, 3215.

[5.19] Sambrook, J.; Russell, D. W. *Molecular Cloning: A Laboratory Manual*; 3rd ed, Cold Spring Harbor; Cold Spring Harbor Laboratory; New York 2001.

[5.20] Steitz, T. A. *J. Biol. Chem.* **1999**, *274*, 17395.

[5.21] Allen, C.; Yu, Y.; Maysinger, D.; Eisenberg, A. *Bioconjugate Chem.* **1998**, *9*, 564.

[5.22] Chambers, S. D.; Donkor, K. K. *Can. J. Anal. Sci. Spect.* **2006**, *51*, 84.

[5.23] Hollo, J.; Szeitli, J. *The Reaction of Starch with Iodine*; Ed.: *Radley, J. A. Starch and Its Derivatives*, 4th ed. London: Chapman and Hall, 1968.

[5.24] Yuasa, H.; Izumi, M.; Hashimoto, H. *Current Topics in Medicinal Chemistry* **2009**, *9,* 76; (b) Bols, M. *Acc Chem Res.* **1998,** *31,* 1*;* (c) Hara, K.; Honda, M. *Agric Biol. Chem.* **1990**, *54,* 1939; (d) Tadera, K.; minami, Y.; Takamatsu, K.; Matsuoka, T. *J. Nutr. Sci. Vitaminol* **2006**, *52*, 149.

[5.25] (a) Granger, M.; Abadie, B.; Mazzei, Y.; Marchis-Mouren, G. *FEBS Lett.* **1975**, *50*, 276; (b) Szedlacsek, S. E.; Duggleby, R. G. *Meth. Enzymol.* **1995,** *249,* 144; (c) Stone, S. R.; Morrison, J. F. *Biochim Biophys Acta* **1986**, *14*, 275; (d) Hille, R.; Massey, V. *Pharmacol Ther.* **1981**, *14*, 249.

[5.26] Ye, M.; English, A. M. *Biochemistry* **2006**, *45*, 12723; (b) Siemann, S.; Brewer, D.; Clarke, A. J.; Dmitrienko, G. I.; Lajoie, G. Viswanatha, T. *Biochim. Biophys. Acta.* **2002,** *1571***,** 190.

[5.27] Maric, S.; Donnelly, S. M.; Robinson, M. W.; Skinner-Adams, T.; Trenholme, K. R.; Gardiner, D. L.; Dalton, J. P.; Stack, C. M.; Lowther, J. *Biochemistry* **2009**, *48*, 5435.

[5.28] Vallee, B. L.; Stein, E. A.; Summerwell, W. N.; Fisher, E. H. *J. Biol. Chem.* **1959**, *234*, 2901.

[5.29] (a) Eftink, M. R. *Methods Biochem Anal.* **1990**, *35*, 117; (b) Burstein, E. A. *Luminescence of Protein Chromophores*. In Model Studies: Science and Technology Results, Vol. 6: Biophysics, VINITI, Moscow 1976; (c) Nilsson, K. P. R.; Ingana, O. *Macromolecules* **2004**, *37*, 9109.

[5.30] Tian, J.; Liu, J.; Tian, X.; Hu, Z.; Chen, X. *J. Mol. Struct.* **2004**, *69*, 1197; (b) Chen, Y.; Barkley, M. *Biochem.* 1998, *37*, 9976; (c) Gentili, P. L. *J. Phys. Chem. B* **2008**, *112*, 16793; (d) Gensch,T. *Photochem. Photobiol. Sci.* **2004**, *3*, 531; (e) Albani, J. R. *J. Fluor.* **2007**, *17*, 406.

CONCLUSION AND FUTURE SCOPE

In this thesis, the interactions between different types of synthetic amphiphiles and protein have been investigated extensively using different types of photophysical techniques like UV-visible, fluorescence and microscopy. Amphiphilic compounds having different types of head group and tail groups have been synthesized and their interactions with different proteins have been studied. Significantly, the influence of 'head group' and 'tail group' nature was found to be different on their photophysics after interaction with different type of proteins. In addition with this, the ionic or the neutral nature of compounds also found to play the essential role in these interaction phenomena. Most importantly, the amphiphilic nature of compounds has been found to have important role in interaction studies with proteins, which is a major finding of this thesis.

A novel amphiphilic fluorophoric molecule was found to have a selective sensing ability for bovine serum albumin (BSA) over other proteins tested at very low concentration. Moreover, the control experiments also reflect that the selective binding of compound towards BSA is due to its amphiphilic nature and the microenvironment created by the macromolecule also plays a crucial role in that process. The thesis has also shown systematically the effect of chelating amphiphilic compounds in chelating the metal from the active sites of polymerase and amylase enzyme and their subsequent inhibitory, which has been also supported by the control experiment. The molecule was also found to be acted differently with the variation in alkyl chain length on their enzymatic activity. The inhibition of enzymatic activity increases with increasing alkyl chain length of compound. The thesis also aimed towards the development of cationic amphiphilic molecule for the suppression of protein-protein interactions at alkaline pH, which is also found to depend on the alkyl chain length.

Therefore, these studies performed in this thesis, reveals the in-sight of amphiphiles and proteins interaction. This also finds several parameters to control the interaction phenomena between proteins and amphiphilic compounds in solutions. These aforementioned facts indicate the significance of nature and structure of amphiphilic molecules *i.e.* the head group and the tail group can control their activity on interaction with proteins. The understanding of such interactions in scale-up process can help in design of sensor for biomolecules, antagonists, therapeutic agents, drugs etc. Besides, scaling down to molecular level to understand more of these interactions can help to engineer at molecular level which can control such interactions in more specific manner.

LIST OF PUBLICATIONS

[1] Artificial Amphiphilic Scaffolds for the Selective Sensing of Protein Based on Hydrophobicity

B. Ojha and G. Das, **Chem. Commun.,** 2079-2081, 46, 2010

[2] The Interaction of 5-(Alkoxy)napthalaen-1-amine with Bovine Serum Albumin and its Effect on the Conformation of Protein

B. Ojha and G. Das, **J. Phys. Chem. B**, 3979-3986, 114, 2010

[3] 2-Alkylmalonic Acid: Amphiphilic Chelator and A Potent Inhibitor of Metalloenzyme

B. Ojha, A. K. Singh, M. D. Adhikari, A. Ramesh and G. Das, **J. Phys. Chem. B**, 10385-10842, 114, 2010

[4] Molecular Recognition of 2-Alkylbenzimidazole: Photophyscial and Structural Studies

B. Ojha and G. Das, **J. Photoch. Photobio. A**, 176–184, 211, 2010

[5] A Subtle Interplay of C-H Hydrogen Bonds in Complexation of Anions of Varied Dimensionality by a Nitro Functionalized Tripodal Podand

S. K. Dey, **B. Ojha** and G. Das, **CrystEngComm.,** 269-278, 13, 2011

[6] Role of Hydrophobic and Polar Interactions for BSA-Amphiphile Composites

B. Ojha and G. Das, **Chem. Phys. Lipids**, 144-150, 164, 2011

[7] Environment-Sensitive Amphiphilic Fluorophore For Selective Sensing of Protein

B. Ojha and G. Das, **Photochem. Photobiol. Sci.**, 554-560, 10, 2011.

[8] Suppression of Protein-Protein Interactions at Alkaline pH by Cationic Amphiphile

B. Ojha and G. Das, (Submitted)